TN-2275

TECHNICAL LIBRARY
AIRESEARCH MANUFACTURING CO.
9851-9951 SEPULVEDA BLVD.
INGLEWOOD,
CALIFORNIA

NACA TN 2275

NATIONAL ADVISORY COMMITTEE FOR AERONAUTICS

TECHNICAL NOTE 2275

A SURVEY OF STABILITY ANALYSIS TECHNIQUES FOR AUTOMATICALLY CONTROLLED AIRCRAFT

By Arthur L. Jones and Benjamin R. Briggs

Ames Aeronautical Laboratory
Moffett Field, Calif.

TECHNICAL LIBRARY
AIRESEARCH MANUFACTURING CO.
9851-9951 SEPULVEDA BLVD.
INGLEWOOD,
CALIFORNIA

Washington
January 1951

TABLE OF CONTENTS

	Page
S U M M A R Y	1
I N T R O D U C T I O N	1
C O M P O N E N T S A N D C O N C E P T S	3
PHYSICAL COMPONENTS OF AN AUTOMATICALLY CONTROLLED AIRCRAFT	4
Error Measuring Devices	5
Control Unit	5
Controlled Plant	6
FUNDAMENTAL ANALYTICAL CONCEPTS	6
Transfer Functions	8
Characteristic Equations	10
Time Lags	11
Delay time	11
Time constants	13
Control Gearing	14
Types of Control	15
Damping	16
Terminology	16
Types of damping	18
Passive Networks in Cascade	24
Feedback Networks	25
T H E O R Y	28
TECHNIQUES OF ANALYSIS	28
One Degree of Control	30

Page

Autopilot as an added term in the equations of motion .. 30

The Routh or Hurwitz criterion 31

Numerical evaluation of roots 32

Stability boundary charts 32

Transient response analysis 34

Airplane response as a transfer function in the control loop 36

Transient response 36

Frequency response 37

Resonance plots 37

Polar plots 41

Logarithmic plots 44

Two Degrees of Control 46

Autopilot as an added term in the equations of motion .. 47

Imlay's method 47

Airplane response as a transfer function in the control loop 47

Greenberg's method 48

EVALUATION OF TECHNIQUES OF ANALYSIS 48

CONCLUDING REMARKS 53

APPENDIX A - ILLUSTRATIVE EXAMPLE 55

APPENDIX B - SYMBOLS AND COEFFICIENTS 78

REFERENCES 84

BIBLIOGRAPHY 87

TABLES 88

FIGURES 103

NATIONAL ADVISORY COMMITTEE FOR AERONAUTICS

TECHNICAL NOTE 2275

A SURVEY OF STABILITY ANALYSIS TECHNIQUES FOR AUTOMATICALLY CONTROLLED AIRCRAFT

By Arthur L. Jones and Benjamin R. Briggs

SUMMARY

A survey of the stability analysis techniques for automatically controlled aircraft is presented. The survey is limited to the techniques commonly applied to linear, continuous-control systems wherein the difference between the output and input quantities is measured continuously and is used in the operation of the system (a closed-loop system). An evaluation of the techniques, based on the kind and amount of information derivable, is included. An illustrative example is also presented to demonstrate the calculations involved for a typical aircraft-autopilot combination.

INTRODUCTION

The application of automatic control to the operation of aircraft has complicated the analysis of the stability of the aircraft motion. Before this innovation no attempt had been made to analyze the effect of directed control, as provided by the human pilot, on the aircraft stability. The omission of this important factor was due for the most part to the apparent impossibility of specifying human response characteristics.[1] Consequently, aircraft stability was evaluated on the basis of the unregulated aircraft motion (or in the case of flight tests on the basis of pilots' opinions). This type of analysis was carried out both with the controls fixed and with the controls free in order to provide as comprehensive a test of the stability as possible.

The combination of the pilot and aircraft represents a closed loop of operations; that is, the pilot observes some output quantity of the aircraft such as its attitude, compares it with the desired attitude, and operates the controls to reduce the difference or error between the actual and desired attitudes. The airplane then changes attitude and the pilot repeats the process of observation, comparison, and control operation until the error is reduced to zero. If the human pilot is replaced by an autopilot, consisting essentially of an error-measuring

[1]Attempts recently have been made to study man as an element of a control system. (See references 1 and 2.)

device and a servo motor, the same closed loop of operations takes place. Furthermore, the response characteristics of the autopilot can be measured or estimated and this information, together with the response characteristics of the aircraft, makes it possible for the autopilot-aircraft combination to be analyzed as a closed-loop automatic-control system or, more concisely, as a servomechanism. In the literature relating to automatic controls there have been attempts made to distinguish between servomechanisms and simple automatic control systems often described as regulators. (See reference 3.) The distinction is quite subtle, however, and has no particular significance in the analysis of automatically controlled aircraft.

At the present time there are two methods of approach in the analysis of the combined aircraft-autopilot stability. One approach follows very closely the "equations of motion" type of analysis familiar to the aeronautical engineers and accounts for the autopilot by means of added stability derivatives, forcing functions, or supplementary equations. (See references 4, 5, and 6.) The other approach follows along the line developed by the mechanical and electrical engineers in their analyses of automatic-control systems and treats the aircraft as merely one component of the control loop. (See references 7, 8, and 9.) Both of these methods are considered herein, and an effort is made to catalogue and correlate the various techniques that have been developed. The techniques covered might well be described as elementary since in the actual process of design and construction of automatically controlled aircraft the analysis techniques often become more elaborate due to the extensions and modifications that are employed.

This survey will be concerned with continuous-control systems only. The discontinuous or "on-off" type of system may be designed to perform similar operations, but the analysis of such systems differs considerably from that of a continuous system. (See reference 10.) Moreover, only linear systems will be considered in this report. Nonlinearities complicate the analysis to the extent that one particular system would probably require as much time for analysis as a whole class of linear systems.

The report will be devoted primarily to discussions of the techniques of analysis of the stability and performance of automatically controlled aircraft in contrast to synthesis techniques for such systems. Analysis, being merely an evaluation of the existing characteristics of a system, is a simpler procedure than synthesis which is concerned with building up of components or the determination of modifications that will provide a system meeting certain standards of stability and performance. The definitions of such standards or criteria are a pressing problem in the development of automatically controlled aircraft at the present time. No attempt will be made herein to formulate such standards, but the fundamental parameters that probably would be used in the formulations will be pointed out and the analyses will be judged on the basis of how completely and how readily these parameters may be evaluated.

The general plan of the report will be to present a brief description of the components and analytical concepts associated with servomechanisms followed by a discussion of the stability analysis techniques. Appendix A contains an application of the techniques to a typical aircraft–autopilot combination. The precise definitions of terms and the detailed descriptions of the techniques, however, will be left to the many and varied references that are mentioned. The symbols and coefficients used in the text are listed and defined in appendix B.

COMPONENTS AND CONCEPTS

In the subsequent discussion the automatically controlled aircraft is considered to be a rather complicated servomechanism. There are many existing definitions of servomechanisms. The following definition suits the nomenclature employed in this report and is based on those given in references 3, 8, and 11: A servomechanism is a combination of elements controlling a source of power which tends to make the output of the device follow a particular input by use of a command signal, the strength of which is a function of the error between the input signal and the fed–back output signal.

Many practical examples of simple servomechanisms are discussed and illustrated in references 3, 11, 12, 13, 14, and 15. For the purposes of this report the following block diagram, with all the components lumped into one box, will serve as the basic schematic illustration of the servomechanisms discussed herein.

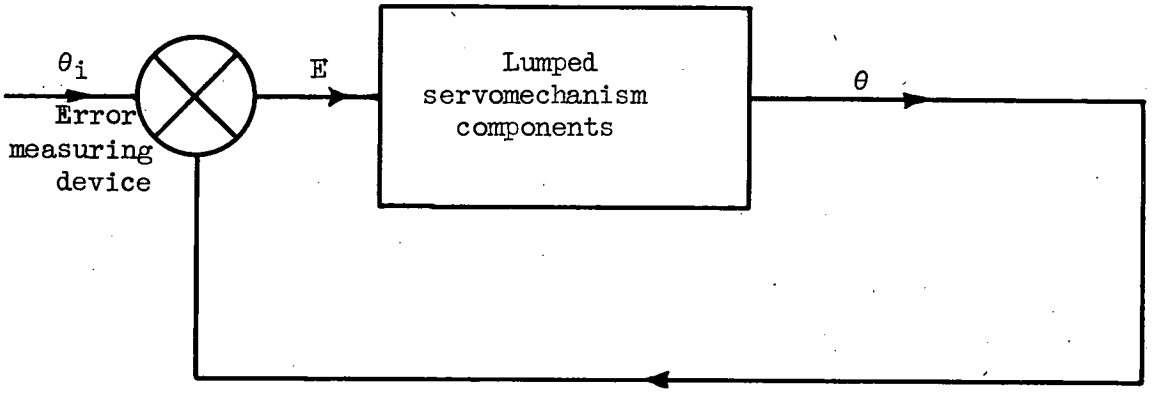

where

θ symbol for the output variable

θ_i symbol for the input variable

E symbol for the error variable, $\theta_i - \theta$

The source of power mentioned in the preceding definition corresponds to the autopilot or to the servo motor part of the servomechanism. The sensing device for the production of an error signal is also part of the autopilot. The airplane is the controlled object and its motion is

the output. The control surfaces of the airplane, actuated by the autopilot, provide the aerodynamic control of the system. The input signal is usually derived from a fixed course that the aircraft is trying to follow or from a target that the aircraft is trying to intercept.

The feeding back of the output to the sensing device provides a follow-up characteristic which makes the system a closed loop and thereby provides the form of control that is the basic characteristic of any servomechanism or regulator. In open-loop control systems, the control acts according to some preset command and is not at all governed by its output action.

In general, servomechanisms may be designed to control quantities other than output position. For instance, the output velocity, a force, a pressure, or almost any physical quantity can be the controlled variable. (See reference 3.) In application to aircraft, however, automatic control will refer almost exclusively to the position of the aircraft. Consequently, the aircraft-autopilot combination may be referred to as an error-sensitive, follow-up, remote-control, positioning servomechanism.

PHYSICAL COMPONENTS OF AN AUTOMATICALLY CONTROLLED AIRCRAFT

As previously indicated, all automatic control systems consist of a unit or "plant" to be controlled and a unit or "controller" to do the controlling. The boundaries separating these components are not too well defined for the many and varied mechanisms that could be classified as automatic control systems. For aircraft application, however, it is probably most convenient to consider the aircraft to be the plant and the rest of the system to be the controller. The controller could be further separated into a measuring device and control unit consisting of an amplifier and a servo motor. A block diagram representing the above breakdown of the automatically controlled aircraft is given as follows:

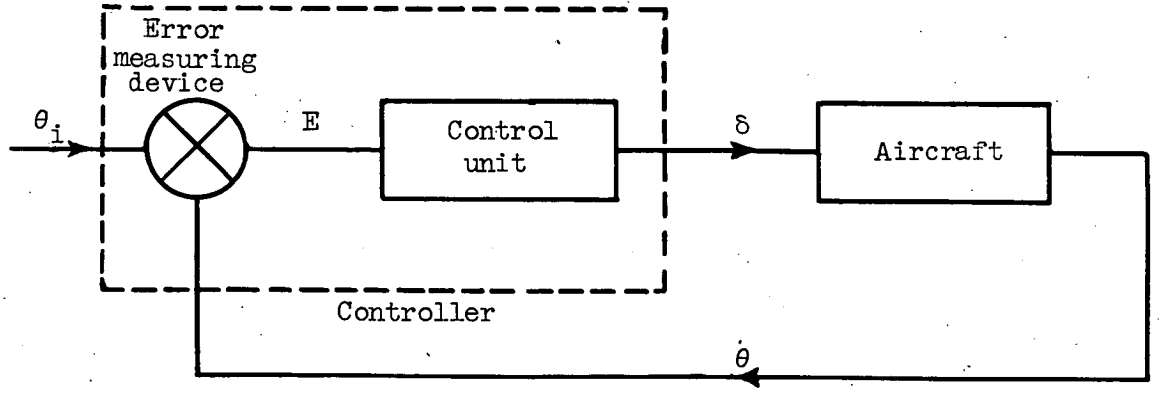

where δ is the deflection of the aircraft control surface as actuated by the control unit. Not all of these components are essential to a servomechanism in general, nor are all servomechanisms restricted to these components, but the breakdown used will be suitable for the cases considered herein.

Error-Measuring Devices

The function of the error-measuring device is to compare the feedback output signal with the input signal and thus determine the error between the desired position and the actual position of the aircraft. The controlled variable could be velocity rather than position but, for aircraft, control of the position is usually desired.

Error-detecting devices can be mechanical, electrical, or of many other forms. (See references 3, 12, 13, 16, 17, 18, and 19.) In aircraft application, however, a gyroscopic device is most often used. The tendency of the axis of the rotor to remain fixed relative to an intial direction in space is utilized to indicate deviations from a set course. Various other instruments such as anemometers, pendulums, etc., can be and are employed.

Control Unit

The control unit in the autopilot-aircraft servomechanism transmits the error signal to the plant with suitable amplification and power to produce the desired output from the plant. This unit is in itself a servomechanism with its own inner feedback loop and usually consists of an amplifier, lead or lag networks, and a servo motor.

The servo motor, which can be of electrical, hydraulic, or mechanical form, provides the torque to operate the controls of the airplane. The amplifier converts the relatively weak error signal to a current sufficient to operate a hydraulic valve or electric device used to control the servo motor.

Phase lead or lag networks may be incorporated within the inner loop to improve the damping and steady-state error of the control-unit servomechanism or may also be added external to the inner loop to provide definite characteristics of damping for the autopilot-airplane combination. The properties of such networks are discussed at greater length in later sections of this report.

Controlled Plant

Whether the aircraft be a conventional airplane, a powered missile capable of sustaining level flight, or a drop bomb with some means of guidance, the dynamic control is achieved by the deflection of aerodynamic control surfaces. Both flap-type control surfaces and variable-incidence control surfaces are used. With the exception of a variable-incidence lifting wing, these control surfaces are usually mounted near the tips of the wings and near the extremities of the body in order to provide moments of sufficient magnitude. The control of the aircraft, therefore, is usually obtained by a torque producing one of three rotations: roll about the longitudinal axis using ailerons, pitch about the lateral axis using elevators, or yaw about the vertical axis using a rudder or rudders.

The aircraft with these control surfaces is a much more complicated plant to control than those usually considered in books and articles on servomechanisms. In particular, more than one of these controls can be in operation at the same time. Thus, up to three degrees of control, two lateral and one longitudinal, must be dealt with as well as possibly six degrees of freedom. An additional degree of control is involved if both an elevator and a variable-incidence wing are used in the longitudinal control.

The combined effects of the actions of two controls, whether they are actuated by separate autopilots or by one autopilot, will complicate the analysis if the resulting modes of motions are interdependent. This situation can occur in the lateral case, for instance, if the ailerons and rudder are simultaneously employed or in the case of a missile so rigged as to destroy the independence of lateral and longitudinal motions provided by the lateral symmetry of most aircraft. Analyses based on one degree of freedom and one degree of control can be extended in special cases, or if approximations are employed to the case of automatically controlled aircraft, as will be evident from the subsequent discussions of the techniques involved. Methods that have been advanced for coping directly with more than one degree of control, however, are rare and will be treated apart from the commonly considered one degree of control problem.

FUNDAMENTAL ANALYTICAL CONCEPTS

The four dynamic response parameters that shall be considered as the basic items for the evaluation of stability and performance characteristics are (1) speed of response, (2) steady-state error, (3) time to damp, and (4) amount of initial overshoot. Reference to these parameters will help to clarify the functional purpose of the various components of the control loop in addition to providing a basis for the

future specification of stability and performance standards. These four items are best described in terms of the transient response (time history) of the motion, and they are illustrated qualitatively in the following diagram of a so-called "underdamped" (references 3 and 13) oscillation:

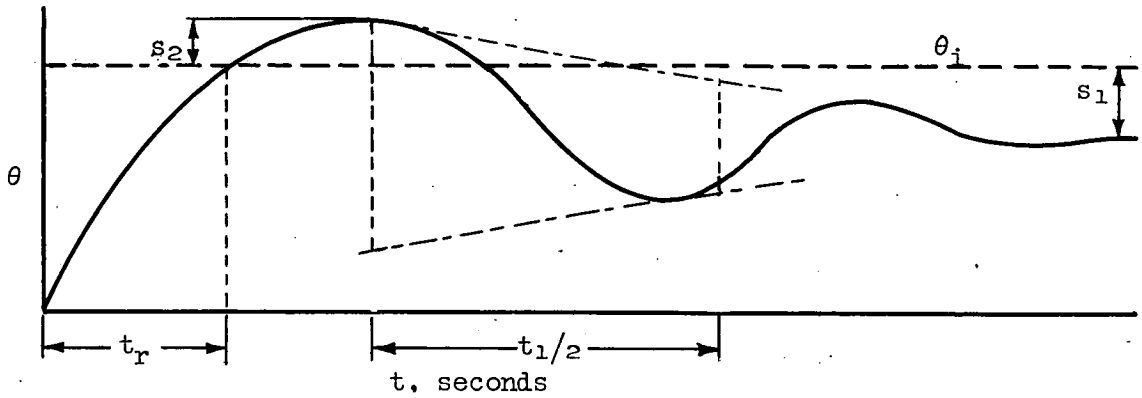

where

$\frac{\theta_i}{t_r}$ approximately the speed of response

s_1 steady-state error

$t_{1/2}$ time to damp to half amplitude

s_2 initial overshoot

For aperiodic motion the overshoot is, of course, missing. The time to damp is often expressed in other ways such as the time for the amplitude to damp by 1/e, the cycles to damp to 1/2 or by 1/e, etc.

The first two dynamic response parameters are affected mainly by the type of control used in the servomechanism and the last two by the type of damping employed, although none of the four parameters is completely independent of either control or damping. Also, both the stability and performance are related to all four parameters. The stability of the system is, of course, almost directly related to the damping. It is impossible to have stability without some positive means of control, however, whether it be proportional, derivative, integral, or otherwise. The problem of stabilizing a servo system, consequently, is inseparably involved with considerations of both control and damping. The improvement of the performance of a servo system is similarly involved.

In the concept of stability used by the aerodynamicist, any positive damping of all the modes of motion (totaling the same as the number of real and conjugate complex pairs of roots of the characteristic equation), oscillatory or aperiodic, constitutes stability. This corresponds to

having all negative real parts for the roots of the characteristic equation of the system. This definition of stability is quite common. An exception to this definition was used by Whiteley in reference 20. Whiteley considers a system to be stable if the response to a disturbance is nonoscillatory with small initial overshoot. The first definition seems to be the most suitable and the most generally applied to stability and therefore will be employed throughout this report. Whiteley's definition is really a definition of satisfactory performance and as such could be usefully employed. The establishment of suitable performance standards, however, is a controversial issue at the present time throughout servomechanism literature, and the general feeling seems to be that the standards will have to fit the intent of the design. Again it should be emphasized that no attempt will be made in this report to establish standards for the stability and performance of automatically controlled aircraft.

Time lags (usually of the exponential type in a continuous control mechanism) usually affect the stability of the system adversely, and, as one or more of these time lags are usually present in a servomechanism, the control and damping problem is immediately evident. In the following sections of the report, discussions of the various types of time lags and of the various types of control and damping will be presented. Inasmuch as pure derivative or integral control is impossible to obtain and the apparatus intended to provide such control is often complicated, discussions of passive lag or lead networks and of feedback networks that will give suitable approximations to integral or derivative control are included.

Transfer Functions

Although stability analysis is concerned ultimately with the servo system as a whole, the investigation of the contribution of each component in the loop to the stability is an important part of the analysis. In order to make such a study it is convenient to utilize the concept of the transfer function.

A transfer function can be thought of as a mathematical operator which relates an output to an input. The operator represents the action of a physical part of the servo loop and it can be obtained in operator form by taking the Laplace transform of the differential equation relating the output to the input. Certain forms of the transfer function also can be obtained by analyzing experimental data. Mathematically speaking, there are many different forms of the transfer function in use in servomechanism analysis, and unfortunately there are some inconsistencies in the terminology associated with these functions. Before discussing any of the differences in terminology, however, the two most common forms of the transfer function will be derived.

For perfectly arbitrary inputs, the differential equation itself can be considered as an elementary type of transfer function. More precisely, however, a transfer function is obtained by transforming the equation using either the Heaviside operator or the Laplace transform technique. The transfer function in this form is extremely useful because of its manageability. To illustrate the derivation of the operator type of transfer function, consider a second-order servomechanism for which the following differential equation holds

$$\ddot{\theta}(t) + 2\zeta\omega_n \dot{\theta}(t) = \omega_n^2 E(t) \qquad (1)$$

Assuming that the initial values are all zero, the Laplace transform of the equation is

$$(p^2 + 2\zeta\omega_n p)\,\theta(p) = \omega_n^2 E(p) \qquad (2)$$

Now rewriting the transformed equation in the following form:

$$\theta(p) = \frac{\omega_n^2}{p^2 + 2\zeta\omega_n p} E(p) \qquad (3)$$

the function $\frac{\omega_n^2}{p^2 + 2\zeta\omega_n p}$ can be considered as operating on $E(p)$ to produce $\theta(p)$. This function, therefore, is the transfer function between E and θ. It is the open-loop transfer function because of the variables involved.

In this operator form the transfer function can be used to determine the effects of a fairly large and general class of inputs on the output of the system. (See reference 11.) The procedure is as follows: The input function is put in operator form, the necessary algebraic manipulations are carried out, and the inverse of the Laplace transform is taken to obtain the time-history solution for the output.

The second type of transfer function oftentimes employed is the frequency-response form. It can be obtained directly from the operator form by substituting $i\omega$ for p. A formal mathematical derivation of this function is given in reference 11.

A few examples of the symbols used for the transfer functions are given below in the frequency-response notation. These functions represent, in particular, the open-loop response of a servomechanism but are typical for all applications of transfer functions:

$$\frac{\theta}{E} = KG(i\omega) \qquad \text{(Reference 3)} \qquad (4)$$

$$\frac{\theta}{E} = K\,|G(i\omega)|\,e^{i\Phi(i\omega)} \qquad \text{(Reference 3)} \qquad (5)$$

$$\frac{\theta}{E} = B + iC \qquad \text{(Reference 7)} \qquad (6)$$

$$\frac{\theta}{E} = Re^{i\epsilon} \qquad \text{(References 7 and 21)} \qquad (7)$$

$$\frac{\theta}{E} = Y(i\omega) \qquad \text{(Reference 11)} \qquad (8)$$

$$\frac{\theta}{E} = \phi P \phi \qquad \text{(Reference 9)} \qquad (9)$$

$$\frac{\theta}{E} = (AR)e^{iPA} \qquad \text{(Reference 9)} \qquad (10)$$

$$\frac{\theta}{E} = F(i\omega) \qquad \text{(Reference 12)} \qquad (11)$$

$$\frac{\theta}{E} = A(i\omega) \qquad (12)$$

In any case the symbols stand for an operator giving a relationship between the input and output of a system or a component of a system.

In regard to the terminology associated with the transfer functions, the source making the greatest distinction between types is reference 11. Therein, the term "transfer function" is reserved for the Laplace transform form and the frequency-response form is called the "frequency-response function." In reference 3 the term "transfer function" is used for all applications except the output-over-input operator $\theta/\theta i$ for the closed loop. The latter is designated as the "frequency response" of the servomechanism. The terminology in reference 11 is similar to that in reference 3 with the exception that there is no particular designation other than "output-input response" given to the θ/θ_i operator. In reference 12 the term "transference" is used for both the Laplace operator and frequency-response form of the transfer function. Reference 22 uses "system transfer function" for θ/θ_i and "loop transfer function" for θ/E.

The application of these functions to the analysis procedures will be discussed in detail in the section of this report on techniques of analysis.

Characteristic Equations

The study of the characteristic equation of a servomechanism is in itself a very convenient means of checking the stability of the system as will be shown in more detail in the discussion of the techniques of analysis. This equation can be formulated by writing the differential equation describing the dynamic behavior of the complete closed-loop system, then reducing the homogeneous form of the equation to a

polynomial. In some cases such as when the lag operator to be described subsequently is used, the homogenous form reduces to a transcendental equation. Generally the reduction is achieved either by substituting a solution of the form $e^{\lambda t}$ into the equation or by writing the equation in operator notation, assuming the initial conditions to be zero. The roots of the resulting algebraic or transcendental equation can then be determined. (See references 3, 23, 24, and 25.) If the roots are real and negative, or if the real parts of the complex roots are negative, the system is known to be stable.

The occurrence of a pair of conjugate complex roots in the solution of the characteristic equation indicates an oscillatory mode of motion. A real root indicates an aperiodic mode. In addition to the damping information provided by the real part of the complex root, the frequency of the oscillatory mode can be determined from the imaginary part.

Time Lags

The discussion of time lags will be divided into two parts. The first part will be on delay time, the period during which no response to a signal takes place. The second part will cover time constants which relate to the lags caused by exponential response to a signal.

Delay Time.- The study of the dynamics of mechanical systems is usually based on a differential equation that ideally represents the application of forces and the resultant acceleration of the masses or inertias. In some cases where the system involves a chain of events, however, an accurate estimate of the response of the system to a signal is not analytically representable unless certain delay times be considered that are not taken into account in the basic differential equation. (See references 26, 27, 28, and 29.) Delay time can be defined as the period between the start of a signal and the start of the resultant output. In electrical systems this kind of time lag is usually enough to be insignificant, but in purely mechanical, hydraulic, or pneumatic systems it is occasionally necessary to evaluate the effects of delay times or dead times as they are sometimes called.

There are a number of ways to incorporate delay time in the analysis of a servo system. The best way, of course, would be to write a differential equation or a set of simultaneous differential equations which would represent perfectly the characteristics of the system. Even a good approximation to this ideal situation, however, is possible only for the case of electrical or electrical-mechanical systems. The combined aircraft and autopilot system is one that usually can be treated as an

electrical-mechanical system. If a frequency-response type of analysis is being used and the experimental results are available for both the aircraft and autopilot, these results can be combined to yield almost exactly the characteristics of the behavior of the coupled components. Furthermore, it is fairly common practice to take the linear theoretical expressions for the aircraft response and the autopilot response, combine them, and proceed with the analysis on the assumption that the time lags are either closely approximated by these expressions or sufficiently small to insure reasonably accurate results.

In cases where an expression for some component of the system or some operation in the system cannot be written, even approximately, a finite time delay is often assumed and a term expressing this delay inserted into the differential equation for the system (making it a differential-difference equation). To illustrate this operation, consider a system defined by a differential equation of the form

$$\varphi(t) = f(D)\, E(t) \tag{13}$$

If the initial conditions are assumed to be zero, the Laplace transform of this equation is

$$L[\varphi(t)] = A(p)\ \ L[E(t)] \tag{14}$$

Now if there is a delay of τ_d seconds in the application of the operations represented by $f(D)$, $E(t - \tau_d)$ must be substituted for $E(t)$ in the above equations. Then by the translation theorem of Laplace transforms

$$L[E(t - \tau_d)] = e^{-p\tau_d}\ L[E(t)] \tag{15}$$

and equation (14) can be rewritten as

$$\begin{aligned} L[\varphi(t)] &= A(p)\ L[E(t - \tau_d)] \\ &= A(p)\ e^{-p\tau_d}\ L[E(t)] \end{aligned} \tag{16}$$

to take into account the time delay. The operator $e^{-p\tau_d}$ is often referred to as the lag operator. Unfortunately, the application of this operator yields a transcendental characteristic equation and, in general, complicates the analysis to such an extent that many investigators have tried using a three-term approximation to the power series expansion of this operator. (See references 6 and 30.) Such an approximation could lead and, in some cases, was reported to lead to erroneous results. Proper applications of the lag operator are demonstrated in references 23 and 27.

Time Constants.- In contrast to the delay time, which represents a fixed time delay between the start of a signal and the resulting response, the time constant concept arises from a certain exponential time response to an input signal, that is, a sort of sluggishness of response that is characteristic of systems having inertia, inductance, or the like. More specifically, the speed of response of a member in the system often can be related to a certain constant or constants that appear as coefficients in the transfer function of the member. These constants, for dimensional reasons, are known as time constants.

For an illustration of a simple case, consider a member of the control loop that has a transfer function of first order

$$A(p) = \frac{1}{1+pT} \tag{17}$$

The symbol T represents the time constant and, in general, it can be related to some physical parameter of the control-loop member. (See references 3 and 12.) The solution of the differential equations for this loop would contain this constant as the inverse coefficient of an exponential term in the manner

$$A(t) = Re^{-t/T} \tag{18}$$

Thus the magnitude of the time constant is seen to give an indication of either the sluggishness of the response or the rate of damping of the response, depending on which phase the motion is in - the approach to the desired condition or the settling down of the overshoot.

It can be seen from equation (18) that the time constant is related to the damping constant associated with oscillations arising in a second-order or higher system. To clarify this relationship consider a simple second-order closed-loop system defined by the equation

$$\ddot{\theta}(t) + 2\zeta\omega_n\dot{\theta}(t) + \omega_n^2\theta(t) = \omega_n^2\theta_i(t) \tag{19}$$

The term $\dot{\theta}(t)$ is the damping term and $2\zeta\omega_n$ is called the damping coefficient for reasons more fully explained in the section of this report on damping. For a second-order mechanical system it can be demonstrated that $2\zeta\omega_n$ is dimensionally equal to 1/sec and that the solution to the equation of motion (19) is of the form

$$\theta = e^{-\zeta\omega_n t}\cos\left(\omega_n t\sqrt{1-\zeta^2} + \epsilon\right) \tag{20}$$

Comparison of the exponential coefficients of equations (18) and (20) shows that the time constant T corresponds, in this case, to twice the reciprocal of the damping coefficient. In many instances where higher-order systems are considered, it can be shown directly that the damping coefficients are functions of the time constants of the first-, second-, or third-order terms in the transfer functions. As the terms become of high order, however, the mathematical and inferential relationships between the time constants of the transfer functions and the damping coefficients and other parameters characterizing the behavior of the complete system become more and more indistinct and the value of the "time constant" concept is lessened.

Various interpretations of the significance of the time constant can be found in references 3, 12, and 26. In reference 12 much attention is devoted to the effects of both sluggishness (corresponding to time constants) and dead time (corresponding to delay time). The combined effects of these two phenomena are studied as well as their individual contributions.

Control Gearing

The concept of control gearing is used primarily by the aeronautical engineer. (See references 6, 7, and 21.) It is the ratio of static control-surface deflection, caused by the autopilot in response to an error signal, to the static error signal. It can be expressed as

$$k = \left| \frac{\delta(i\omega)}{E(i\omega)} \right|_{\omega=0} \tag{21}$$

This parameter merely expresses the ratio of magnitudes of the input and output of the servo controller (autopilot) and does not give any indication of phase lag or lead. In terms of the transfer function of the autopilot it is

$$k = \left| A_p(i\omega) \right|_{\omega=0} \tag{22}$$

The control gearing concept is especially useful in defining stability boundaries as was done in reference 6, which typifies the aeronautical dynamic-stability approach to the problem of analyzing automatically controlled aircraft. It also has been employed in the frequency-response type of analysis in reference 7 where the critical control gearing k_{cr}, which corresponds to neutral stability, was investigated.

It should be pointed out that the sensitivity or gain, defined by the symbol K in reference 3, is not necessarily equal to the control gearing but is related to it by

$$K = \frac{k}{|G|_{\omega=0}} \tag{23}$$

where $|G|$ is the absolute magnitude of the frequency dependent part of the transfer function of the autopilot expressed as $KG(i\omega)$.

In reference 31, the inverse of the control gearing is called the static follow-up ratio and is used as a parameter.

Types of Control

In servomechanism terminology the term "control" refers to the type of signal fed to the control unit. The intent of the signal, of course, is to produce an output that will coincide with the input. Consequently, the signal is generally made a function of the error between the input and output, although control signals based on the input signal or directly on the output signal have been investigated and used.

The four kinds of control that are most commonly considered in analysis are: (1) proportional control; (2) proportional plus integral control; (3) proportional plus derivative control; and (4) proportional plus a combination of integral and derivative control. (See references 13 and 20.) Discussions of more complicated forms of control can be found in references 20 and 32.

The use of proportional control implies that a signal directly proportional to the error is controlling the source of power so that the control surface of the aircraft will be deflected in a direction tending to reduce the error. This results in zero steady-state error for a step input in the absence of external stiffness load. Addition of integral control, on the other hand, provides a zero steady-state error for a constant velocity input and also for a step input in the presence of external stiffness load. Integral control cannot be added to an unstable system as a direct means of stabilization, but indirectly it may be used to increase the stability of an already stable system by permitting the use of a lower gain factor or control gearing. Addition of derivative control or error-rate control, as it is sometimes called, provides anticipation of the change in error that is to take place by feeding the derivative of the error signal to the power source. This speeding up of the response by use of derivative control, in contrast to the slowing down caused by the use of integral control, improves the damping of the transient oscillations. The effect of adding both the derivative and integral control signals can best be expressed in the words of Whiteley (reference 20), "...it may be deduced that a combination integral and differential-of-error terms is a desirable arrangement, the former to control rates of response and achieve specified steady-state errors, and the latter to promote stability."

The effects of these various types of control on the damping will be discussed in the following section on damping.

The more subtle characteristics of these controls are discussed at some length in references 3, 11, 12, 13, 20, and 26. Methods of approximating these controls by use of lag or lead networks or feedback loops are discussed in later sections of this report.

Damping

The damping of a servo system is very closely related to the stability of the system. Without damping of some kind, the oscillations usually arising as one of the modes of motion would be sustained if not divergent. The aperiodic modes of motion are also affected by the damping and care must be taken not to have too much damping present or these modes and the over-all response of the servo system may become sluggish.

The terminology associated with damping seems to have been developed in the study of simple linear, second-order systems having viscous damping. Some of the constants involved have been labeled with an assortment of names by various authors. In order to make the following discussions on the damping of ordinary second-order servomechanisms and higher-ordered aircraft-autopilot systems as clear as possible, a short summary of the terminology used will be given.

Terminology.- The differential equation for a linear second-order system may be written in the following form:

$$J \frac{d^2x}{dt^2} + f \frac{dx}{dt} + \mu x = 0 \tag{24}$$

where

x some dependent variable

t time, the independent variable

J mass or moment of inertia

f the damping coefficient

μ the spring constant

The roots of the characteristic equation of the preceding differential equation are

$$r_1, r_2 = \frac{-f \pm \sqrt{f^2-4J\mu}}{2J} \tag{25}$$

Two parameters can be chosen such that these roots can be expressed in terms of two quantities instead of three. These two parameters are ω_n the natural frequency of the system, and ζ a dimensionless damping ratio. In terms of the previous constants these parameters are

$$\omega_n = \sqrt{\frac{\mu}{J}} \tag{26}$$

$$\zeta = \frac{f}{f_{cr}} = \frac{f}{2\sqrt{\mu J}} = \frac{\text{damping coefficient}}{\text{critical damping coefficient}} \tag{27}$$

The critical damping coefficient f_{cr} is the value of f for which the two roots r_1 and r_2 become real and equal and the oscillations are changed into aperiodic modes.

The differential equation can now be written in the following form:

$$\frac{d^2x}{dt^2} + 2\zeta\omega_n \frac{dx}{dt} + \omega_n^2 x = 0 \tag{28}$$

and the roots of the corresponding characteristic equation become

$$r_1, r_2 = -\zeta\omega_n \pm i\omega_n\sqrt{1-\zeta^2} \tag{29}$$

where $\omega_n\sqrt{1-\zeta^2}$ is the actual frequency ω of the damped oscillations or, as it is sometimes called, the frequency of the transient response. When ζ is small ω_n is a good approximation to the actual frequency. The equation for the time response is of the form

$$x(t) = R_1 e^{r_1 t} + R_2 e^{r_2 t} \tag{30}$$

or

$$x(t) = e^{-\zeta\omega_n t}(R_3 \cos \omega_n\sqrt{1-\zeta^2}\, t + R_4 \sin \omega_n\sqrt{1-\zeta^2}\, t) \tag{31}$$

The term $e^{-\zeta\omega_n t}$ contributes the damping and the coefficient $\zeta\omega_n$ is called diversely the damping constant, the damping coefficient (which unfortunately is also the name associated with f in the differential equation) in reference 33, the damping rate in reference 13, and occasionally the damping factor.

The inverse of this quantity $1/\zeta\omega_n$ can be referred to as a time constant. It represents the time required for the amplitude of the oscillations of the dependent variable to decrease by a factor of $1/e$. In this sense, it is similar to the time constants of the first-order terms discussed in the section on time constants. The number of cycles for the amplitude to damp by a factor of $1/e$ would be given by $\omega/2\pi\zeta\omega_n$ or $\sqrt{1-\zeta^2}/2\pi\zeta$. The aeronautical engineer often uses the time to damp to $1/2$ amplitude $t_{1/2}$ as a damping criterion. This quantity is related to $\zeta\omega_n$ in the following manner:

$$t_{1/2} = \frac{0.693}{\zeta\omega_n} \tag{32}$$

By taking the quotient of the period P where

$$P = \frac{2\pi}{\omega} \tag{33}$$

and the time constant $1/\zeta\omega_n$ it is possible to obtain a dimensionless measure of the damping called the logarithmic decrement

$$d = \frac{P}{1/\zeta\omega_n} = \frac{2\pi\zeta\omega_n}{\omega} = \frac{2\pi\zeta}{\sqrt{1-\zeta^2}} \tag{34}$$

It can be shown that

$$d = \log \frac{x(t)}{x(t+P)} \tag{35}$$

Hence, the logarithmic decrement is the logarithm of the ratio of displacements one period apart. The inverse of the logarithmic decrement $1/d$ is equal to the cycles required for the amplitude to decrease to $1/e$ of its value.

Types of Damping.- There are two kinds of damping usually associated with simple second-order servomechanisms, namely, viscous damping which is always present to some degree whether desired or not and the so-called error-rate damping. The latter is also known as derivative and kinetic damping. In some instances the viscous damping performs its stabilizing service without dissipating as heat loses too much of the power provided by the servo motor. When this favorable condition does not exist, however, there are two possible ways to reduce the energy losses of the viscous damping. One way is to use simulated viscous damping often referred to as tachometric feedback, which absorbs no energy from the servo motor, to replace the viscous damping to as great

an extent as possible. For a detailed discussion of simulated viscous damping see reference 13. The other way to reduce the losses is to keep the viscous friction as small as possible and yet stabilize the system by supplementing the viscous friction with error-rate damping.

The types of damping that are present in an aircraft-autopilot combination are shown in the following diagram:

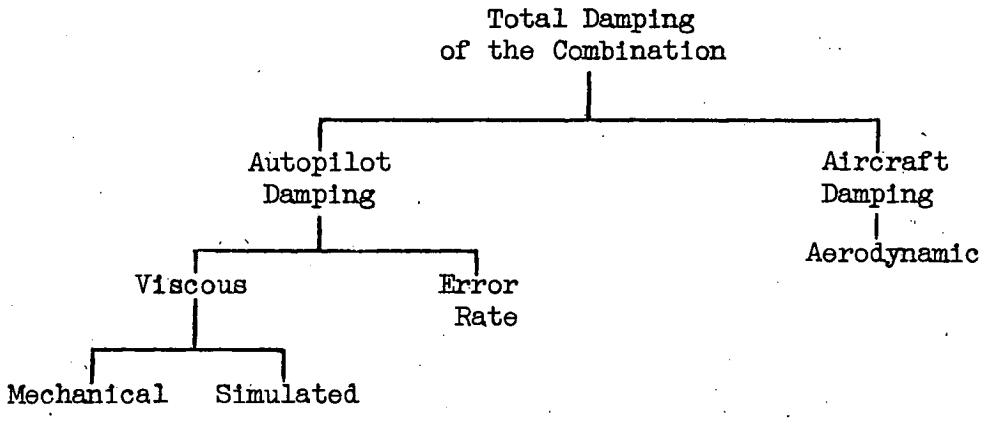

The autopilot damping is similar to the damping of a simple second-order servomechanism. The aerodynamic damping corresponds closely to the actual viscous damping in the autopilot. When the aircraft and autopilot are combined to form a servomechanism, the resulting modes of motion and the damping of these modes are not simply the sum of those of the individual components. The feedback arrangement that is the basic element in obtaining automatic control changes the characteristics of the modes of motion although the total number of modes of motion is not changed.

Some calculations showing the relative magnitudes of the damping factors involved will be undertaken to indicate these effects more explicitly. It will be advantageous to simplify the expression for the airplane-autopilot response in order to obtain a form that can be compared more or less directly to the second-order form of servomechanism previously discussed. The first step in this development is to combine the three equations of longitudinal motion used in the illustrative example in appendix A with the assumed autopilot equation

$$(0.058\,D^2 + D + 37.5)\,\delta = -37.5\,k\,E \qquad (36)$$

where

k control gearing

δ control surface deflection

This is easily done by inserting the autopilot equation as a forcing function in the equation for the angular degree of freedom (a stability analysis approach that will be described in the discussion of the techniques of stability analysis). The resulting forms of the equation are

$$\left(-C_{T_o}\cos\alpha_o - \frac{\partial C_L}{\partial \alpha}\right)\alpha - 2\tau D\alpha + 2\tau D\theta + \left(-2C_{L_o} - 2C_{T_o}\sin\alpha_o - \frac{\partial C_L}{\partial u'}\right)u' = 0 \quad \text{(Lift)} \quad (37)$$

$$\left(\frac{\partial C_D}{\partial \alpha} - C_{L_o}\right)\alpha + \left(C_{L_o} + C_{T_o}\sin\alpha_o\right)\theta + \left(2C_{D_o} - 2C_{T_o}\cos\alpha_o + \frac{\partial C_D}{\partial \mu'}\right)\mu' + \left(\frac{1}{\tau}\frac{\partial C_D}{\partial \dot{\mu}'} + 2\right)\tau D\mu' = 0 \quad \text{(Drag)} \quad (38)$$

$$\frac{\partial C_m}{\partial \alpha}\alpha + \frac{\partial C_m}{\partial \dot{\alpha}}D\alpha + \frac{\partial C_m}{\partial \dot{\theta}}D\theta + \left(\frac{1}{\tau^2}\frac{\partial C_m}{\partial \ddot{\theta}} - 2K'\right)\tau^2 D^2\theta + \frac{\partial C_m}{\partial u'}u' = -\frac{\partial C_m}{\partial \delta}\left(\frac{-k\ 37.5\ E}{0.058\ D^2 + D + 37.5}\right) \quad \text{(Pitching Moment)} \quad (39)$$

Now it is a very common procedure in the case of longitudinal motion in level flight to assume that the longitudinal perturbation velocity u' can be neglected and that conditions can be further controlled such that equation (38) can be eliminated. This procedure eliminates one degree of freedom and leaves the two following simultaneous differential equations:

$$\left(-C_{T_o}\cos\alpha_o - \frac{\partial C_L}{\partial \alpha}\right)\alpha - 2\tau D\alpha + 2\tau D\theta = 0 \quad (40)$$

$$\frac{\partial C_m}{\partial \alpha}\alpha + \frac{\partial C_m}{\partial \dot{\alpha}}D\alpha + \frac{\partial C_m}{\partial \dot{\theta}}D\theta + \left(\frac{1}{\tau^2}\frac{\partial C_m}{\partial \ddot{\theta}} - 2K'\right)\tau^2 D^2\theta = \frac{\partial C_m}{\partial \delta}\left(\frac{37.5\ k\ E}{0.058\ D^2 + D + 37.5}\right) \quad (41)$$

Now combining these to get one equation in θ and E yields

$$\left\{\tau^3 D^3\left(\frac{2}{\tau^2}\frac{\partial C_m}{\partial \dot{\theta}^{\bullet}} - 4K'\right) + \tau^2 D^2\left[\frac{2}{\tau}\frac{\partial C_m}{\partial \dot{\alpha}} + \left(C_{T_o}\cos\alpha_o + \frac{\partial C_L}{\partial \alpha}\right)\left(\frac{1}{\tau^2}\frac{\partial C_m}{\partial \dot{\theta}^{\bullet}} - 2K'\right) + \right.\right.$$

$$\left.\left.\frac{2}{\tau}\frac{\partial C_m}{\partial \dot{\theta}}\right] + \tau D\left[2\frac{\partial C_m}{\partial \alpha} + \left(C_{T_o}\cos\alpha_o + \frac{\partial C_L}{\partial \alpha}\right)\frac{1}{\tau}\frac{\partial C_m}{\partial \dot{\theta}}\right]\right\}\theta$$

$$= \left(C_{T_o}\cos\alpha_o + \frac{\partial C_L}{\partial \alpha} + 2\tau D\right)\frac{\partial C_m}{\partial \delta}\left(\frac{k\ 37.5\ E}{0.058\ D^2 + D + 37.5}\right) \qquad (42)$$

In order to put this in the form of a torque balance equation as commonly written for the second-order servomechanism τD can be factored out of the left-hand side of the equation and the signs of all the terms reversed (to make the numerical values of the coefficients positive):

$$\left(4K' - \frac{2}{\tau^2}\frac{\partial C_m}{\partial \dot{\theta}^{\bullet}}\right)\tau^2 D^2\theta + \left[\frac{2}{\tau}\left(-\frac{\partial C_m}{\partial \dot{\alpha}}\right) + \left(C_{T_o}\cos\alpha_o + \frac{\partial C_L}{\partial \alpha}\right)\left(2K' - \frac{1}{\tau^2}\frac{\partial C_m}{\partial \dot{\theta}^{\bullet}}\right) + \right.$$

$$\left.\frac{2}{\tau}\left(-\frac{\partial C_m}{\partial \dot{\theta}}\right)\right]\tau D\theta + \left[2\left(-\frac{\partial C_m}{\partial \alpha}\right) + \left(C_{T_o}\cos\alpha_o + \frac{\partial C_L}{\partial \alpha}\right)\left(-\frac{1}{\tau}\frac{\partial C_m}{\partial \dot{\theta}}\right)\right]\theta$$

$$= \frac{1}{\tau D}\left(C_{T_o}\cos\alpha_o + \frac{\partial C_L}{\partial \alpha} + 2\tau D\right)\left(-\frac{\partial C_m}{\partial \delta}\right)\left(\frac{k\ E\ 37.5}{0.058\ D^2 + D + 37.5}\right) \qquad (43)$$

In this form the coefficient of the angular velocity $D\theta$ is easily recognized as the aircraft equivalent of the damping coefficient of the second-order servomechanism equation. The autopilot damping is shown by the characteristic equation of the autopilot in the denominator of the right-hand side of equation (43). In order to get some idea of the relative amounts of the damping that the airplane and autopilot possess uncombined, the numerical values used in the illustrative example of appendix A are inserted in equation (43) to give

$$[(0.0231)\ D^2 + (0.0342 + 0.0656 + 0.0704)(0.967)\ D + (1.278 + 0.187)]\ \theta$$

$$= \frac{(5.325 + 1.933\ D)(0.6299)\ 37.5\ k\ E}{(0.967)\ D(0.058D^2 + D + 37.5)} \tag{44}$$

or

$$[(0.0231)\ D^2 + (0.1645)\ D + 1.465]\ \theta = \frac{(5.325 + 1.933\ D)(0.6299)\ 37.5\ kE}{(0.967)\ D(0.058\ D^2 + D + 37.5)} \tag{45}$$

Putting the equation in the desired form,

$$[(D^2 + 7.12\ D + 63.4)]\ \theta = \frac{37.5\ (5.325 + 1.933\ D)(0.6299)\ k\ E}{(0.0231)\ D\ (D^2 + 17.25\ D + 647)(0.058)(0.967)} \tag{46}$$

and then in transfer function notation yields

$$\theta = A\theta_s\ A_p\ E \tag{47}$$

where for the airplane

$$A_{\theta_s} = \frac{\theta}{\delta} = \frac{(5.325 + 1.933\ D)(0.6299)}{(0.967)\ D\ (D^2 + 7.12\ D + 63.4)(0.0231)} \tag{48}$$

yielding

$$\zeta\omega_n = \frac{7.12}{2} = 3.56;\quad \omega_n = \sqrt{63.4} = 8.0$$

and where for the autopilot

$$A_p = \frac{\delta}{E} = \frac{37.5\ k}{(0.058)(D^2 + 17.25\ D + 647)} \tag{49}$$

yielding

$$\zeta\omega_n = \frac{17.25}{2} = 8.63;\quad \omega_n = \sqrt{647} = 25.5$$

This comparison shows that the airplane has about half the damping constant that the autopilot has and has a natural frequency of 8.0 radians per second; whereas the autopilot has a natural frequency of 25.5 radians per second. (The actual frequencies of the oscillatory modes are 7.2 and 23.9 radians, respectively.) In terms of the time to damp to half amplitude, the airplane requires 0.19 second; whereas the autopilot requires only 0.08 second.

When the two units are combined into a complete automatic control system the behavior of the resulting servomechanism is not the simple sum of the behaviors of the individual parts as mentioned previously. The basic feedback loop to the error detector makes the equation for the response (references 3, 11, 22, and 34)

$$\frac{\theta}{\theta_i} = \frac{\theta/E}{1+\theta/E} = \frac{A_{\theta_s} A_p}{1 + A_{\theta_s} A_p} \tag{50}$$

The new characteristic equation is $1 + A_{\theta_s} A_p = 0$ which yields a fifth-order equation that is no longer factorable into distinct airplane and autopilot functions. Thus the new modes of motion are a complex combination of the autopilot and airplane modes.

Numerically the new characteristic equation is

$$(0.967)\, D\, [(0.0231)\, D^2 + (0.1645)\, D + 1.465](0.058\, D^2 + D + 37.5) + (5.325 + 1.933\, D)(0.6299)\, k\, 37.5 = 0 \tag{51}$$

or

$$D^5 + 24.4\, D^4 + 833\, D^3 + 5700\, D^2 + 76{,}200\, kD + 97{,}100\, k = 0 \tag{52}$$

The roots to this equation were determined for $k = 1.0$ and $k = 0.2$:

$$\left.\begin{aligned} &k=1.0,\ \lambda_1=-1.39;\ \lambda_{2,3}=-1.97 \pm 10.5\ i;\ \lambda_{4,5}=-9.52 \pm 22.8\ i \\ &k=0.2,\ \lambda_1=-4.28;\ \lambda_{2,3}=-1.76 \pm 1.89\ i;\ \lambda_{4,5}=-8.29 \pm 24.8\ i \end{aligned}\right\} \tag{53}$$

It can be seen from an inspection of the values for the damping constants (the negative of the real parts of the roots) and the actual frequencies (the numerical values of the imaginary parts of the roots) that the oscillatory mode corresponding to $\lambda_{4,5}$ has a close correspondence to the mode of oscillation of the autopilot alone. It is also the mode least affected by the variation in the strength of the feedback of the closed loop as shown by small changes in the damping and frequency characteristics caused by the variation in the control gearing k. The other oscillatory mode $\lambda_{2,3}$ corresponds somewhat to the airplane mode although it is apparent that these two modes show large differences in the damping and frequency characteristics. The $\lambda_{2,3}$ mode and the aperiodic mode λ_1 are quite markedly affected by the variation in feedback. It is important to note that with regard to the determination of the mode or modes that will be predominant in the output motion of the aircraft-autopilot combination, the magnitudes of the various modes must be calculated in addition to the damping and frequency characteristics.

A check on these results for k=1 was made by calculating the roots of the characteristic equations resulting from the combination of the autopilot with the unmodified equations of motion for the aircraft and with the equations of motion modified by an approximate factorization of the stability quartic. The values of the damping constants obtained are given in table I. These additional analyses both revealed that in the uncombined condition the aircraft possessed a slowly divergent aperiodic mode. This divergent mode disappeared, however, when the autopilot and aircraft were combined in closed-loop operation. The values of the damping constants for the oscillatory modes were in good agreement among the three analyses.

Passive Networks in Cascade

In cases where it is not suitable mechanically to add control in the form of derivatives or integrals of the error, the damping or performance of a system can be improved by the insertion of passive networks in cascade. Passive networks in cascade are networks containing no source or sink of energy that are inserted in series with the other elements of the loop. These networks are usually inserted near the input end of the main servo sequence and are referred to as "input networks" in reference 20. These passive networks only approximate the effects of pure derivative-error or integral-error control by the addition of phase lead or lag to the system. The fact that such networks can be employed advantageously is emphasized in references 3 and 20.

The process of analyzing the changes in a servomechanism loop required to obtain the proper system behavior can be done quite simply on the polar type of plots of the frequency-response methods of analysis (described under the section Techniques of Analysis). The transfer locus of the servomechanism must conform to a rather specific pattern in order that the system be stable and otherwise satisfactory. The shape of the curves can be changed over certain frequency ranges by the use of these passive networks. Thus a passive network is usually designed to give phase lag or lead in such a manner that when its transfer locus is added to that of the rest of the servo loop the resulting locus has the desired shape. In reference 3, this procedure is referred to as reshaping the G locus. To illustrate, consider a simple servomechanism with a frequency-response function of the following form:

$$\frac{\theta}{E} = A_1 = \frac{1}{i\omega(i\omega T_1+1)} \tag{54}$$

where T_1 is a time constant. The polar plot of this transfer function is given in the sketch. As it stands, the locus indicates a zero position error type of servomechanism because at the low frequencies it is asymptotic to the negative imaginary axis. Now if it were desired to change this servo system to a zero-velocity-error type, for which the low-frequency asymptote lies along the negative real axis, the following transfer function corresponding to an integrating network could be used:

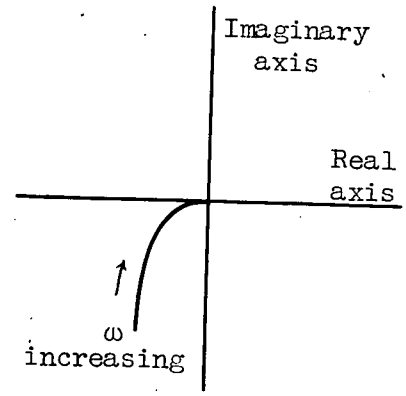

$$A_2 = 1 + \frac{1}{i\omega T_2} \tag{55}$$

where T_2 is a time constant of the network. The network locus has the shape shown in the accompanying sketch. Adding the network to the initial servo loop gives the following transfer function:

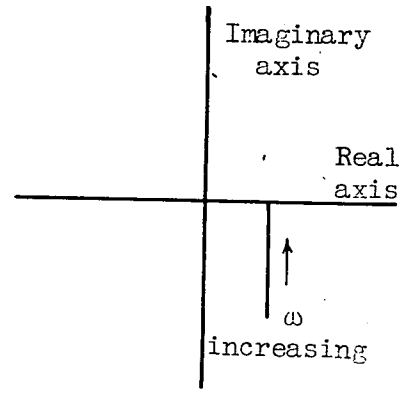

$$\frac{\theta}{E} = A_1A_2 = \frac{i\omega T_2 + 1}{T_2(i\omega)^2\,(i\omega T_1 + 1)} \tag{56}$$

and the transfer locus takes the shape indicated in the accompanying sketch.

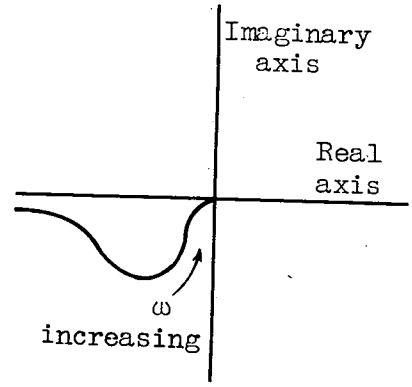

Feedback Networks

When passive networks in cascade cannot be used to provide the approximate derivative or integral control desired, feedback networks are often used. (See reference 3, pp. 206, 217, 224. See also reference 20.) In fact, it is frequently more desirable in practice to use feedback rather than cascaded networks. (See references 3, 20, and 32.) The servomechanism itself is a degenerative feedback system in that the output in some form is fed back to reduce the error. An auxiliary feedback loop in the system can be either degenerative or regenerative although the latter requires a more critical adjustment. Feedback is usually obtained from a parallel circuit in the loop that provides for

the addition of a later operative quantity to an earlier one, the earlier quantity usually being the error signal. Feedback in a broad sense can also be obtained by inserting a dynamic element in the basic servomechanism feedback from the output to the error-measuring device. (See reference 3, pp. 224 and 225.) The parallel feedback circuits can be passive or dynamic although passive networks are usually preferred for the sake of their simplicity.

Designing feedback networks to perform a particular control or stabilizing function or to modify the performance of the servo system in some particular way is not as straightforward and simple a procedure as was the derivation of passive lag or lead networks. Such a synthesis problem is most easily solved if the feedback network can be made substantially equivalent to a suitable cascaded network. As an example of this process, consider a servo system of the following form:

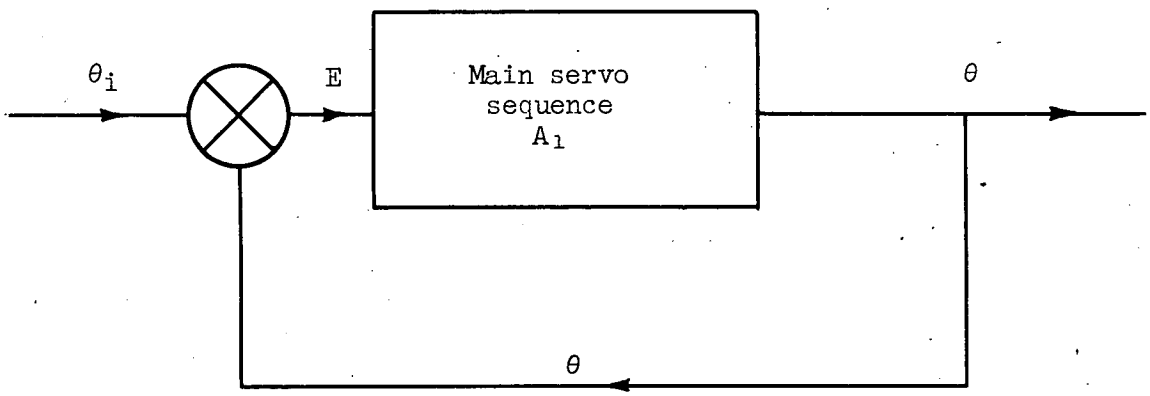

$$\frac{\theta}{E} = A_1 \tag{57}$$

$$\frac{\theta}{\theta_i} = \frac{A_1}{1+A_1} \tag{58}$$

If a parallel feedback loop is added in the following manner

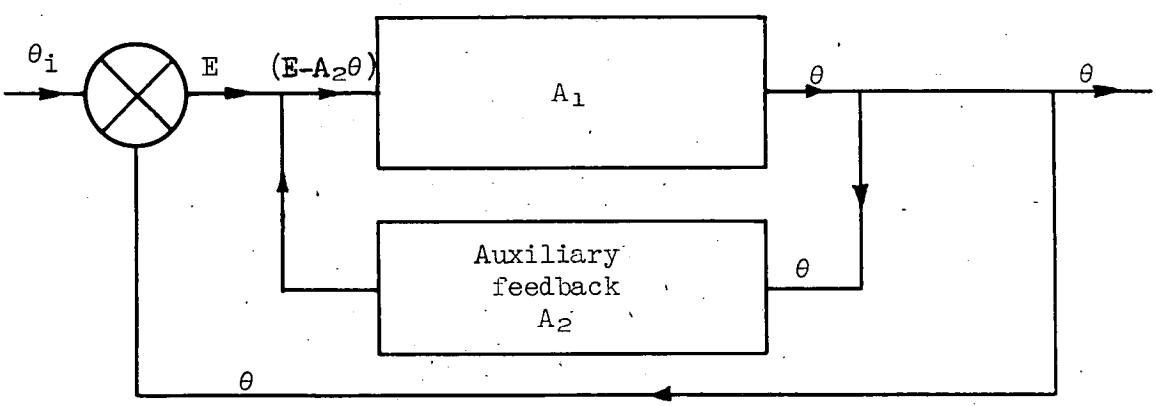

the open–loop and closed–loop responses become

$$\frac{\theta}{E} = \frac{A_1}{1+A_1A_2} \tag{59}$$

and

$$\frac{\theta}{\theta_i} = \frac{A_1}{1+A_1A_2+A_1} \tag{60}$$

Now it is desired to find the form of A_2 in terms of the equivalent modification to the basic loop by a cascaded network A_3 shown as follows:

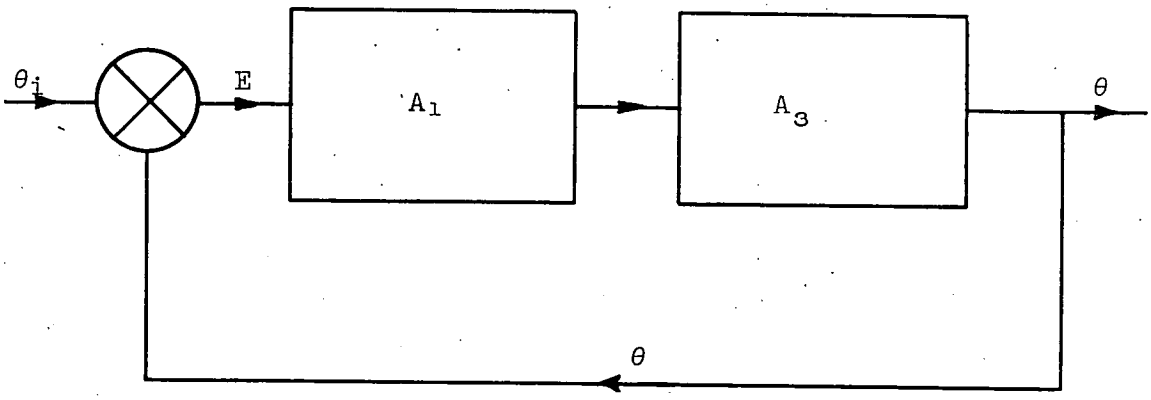

For the cascaded network the open– and closed–loop responses are

$$\frac{\theta}{E} = A_1A_3 \tag{61}$$

and

$$\frac{\theta}{\theta_i} = \frac{A_1A_3}{1+A_1A_3} \tag{62}$$

Thus to get A_2 in terms of A_3 the open–loop responses can be equated yielding

$$A_1A_3 = \frac{A_1}{1+A_1A_2} \tag{63}$$

or

$$A_2 = \frac{A_1 - A_1 A_3}{A_1^2 A_3} \tag{64}$$

$$A_2 = \frac{1}{A_1}\left(\frac{1}{A_3} - 1\right) \tag{65}$$

for the feedback form as a function of the equivalent passive network.

Whiteley in reference 20 says "Combinations of input networks and feedback networks can of course be used; practical considerations may well determine what role shall be assigned to the input and feedback meshes. Generally it would be preferable to assign the differentiating functions to the input network, and the integrating functions to the feedback."

A table of equivalent feedback and passive networks is given in reference 20.

THEORY

TECHNIQUES OF ANALYSIS

In describing the techniques of stability analysis that are commonly applied to servomechanisms, it is convenient to establish at the outset the number of degrees of freedom and degrees of control to be investigated and to classify the techniques accordingly. The number of degrees of freedom of a system is equal to the number of independent variables required to describe the behavior of the system. The number of degrees of control, on the other hand, is equal to the number of controlling elements that directly produce the output of the system. For instance, the conventional aircraft has three degrees of control provided by the rudder, elevator, and aileron.

The analysis of ordinary second-order seryomechanisms, as generally carried out in the existing literature on the subject, is usually concerned with one degree of freedom and one degree of control; whereas the conventional aircraft has six degrees of freedom and three degrees of control. Fortunately, however, the motion of the conventional aircraft can be separated into two categories: longitudinal motion and lateral motion, by virtue of the lateral symmetry of the aircraft. (See reference 35.) The longitudinal motion generally is considered to have three degrees of freedom, a longitudinal velocity, a vertical velocity, and an angular velocity of pitch about the lateral axis. In some instances it is convenient and permissible to assume the longitudinal velocity constant and consider only two degrees of freedom. In the longitudinal

case the elevator usually provides the only degree of control. The lateral motion has three degrees of freedom, a lateral or sideslipping velocity, an angular velocity of roll about the longitudinal axis, and an angular velocity of yaw about the vertical axis. There are usually two degrees of control available in the lateral case: An aileron produces rolling motion, and a rudder produces yawing motion. Analyses of the lateral motion of aircraft have been carried out based on the assumption that the rolling or yawing degree of freedom can be isolated, but in general all the lateral motions are coupled to the extent that separation is not advisable.

As far as the classification of stability analysis techniques for automatically controlled aircraft is concerned, the number of degrees of freedom will not be used directly inasmuch as the linearized differential-equation type of analysis treats the aircraft as a whole so that all three degrees of freedom in one category are stabilized simultaneously. Thus the discussion of the techniques of analysis will be divided into two parts: the first relating to one degree of control and the second to two degrees of control. As yet an aircraft with more than two degrees of control for one category of motion has not been produced.

In the development of guided missiles, many unconventional designs have been evolved, some of which have more and some less geometrical symmetry than the lateral symmetry characteristic of conventional aircraft. In such cases the degrees of freedom, their coupling, and their relationship to the degrees of control must be established before the analysis is attempted. It seems likely, however, that the classification of analysis techniques for such aircraft should be made on the basis of the numbers of degrees of control for any one category of motion.

The autopilot is not always introduced in the form of a differential equation based on its physical and dynamic characteristics. When satisfactory mathematical expressions for the autopilot are not available, many investigators make use of a lag factor or a lag operator to simulate the action of the autopilot. These artifices were discussed to some extent in the section on delay time. It should be pointed out, however, that the use of the lag operator makes the characteristic equation transcendental and consequently difficult to handle. Most of the techniques to be described can, in principle, handle the transcendental characteristic equation though it may not be practical to do so.

In appendix A sample calculations are presented for a high-subsonic-speed fighter type of aircraft that include an application of each of the following techniques.

One Degree of Control

In the consideration of automatic control it was only natural that the aeronautical engineer should attempt to perform an analysis by modifying the well-known set of simultaneous differential equations representing the motion of an airplane. (See references 35 and 36.) Two artifices were used. One was to include the autopilot action in the form of an added stability derivative (references 4 and 5) and the other was to include the autopilot action as part of a forcing function. (See reference 6.) These operations are equivalent. The obvious effect of adding the autopilot in this manner is to raise the order of the equations and thereby introduce new modes of motion of the aircraft.

A different approach is used by the servomechanism engineers, one that follows more or less the techniques of network or circuit analysis used to a great extent by the electrical engineers. In this approach the airplane is included as one member of the control loop and its dynamic response characteristics are lumped with those of the other components of the loop when the over-all response characteristics of the system are to be evaluated.

As should be expected these two approaches provide essentially the same initial equations representing the system though they may appear to be in radically different form. The characteristic equations obtainable by these methods for a given system should be identical. The technique discussed under the two separate headings either have been developed through the approach within which they are included or they are most frequently applied in that type of approach to the problem. Actually none of the techniques discussed is restricted to application by one approach or the other.

For systems having complicated feedback hookups between the components identified as the control unit and the aircraft, the resulting interaction of these components makes it impossible to treat them as cascaded elements. In such cases the combination of the autopilot equation with the equations of motion is complicated and results in a higher order system of equations than that obtained by the simple substitution permissible with cascaded elements. The transient-response analyses for such systems would probably be so involved as to make the procedures impracticable except where an analogue computer were available. The frequency-response techniques, on the other hand, can handle the feedback complications rather neatly. (See references 3 and 22.)

Autopilot as an added term in the equations of motion.- The types of analyses relating to this approach are essentially closed-loop analyses; that is, the motion of the aircraft-autopilot combination is analyzed with the system completely assembled and operative. Open-loop analyses, where the chain of operations is broken at some point in the

loop such as the output feedback to the sensing device, are used in the servomechanism type of analysis. The open-loop analyses lend themselves more readily to the synthesis of automatic control systems than do the closed-loop type. (See reference 34, page 518.)

The Routh or Hurwitz criterion:- The simplest and usually most rapid test of the stability of a dynamic system is to apply the Routh criterion. (See reference 37.) This criterion was put in the form of some easily written determinants by Hurwitz. It determines whether or not all of the roots of the characteristic equation have negative real parts, thus indicating whether or not subsidence of aperiodic modes and damping of the oscillatory modes exist.

The first step in the application of this technique is to write down the characteristic equation in the following form:

$$a_0 D^n + a_1 D^{n-1} + \ldots + a_n = 0 \tag{66}$$

where $a_0, a_1, \ldots, a_n$ are real constants and $a_0 > 0$. A necessary condition for all the roots of the above polynomial to have negative real parts is that all of the coefficients be positive.

According to the Hurwitz criterion, the following determinants must be positive for a stable system:

$$\textcircled{1}\quad a_1, \qquad \textcircled{2}\quad \begin{vmatrix} a_1 & a_3 \\ a_0 & a_2 \end{vmatrix}, \qquad \textcircled{3}\quad \begin{vmatrix} a_1 & a_3 & a_5 \\ a_0 & a_2 & a_4 \\ 0 & a_1 & a_3 \end{vmatrix}, \qquad \textcircled{4}\quad \begin{vmatrix} a_1 & a_3 & a_5 & a_7 \\ a_0 & a_2 & a_4 & a_6 \\ 0 & a_1 & a_3 & a_5 \\ 0 & a_0 & a_2 & a_4 \end{vmatrix}, \ldots$$

$$\textcircled{n-1}\quad \begin{vmatrix} a_1 & a_3 & a_5 & \ldots & 0 \\ a_0 & a_2 & a_4 & \ldots & 0 \\ 0 & a_1 & a_3 & \ldots & 0 \\ 0 & a_0 & a_2 & \ldots & 0 \\ 0 & 0 & a_1 & \ldots & 0 \\ \ldots & & \ldots & & a_n \\ 0 & 0 & 0 & \ldots & a_{n-3} a_{n-1} \end{vmatrix}, \qquad \textcircled{n}\quad \begin{vmatrix} a_1 & a_3 & a_5 & \ldots & 0 \\ a_0 & a_2 & a_4 & \ldots & 0 \\ 0 & a_1 & a_3 & \ldots & 0 \\ 0 & a_0 & a_2 & \ldots & 0 \\ 0 & 0 & a_1 & \ldots & 0 \\ \ldots & & \ldots & & 0 \\ 0 & 0 & 0 & \ldots & a_{n-2} a_n \end{vmatrix} \tag{67}$$

For a system of nth order there are n of these determinants. A derivation of the Hurwitz criterion is given in reference 38. In this reference, the criterion is stated in the following form:

"The roots of a polynomial with real coefficients have negative real parts if and only if the above determinants are positive, provided the coefficient a_0 is positive."

Routh, in reference 37, has derived this same criterion. The derivation used by Routh is based on the theorem of Sturm. (See reference 25.) It is somewhat easier to use the Hurwitz form, since it can be written conveniently in terms of the determinants. These criteria are applicable to polynomials of any order.

In most cases it is not necessary to compute all n of the Hurwitz determinants. Certain of them may be redundant. Consider, for instance, the case of a fourth-order polynomial. The Hurwitz determinants are

$$\left.\begin{aligned} (a_1 a_2 - a_0 a_3) &> 0 \qquad \text{(a)} \\ a_3 (a_1 a_2 - a_0 a_3) - a_1^2 a_4 &> 0 \qquad \text{(b)} \end{aligned}\right\} \tag{68}$$

Since all of the coefficients must be positive, it is clear that condition (68a) can be derived from condition (68b). The determinant (68a) is therefore superfluous. In the case of high-order polynomials, much labor can be saved if superfluous determinants can be found and eliminated.

Numerical evaluation of roots:- In general, the characteristic equations of linear systems are polynomial equations that can be solved by well-known methods. No details of such methods will be given here, but the Graeffe root squaring method (reference 24) and an iteration process which can be carried out to obtain any desired accuracy (reference 3, pp. 89-91) are recommended.

In the case of the transcendental characteristic equation, such as arises through the use of the lag operator, a graphical method of solution is recommended. Such a solution is given in reference 23.

Stability boundary charts:- Basically this method is an extension of the Routh or Hurwitz criterion method. If the influence of two variables on the stability of the motion is of interest, a plot can be made showing stability boundaries with these two variables as coordinates. An example describing the construction of such a chart is given in appendix A. The criterion for establishing the stability boundaries is the vanishing of the real parts of the roots of the characteristic equation.

Many different forms of such charts are employed in various fields of mechanics for the purpose of dynamic stability analysis. (See references 6, 26, 39, 40, 41, and 42.) For instance, if the values of the period and damping of the motion are of more interest than the absolute stability boundaries, lines of constant period and damping may be substituted for the stability boundaries or even superimposed on them if desired. The superposition of such lines and boundaries could be extended to cover even more criteria, but the chart would soon become a confusing network of lines.

Presumably any two independent variables of interest, usually relating to the physical properties of the system, such as stability derivatives, control gearings, moments of inertia, or a coefficient representing an algebraic combination of such parameters, can be used as the two coordinates. The stability characteristics for which the boundaries or lines of constant magnitude are constructed are usually related to the output or behavior of the system. These characteristics are often in the form of stability boundaries, damping and period constants, regions of optimum performance, etc.

Examples of such charts and methods of construction are given in references 6, 26, 38, 39, 40, 43, 44, and 45.

The theory underlying the construction of the stability boundary chart in particular, such as those constructed in appendix A, will now be discussed.

The characteristic equation of the system gives the roots for all the possible modes of motion. Routh (reference 37) and Hurwitz (reference 25) have determined that if the coefficient of the constant term of the characteristic equation is positive and if certain inequalities, developed by Routh as discriminants and also obtainable from the Hurwitz determinants, are satisfied, the real parts of all the roots will be negative and all modes of motion will be stable. (For proof of this see reference 25.) By equating this coefficient of the constant term to zero and by considering the inequalities to be equalities it is possible to establish the boundaries of a stable region in terms of any two independent variables involved in the coefficients of the characteristic equation. For any characteristic equation of polynomial form (for the case of transcendental characteristic equations, see reference 23) the number of determinants that exist is equal to n, the order of the equation. In general, then, it would seem that $n+1$ functions must be plotted to determine the region of stability. Actually only two functions must be plotted to determine the stability boundary. The locus of $a_n=0$, where a_n is the coefficient of the constant term, and the locus of the $n-1$ determinant give the complete boundary.

The locus of $a_n=0$ forms the boundary between stable and unstable aperiodic modes. This statement is based on the fact that in proceeding from a stable to an unstable condition the coefficient a_n, which is equal to the product of all the roots, is the first to change the sign if one real root does but it is not affected by changes in sign of the real parts of the complex roots.

The locus of the $n-1$ determinant forms the boundary between the stable and unstable oscillatory modes. This can be shown[2] by taking $i\omega$, the value of the root to the characteristic equation which would yield neutral oscillatory stability, and substituting it for D in the characteristic equation. Then separating the real and imaginary parts and applying Sylvester's elimination theorem (reference 25) ω can be eliminated from the separated equations leaving a determinant which is precisely the $n-1$ Hurwitz determinant.

A variation of this method of determining the oscillatory boundary has been developed which uses numerical values of ω in the characteristic equation rather than the locus of the $n-1$ Hurwitz determinant. This numerical process seems to be somewhat simpler and provides, additionally, the values of the frequencies at various points along the boundary. Details of the construction of such a boundary are given in references 38 and 46. The procedure, generally speaking, is to substitute the root $i\omega$ into the characteristic equation, set the real and imaginary parts equal to zero, and solve the resulting equations simultaneously (in terms of the two chosen independent variables) for a sufficient range of values of ω to define the oscillatory boundary. Application of this method for obtaining lines of constant damping and frequency is very easily carried out. Such procedures using the numerical value of ω are described in references 23 and 44.

Hence, to summarize the technique of plotting the stability boundaries, it can be said that the oscillatory mode part of the stability boundaries can be determined analytically from the $n-1$ Hurwitz determinant or numerically using $i\omega$ as a root of the characteristic equation. The portion of the boundary separating the regions of stable and unstable aperiodic modes is the locus of the coefficient of the zero-order term.

Transient response analysis:- If more information is desired than can be obtained from application of the first three techniques discussed, the transient response, that is, the time history of the motion following a disturbance, can be investigated. Various kinds of step and pulse inputs are ordinarily

[2]Proof communicated to the authors by Mr. Harry Greenberg.

applied in the calculations or experimentation used to obtain the transient response. The unit step function is perhaps the most commonly employed input. It is discussed at greater length in the section on evaluation of techniques. The transient response can be obtained analytically in at least four ways: (1) by the classical methods for solution of simultaneous differential equations, (2) by the operational method of solution, (3) step-by-step calculations, and (4) by the use of an analogue computer. For the first two of these methods the roots must be known. Expressions for the roots can easily be written down for most second-order systems. For higher-order systems it is usually more practical to solve for the roots numerically, which necessitates application of one of the techniques previously discussed. The roots need not be obtained in the application of the other two methods. They can be estimated roughly, however, from the resulting curves showing the time histories of the motion. If the frequency-response data are available the transient response can, of course, be obtained by Fourier synthesis.

The usual procedure followed in applying the first two methods is to formulate the characteristic equation, determine its roots, formulate the complementary and particular solutions, and insert the known boundary or initial conditions in order to evaluate the undetermined coefficients. Generally speaking, the character of the transient response is determined by the characteristics of the servomechanism itself and is independent of the form of input function. Thus the particular solutions are used solely to determine the steady-state error, even though various transients result from various input functions, and the transient response is obtained solely from the complementary solution.

The application of analogue computers to obtain the time-history solutions is a very powerful technique. A discussion of the details of using computers is not within the scope of the report. However, it is obvious that in order to carry out the calculations on such machines the numerical values of the constant coefficients and of the constants related to the initial and boundary conditions must be known. These analogue computers can be applied to solve linear systems of any order within the limits imposed by the size of the machine. Investigation of nonlinear systems is also possible.

Examples of transient solutions using the airplane stability equations, with the autopilot included or at least approximated by a lag factor, can be found in references 23, 36, and 37. For fourth-order systems representing an uncontrolled aircraft, references 47 and 48 give transient response solutions. In general, however, the automatically controlled systems of fourth or higher order are more readily analyzed using the

frequency response techniques to be described later. Consequently, most of the solutions for such systems appear in the frequency-response form.

Airplane response as a transfer function in the control loop.- The techniques to be discussed in this approach will be divided into two groups: the first representing transient response analyses; the other representing frequency response analyses. As was the case for the previously discussed techniques, those in the transient response group will be basically closed-loop analyses; whereas those in the frequency response group will be essentially open-loop analyses.

The results of the open-loop techniques are always capable of being interpreted in terms of the closed-loop performance, otherwise there would be no point in carrying out such analyses. The transient response is the most pertinent for judging the results of the analysis and, consequently, the open-loop and closed-loop frequency response techniques must provide results that can be related to the transient response.

Transient response:- As mentioned previously the initial equation or set of equations developed for the dynamic analyses of servomechanisms may have been obtained by either of two formally different approaches considered in this report, but the equations so derived will be independent of the approaches except possibly for their mathematical form. Thus it is reasonable that the discussion of the technique of transient response analysis under the aircraft equations of motion approach will, in general, be applicable to the servomechanism-loop approach also.

Examples of the use of transient response techniques in conjunction with this servomechanism-loop approach are of interest, however, and are worthy of mention. This technique is applied extensively in reference 13 to the second-order servomechanisms with various types of control and damping. Classical methods are used therein to solve the differential equations encountered because, as the authors stated, in contrast to the more advanced process of operational calculus these methods more readily afforded an understanding of the physical phenomena involved. Examples of both the classical and operational solutions for second-order servomechanisms are given in reference 3. Reference 20 applies the operational methods and gives a "standard form" criterion for use in analyzing and modifying the stability and performance of the system. These criteria are established for systems of the order of two to six and are based on an initial overshoot of from 10 to 20 percent. A table of characteristic equations with numerical values of the coefficients is given. The equations listed correspond to various percentages of overshoot and are intended for use as a basis of comparison,

that is, a standard. The method, however, is not necessarily restricted to those standard forms chosen in reference 20. If different performance characteristics are required the standard forms can be suitably altered. A third-order system is analyzed by classical methods in reference 41 and by operational transient-response methods in reference 26.

With the possible exception of the "standard form" technique, however, the fourth and higher order systems probably can be more readily analyzed by the frequency-response techniques to be discussed.

Frequency response:- Recently the method of frequency-response analysis has become a very popular method for studying servomechanisms. Basically this method is a study of the effects of a sinusoidal input of various frequencies on the amplitude ratio and phase characteristics between the input and the response, or output, which is sinusoidal also. The method is applicable to both experimental and analytical techniques. This versatility, plus the fact that it is a relatively fast method for purposes of synthesis, if not analysis, accounts in part for its popularity.

A good introduction to this method is given in reference 3, pages 92-96, which includes discussions of certain general relationships between transient and frequency behavior and a treatment of the preparation of system data into a form convenient for analysis and synthesis by frequency-response techniques. A short discussion of the various techniques is given in the following paragraphs.

(1) Resonance plots

(a) General applications

If the sinusoidal input is written as

$$\theta_i = R_1 \cos \omega t \tag{69}$$

the resulting output will be of the form

$$\theta = R_2 \cos (\omega t + \epsilon) \tag{70}$$

where ϵ is the phase angle between the output and input. These expressions may be considered as the real parts of

$$\theta_i = R_1 e^{i\omega t} \tag{71}$$

and

$$\theta = R_2 e^{i(\omega t + \epsilon)} \tag{72}$$

by virtue of the well-known expansion of a complex exponential function into sine and cosine components

$$e^{i\omega t} = \cos \omega t + i \sin \omega t \tag{73}$$

With the input and output expressions written in this exponential notation it is easy to obtain a form for the closed loop transfer function of the system. Thus

$$\frac{\theta}{\theta_i} = \frac{R_2 e^{i(\omega t + \epsilon)}}{R_1 e^{i\omega t}} \tag{74}$$

or

$$\frac{\theta}{\theta_i} = \frac{R_2}{R_1} e^{i\epsilon} \tag{75}$$

where $\frac{R_2}{R_1}$ is the amplitude ratio.

Plots of the amplitude ratio of the output to input $\frac{R_2}{R_1}$ or $\left|\frac{\theta}{\theta_i}\right|$ and of the phase angle ϵ against frequency ω give the basic closed-loop form for the frequency-response characteristics of a system and are often called resonance plots. Some typical resonance curves for servomechanisms are given below:

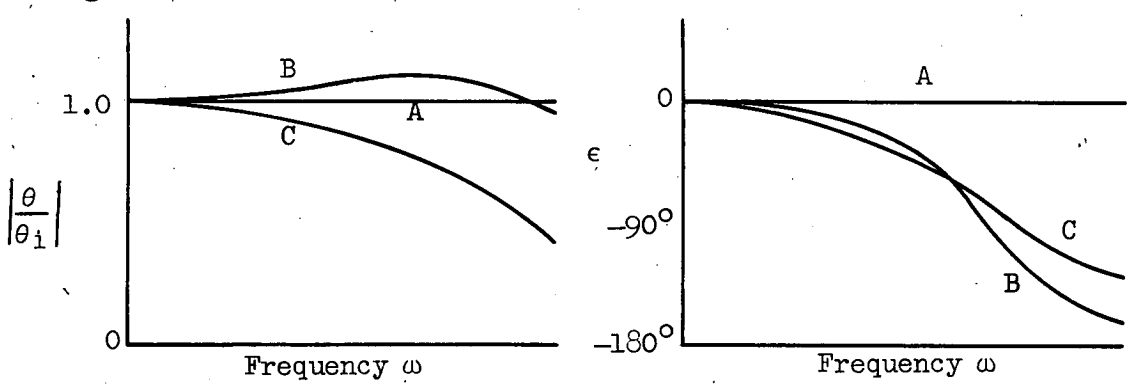

The frequency-response characteristics are most readily related to the transient response when presented in this form. It is not convenient to determine quantitative stability data such as critical control gearings, etc., however, from these

closed-loop resonance plots. It is possible, though, to determine the existence of a steady-state error from the shape of the amplitude-ratio curve at $\omega = 0$. For a displacement type of input such as a step function there is no steady error if the frequency-response ratio of the amplitudes $\frac{\theta}{\theta_i}(i\omega)$ is 1.0 and the phase angle is zero at $\omega = 0$. For zero steady-state error with constant speed or constant acceleration inputs, there is the further requirement that the first and second derivatives, respectively, of the amplitude-ratio curve and the phase-angle curve must be zero at zero frequency.

Generally speaking, the evaluation of the behavior of closed-loop systems by frequency-response methods starts with the determination of the open-loop response (discussed later) which is then related to the closed-loop resonance plots and to the transient response through the implicit correlations that exist between these techniques.

The relationship between the sinusoidal behavior as indicated on the resonance plots and transient behavior is discussed at some length in reference 3. (See pages 104-106.) To summarize these relationships briefly, consider the following figure which has typical curves for the closed-loop transient response and the closed-loop frequency response for several values of the damping ratio ζ. These curves are representative of a second-order servomechanism, but they are sufficiently general for illustrative purposes.

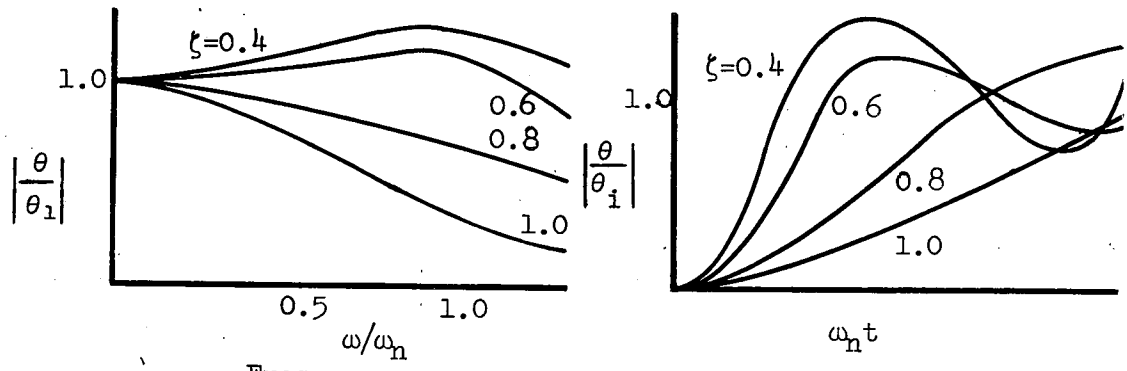

The peak amplitudes on the frequency-response curves indicate resonance and the frequency at resonance for any given damping ratio ζ is a fairly good quantitative indication of the frequency of the transient oscillation. Also the magnitude of the peaks can be taken as a good indication of the relative

damping of the transient response. For damping ratios of approximately 0.6 or less the peak overshoots for corresponding curves can be fairly well correlated quantitatively. The speed of response to transient signals can be predicted from the frequency-response curves since a high resonant frequency would indicate a high natural frequency and, consequently, a high speed of response to an input signal. Thus the frequency-response curve for $\zeta = 0.4$ has its peak at the highest value of ω/ω_n of the curves shown and on the transient-response plot this value of ζ is seen to give the quickest response. The transient curve for $\zeta = 0.4$ also shows the greatest overshoot as could be anticipated from the relatively large magnitude of the peak on the $\zeta = 0.4$ curve of the frequency response. For systems of order higher than the second it is possible that a high peak on the frequency-response curve will indicate a small oscillation in the transient-response curve before reaching θ_i rather than an overshoot of θ_i. It is usually possible to predict an overdamped transient response if the curve for the frequency response has no peak. For the cases illustrated, however, the curves for values of ζ between 0.707 and 1.0, show no peak on the frequency-response curves but the transient curves show a slightly underdamped, rather than overdamped, response.

The phase shift between ϑ and θ_i is also an important characteristic and the magnitudes of the phase shifts that are shown on the frequency-response curves can be used to explain certain characteristics of the transient response. Limits are often set on these magnitudes in order to provide for suitable transient-response characteristics.

(b) Greenberg's Method

By plotting the resonance curves for the aircraft and autopilot separately, Greenberg (reference 7) was able to find the critical control gearing for a system having all the other parameters fixed. The critical control gearing k_{cr} is specified as the value of the gearing between the autopilot and the aircraft control surface that provides neutral oscillatory stability (hunting oscillations) at the critical frequency. The critical frequency is the frequency at which the total phase lag of the aircraft-autopilot combination is either 0° or 180° (depending on the definitions of the signs of the phase angles). The procedure for finding the critical control gearing corresponds to the method of finding the gain margin of the system which will be described later.

The same plotting technique is used in reference 21 by Jones and Sternfield, but the stability condition applied in this case was, essentially, that the total phase lag shall be less than 180° when the product of the amplitudes is unity.

This procedure corresponds to the method of determining the phase margin for the system as described later.

(2) Polar plots.- The use of polar plots showing the magnitudes and phase angles of the frequency-response characteristics by curves tracing the vector loci are possibly the most frequently used type of diagrams in automatic-control-system analysis at the present time. These loci show the variations of the vector quantities such as $\frac{\theta}{\theta_i}$, $\frac{\theta}{E}$ or $\frac{E}{\theta}$ over the frequency range $0 < \omega < \infty$ as continuous curves plotted in the complex plane. Of the various vector quantities that could be plotted the vector locus of $\frac{\theta}{E}$, more commonly known as the transfer function locus, is the most useful. The quantity $\frac{\theta}{E}$ represents the open-loop transfer function of the system.

(a) Open-loop transfer locus plots (Nyquist diagrams)

The open-loop transfer locus $\frac{\theta}{E}$ is related to the overall frequency-response characteristic of the closed-loop system $\frac{\theta}{\theta_i}$ in the following manner:

$$\frac{\theta}{\theta_i} = \frac{\theta/E}{1 + \theta/E} \tag{76}$$

The open-loop response is often preferred to the closed-loop response in both analysis and synthesis because it is more easily obtained and is more useful in studying the effects of system parameter changes on the closed-loop stability characteristics. The closed-loop response can be obtained readily from the open-loop response curves by a simple graphical relationship that is demonstrated on the sketch of the open-loop transfer locus plot.

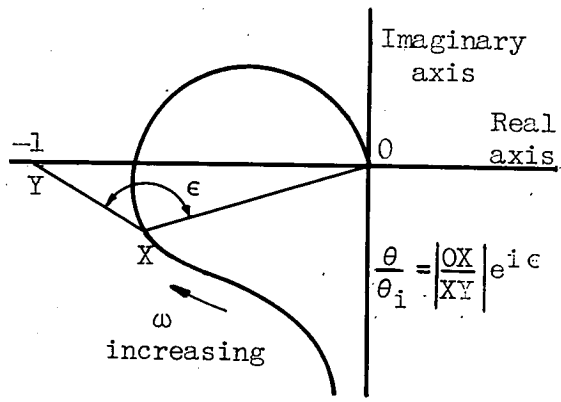

In using this type of plot to determine the behavior of a system it is convenient to consider three separate regions of the locus and inspect them individually. These regions are the low-frequency region, the region near the point $-1 + 0i$, and the high-frequency region near the origin.

From the low-frequency region it can be determined whether the system is a zero-position error, a zero-velocity error, or a

zero-acceleration-error servomechanism according to the axis the locus approaches at zero frequency. These classifications are related to the number of integrations in the loop and their significance is discussed at some length in references 3 (pages 166-168) and 20.

The region near the point $-1 + 0i$ relates to the stability of the system and it is by far the most important region. The high-frequency region may possibly yield information regarding the over-all complexity of the physical system.

From the $-1 + 0i$ region it can be determined whether or not the system is stable by use of the Nyquist criterion, what the gain and phase margins are, and some indication of the magnitude of the peak response, which relates to the maximum overshoot, and of the resonant frequency.

The Nyquist criterion can be best explained by relating it to the roots of the characteristic equation $1 + \theta/E = 0$. It was stated previously that if any of the real parts of the roots of this equation were positive the system was unstable. This is equivalent to saying that all the roots, when plotted on the complex p plane, must lie to the left of the imaginary axis for stability. Roots lying on the axis give neutral stability and roots lying to the right of the axis indicate divergence of the motion. The Nyquist criterion, however, relates to the frequency-response plot of the transfer locus on the θ/E plane. The relationship between the transfer locus plot and the location of the roots on the p plane is involved with the mapping of regions from one plane to the other. It can be shown that the imaginary axis of the p plane, defining the boundary between the stable and unstable roots, maps as the transfer locus on the θ/E plane. Furthermore, as shown in references 3, 11, 13, and 49, if the transfer locus encloses the point $-1 + 0i$ there are roots on the right-hand side of the imaginary axis of the p plane and the system is unstable. If the transfer locus passes through the point $-1 + 0i$ neutral stability is indicated. In the manner just stated, this criterion is rather vague and applies only to simple systems having no multiple loops. A more specific "rule of thumb" for the stability of single-loop systems is given in reference 13. The rule says, in effect, that, if a line originally coinciding with the imaginary axis on the θ/E plane can be fitted to the transfer locus through a clockwise rotation and a suitable distortion without sweeping over the $-1 + 0i$ point, the system is stable. Another quick test for single-loop systems is to trace along the locus in the direction of increasing frequency and if the $-1 + 0i$ point lies to the left of the curve as the tracing proceeds to the origin the system is stable.

These simple tests may need modification when the system is complicated by multiple loops. In general, the Nyquist criterion requires that for stable systems, that is, systems having no positive real parts in the roots of the characteristic equation, the number of times that the locus encircles the $-1 + 0i$ point shall be equal to the number of poles of the transfer function. Such poles may exist in a complicated system inasmuch as one of the subsidiary loops may be unstable by itself, while the closed-loop system is stable. A proof of the Nyquist criterion covering multiple-loop systems is given in reference 11 and references 3 and 49 give an extensive treatment of the subject.

The phase and gain margins give some idea of the degree of stability, although the degree of stability can be found only by knowing the values of the roots of the characteristic equation. The gain margin, designated as G_m in the following figure, is defined as the reciprocal of the magnitude of the transfer-function vector at the phase angle of -180°. Defined in this manner the gain margin can be interpreted easily as decibels below the zero decibel level on the logarithmic plots to be discussed. Another definition of gain margin, namely, the difference between the magnitude of the transfer function and the $-1 + 0i$ point at a phase angle of -180°, has also been used, but it is not a practical concept.

In cases where the transfer locus crosses the negative real axis more than once there can be as many values of gain margin as there are crossings. This situation occurs in the illustrative example presented in appendix A. The phase margin, designated as γ_m in the following figure, represents the amount by which the phase of the transfer function falls short of being -180° when the amplitude of the transfer function vector is 1.

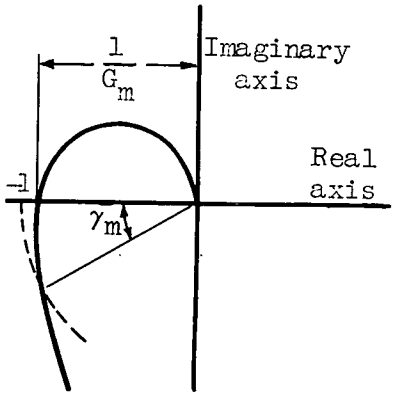

An indication of the magnitude of the peak response and of the resonant frequency can be obtained from the transfer locus plots by superimposing contour lines of constant magnitude and constant phase for the θ/θ_i vector. Examples of such contour lines designated by M and N, respectively, are shown on the following chart:

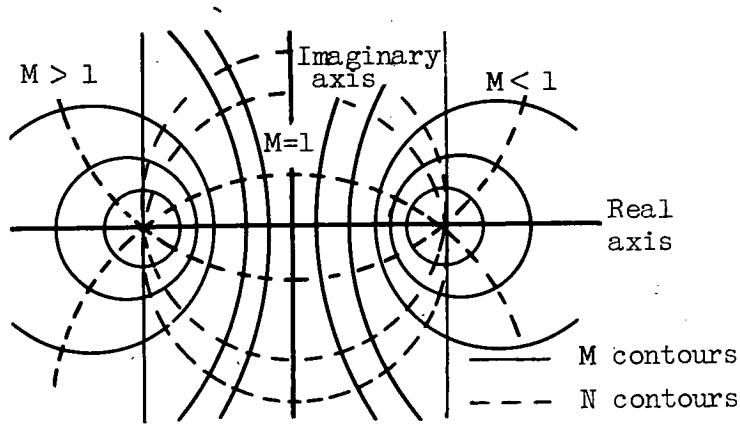

It is obvious that by use of these M–N contours it is possible to mark off zones on the plot through which the transfer locus must pass in order that the magnitude and phase lag of θ/θ_i shall fall within prescribed bounds. Furthermore, the M circle which is tangent to the transfer locus gives the peak magnitude of the θ/θ_i response and the frequency at which this occurs will be the resonant frequency.

The most obvious application of these contours is in the reshaping of the locus to obtain better response characteristics. By vectorial addition on the locus plot the effect of inserting a new component in the loop can be determined fairly easily. The effects of increasing the gain of the system are quite readily observed on the polar plots.

(b) The inverse open–loop transfer locus and others.

Other polar plots of various vector quantities relating to the open–loop or closed–loop response are sometimes employed. The inverse transfer locus E/θ and the closed–loop–system response locus θ/θ_i are seen fairly often.

The inverse transfer locus shown below has one advantage in that the θ_i/θ response can be determined by simple visual inspection rather than by graphical construction. (See references 3, 22, and 32.) The use of one or the other of these two locus plots, however, is largely a matter of experience and personal preference.

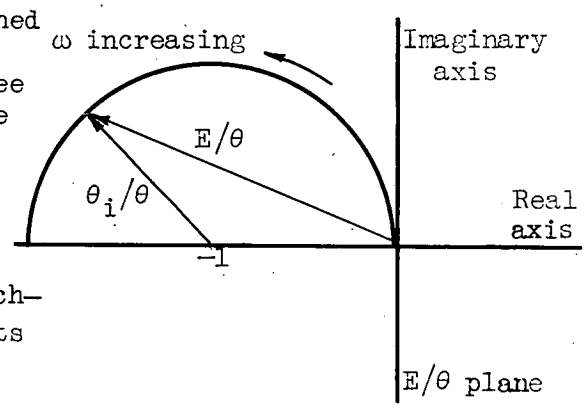

(3) Logarithmic plots.– The technique of employing logarithmic plots of the amplitude ratio and phase shift against frequency is useful

primarily in synthesis, that is, in the prediction of the effects of adding corrective networks to the system. In this method the phase angle and the log of the amplitude ratio of the transfer function (usually given in decibels, db, which is defined as 20 times the common logarithm of the amplitude ratio) are plotted against the log of the frequency as shown in the following sketch:

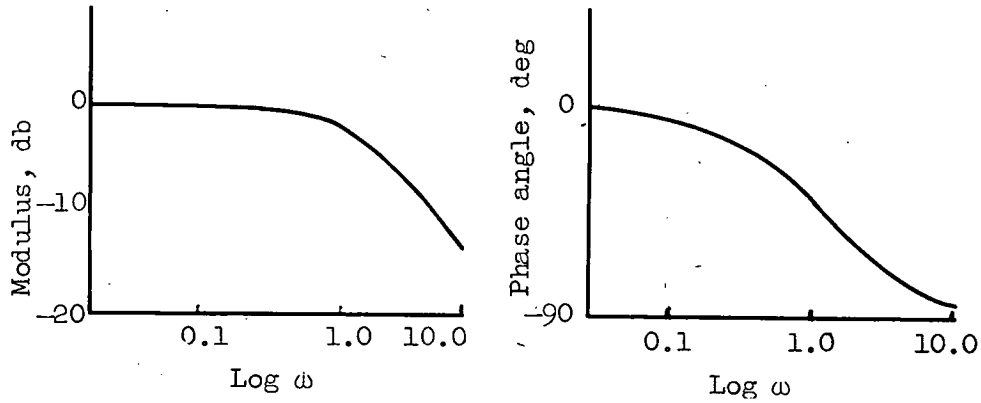

The use of logarithms makes it possible to add ordinates directly rather than vectorially when altering the response curve to take into account the addition of some component to the loop. Furthermore, the log moduli of first-order components of the loop plot either as straight lines or approximately as straight-line segments. Second-order components can be handled conveniently using previously prepared families of logarithmic curves with the damping factor as the parameter. Thus servomechanisms made up of first- or second-order components in cascade can be rather quickly plotted on the log modulus graphs. There is also a special way of handling the phase-angle plots that permits rapid manipulation of these curves. Very good descriptions of the logarithmic plot techniques are given in references 3 and 11.

In order to relate the open-loop characteristics of the transfer function to the closed-loop characteristics a cross plot can be made with the magnitude of the transfer function in decibels plotted against the phase angle for various frequencies. On this type of plot the M and N contour lines can be superimposed to determine the closed-loop characteristics. A sketch of this type of plot is given.

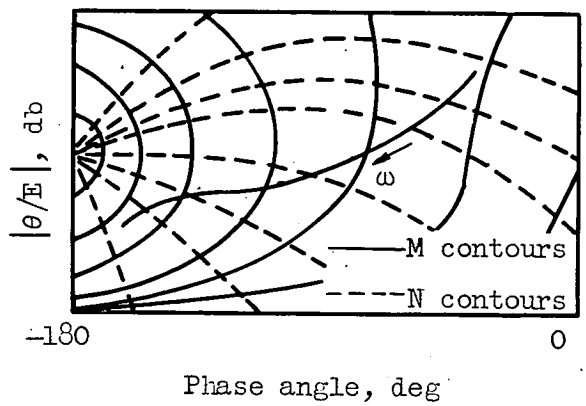

The point of zero decibels magnitude and -180° phase shift now becomes the instability point to be avoided.

The manner in which the gain must be changed to stay within a certain limit of $\left|\frac{\theta}{\theta_i}\right|_{max}$ at resonant frequency and the effects of adding components and changing the transfer-function locus shape can be determined on these logarithmic-coordinate plots in much the same manner that it was on the polar plot. The gain margin and phase margin also can be determined from these plots.

This method of analysis can be applied to systems having higher than second-order components as is demonstrated in appendix A; but the facility of the method is definitely reduced unless the system can be broken down into first- and second-order elements. In the case of the longitudinal motion of an aircraft the fourth-order equation representing the aircraft can be approximately factored as shown in appendix A. It is relatively easy to plot the quadratic factors and the example in appendix A shows that the results for the approximate factorization are not appreciably different from the curves for the quartic equation.

Two Degrees of Control

As indicated previously the airplane, considered kinematically, is a slightly more complex object to control than those considered in the ordinary treatises on servomechanisms. Having six degrees of freedom, the airplane usually requires as many as three degrees of control to get satisfactory stability and performance. It is a well-established fact, however, that the motion of the conventional airplane can be divided into two categories, longitudinal and lateral, each with three degrees of freedom. The longitudinal motion, usually controlled by the elevator only, has been covered in the previously discussed analyses pertaining to one degree of control. The lateral motion, on the other hand, is usually controlled by some combination of the aileron and rudder deflections. In the lateral case it is theoretically possible to make the deflections of both the aileron and the rudder functions of the displacements and velocities of roll and yaw, of the sideslip velocity, of the accelerations in roll and yaw, etc. Practical limitations, however, have so far restricted the analysis of lateral controls to two cases: (1) the so-called "cross-coupled" control (see reference 6) where the aileron and the rudder deflections are proportional to both displacement in bank and displacement in yaw (i.e., azimuth); and (2) the so-called "simple" control where the aileron deflection is proportional to displacement in bank and the rudder deflection is proportional to displacement in yaw (azimuth). Even in the last and most

simplified case, however, the analysis of the stability of the over-all lateral motion is greatly complicated due to the inherent coupling of the three individual lateral motions. The existing theoretical treatments of the two degrees of control arrangement are restricted to the latter case except for one brief treatment of cross-coupled control in reference 6.

Autopilot as an added term in the equations of motion:- As in the case of one degree of control, this approach leads to the closed-loop type of analysis.

Imlay's method.- In this method the autopilot is introduced through a forcing function added to the equations of motion of the airplane. In the particular application of this method by Imlay, reference 6, an approximate delay time expression is used to simulate the action of the autopilot. This artifice is not essential to the method and with the now existing knowledge of servo systems it is possible to write expressions that will give a good linear representation of their action.

Imlay considered the "cross-coupled" control briefly. In spite of the complexity of the expressions resulting from this type of control he was able to determine the control gearings to give the special case of equal roots. This solution corresponds to motion with no oscillatory components and having all the aperiodic modes equally damped. It was a satisfactory solution at the lift coefficient investigated but the same control gearings caused instability at higher lift coefficients. Further study of this control was dropped in favor of a more complete investigation of the simple control.

Simple control was investigated by the technique of developing stability boundary charts. The two variable parameters upon which the chart was based were the two control gearings, $\frac{\partial \delta_r}{\partial \psi}$ for the rudder, and $\frac{\partial \delta_a}{\partial \varphi}$ for the aileron. This technique involves the establishment of criteria in the form of algebraic inequalities by the Routh or Hurwitz methods and the subsequent study of these inequalities in terms of the two variable parameters in order to be able to chart the stability boundaries. For a system represented by a fourth degree equation, such as the airplane uncontrolled, this procedure is fairly long and tedious. For systems involving higher order equations, such as an aircraft-autopilot combination yielding a sixth-order equation, the procedure may become so laborious as to be prohibitive.

Airplane response as a transfer function in the control loop:- In addition to Greenberg's method discussed below, the open-loop polar-plot technique (Nyquist diagrams) could undoubtedly be applied to the analysis of aircraft-autopilot systems having two degrees of control.

A system using this type of control falls into the category of multiple-loop systems which the Nyquist diagram technique can handle, in principle, no matter how complicated the system might be. The details of the application of this technique to the particular case of an aircraft-autopilot combination having two degrees of control are not available, however, at the present time.

Simplified methods of handling two degrees of control are desirable and perhaps could be developed by neglecting the coupling of the control effects as a first approximation or by the use of some similar artifice. There is also room for the development and presentation of more powerful analytical techniques, especially if the time required for their application can be held within reasonable bounds. It is possible, however, that the use of a simulator, such as an analogue computer, will always provide the best combination of simplicity and versatility for the analysis of systems having two degrees of control.

Greenberg's method.– This method (reference 50) is an application of the frequency-response type of analysis to the calculation of the stability of an airplane with two independent autopilots or, in Imlay's terminology, with "simple" control. It is an extension of Greenberg's earlier paper, reference 7, on the application of frequency-response methods to obtain the critical control gearing for one degree of control.

The method makes use of a type of resonance plot similar to that found in reference 7. The calculations involved are, naturally, much longer and more tedious than those for one degree of control. Basically the method gives only discrete points of the stability boundary using the control gearings as the variables, but it could be applied a number of times in order to get a fairly accurate layout of the boundary. Whether this would be more or less time consuming than Imlay's method is questionable.

EVALUATION OF TECHNIQUES OF ANALYSIS

Although no specific performance or stability standards are to be set up in this report, an attempt will be made in the present section to evaluate the techniques of analysis on the basis of their usefulness in providing information about the parameters affecting performance and stability. In the discussion of fundamental analytical concepts the four parameters chosen for consideration were (1) speed of response; (2) steady state error; (3) time to damp; and (4) amount of initial overshoot. It was pointed out that these items could be reasonably, though not absolutely, paired off under the headings of control and damping parameters. Furthermore, the damping and control can be rationally paired off with stability and performance, respectively, although, here again, the division is not absolute. Thus the following diagrammatical outline is developed relating the four parameters to the behavior of the system in terms of performance and stability:

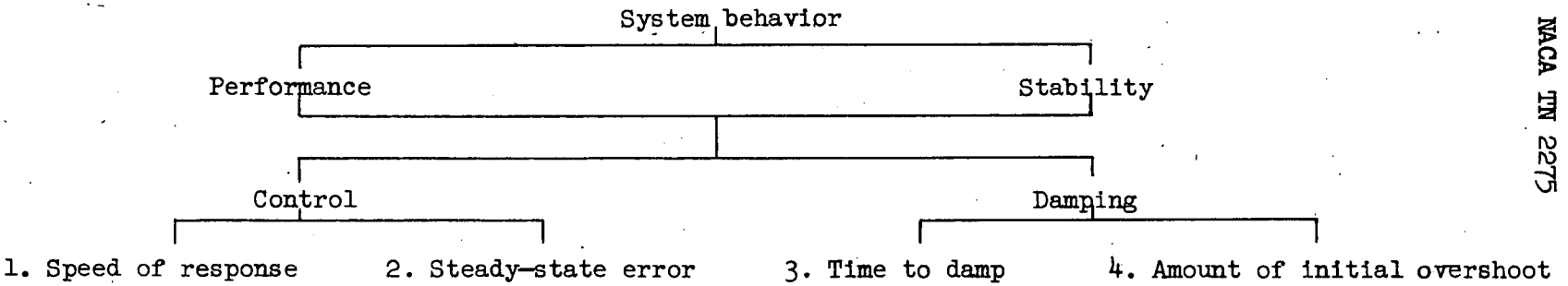

The techniques of analysis can be outlined in the following manner:

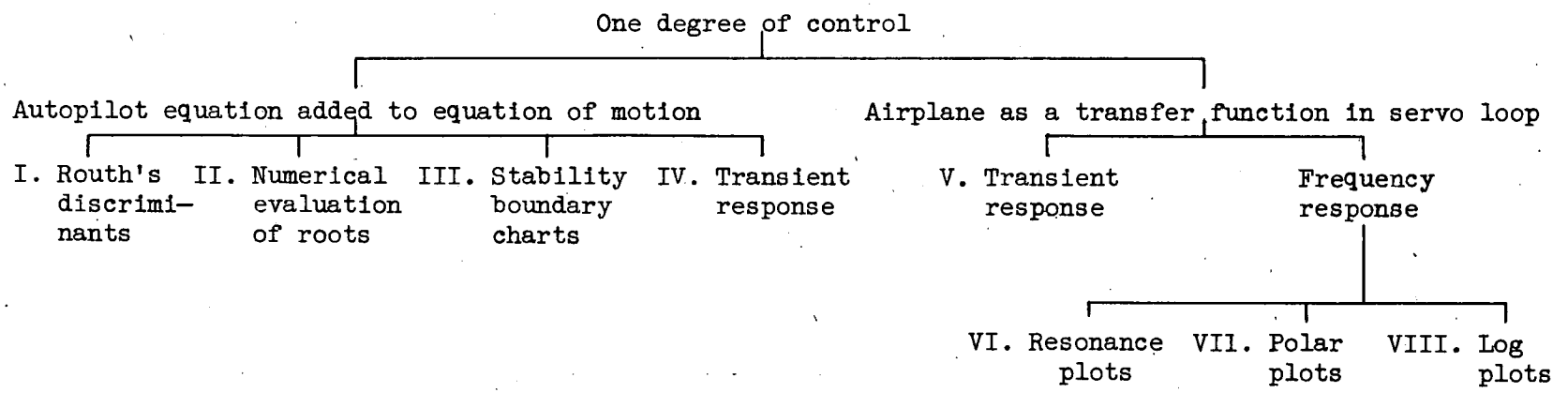

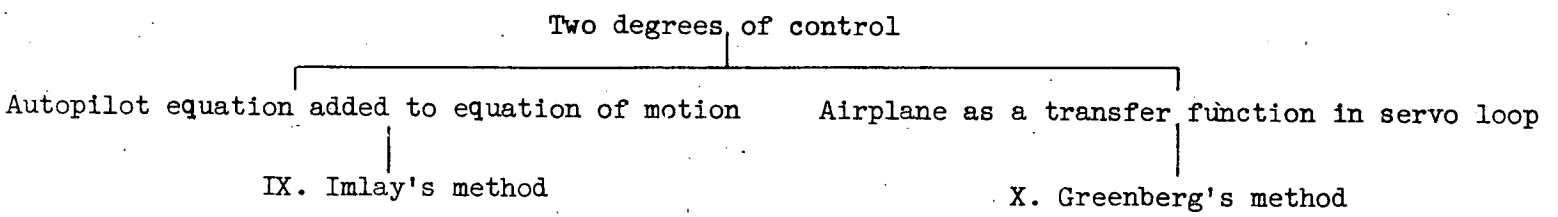

I. Routh's Discriminant

This technique merely provides the answer as to whether stability does or does not exist. Thus it is only useful for obtaining qualitatively information relating to parameter 3.

II. Numerical Evaluation of Roots

The numerical evaluation of the roots provides information regarding the time to damp (parameter 3). Furthermore from the complex roots, the natural frequency of the oscillatory modes can be calculated and used to estimate roughly the speed of response (parameter 1).

III. Stability Boundary Charts

Basically the use of stability boundary charts permits combinations of various values of two independent variables to be charted into regions of stability or instability. In this respect it is slightly more flexible than technique I but gives essentially the same information. It is possible, however, to superimpose a lattice of lines of constant damping and period on such a chart. With this supplementary feature, it is possible to use the charts to determine quantitatively the time to damp and to estimate the speed of response as can be done using technique II.

IV. and V. Transient Response

From a graph showing the transient response, information concerning all four parameters can be obtained. The determination of the transient response by theoretical procedures, however, such as described in the discussion of the techniques of analysis, is usually restricted to certain standard types of input signal. The information obtained, consequently, might seem to be relevant only for operating conditions under which such signals or similar disturbances occurred. Experience has shown, however, that this procedure is a satisfactory one and can be used rationally for analysis and synthesis of servomechanisms. The response to a step input, for instance, can be used to evaluate the response to random signals or disturbances, or it can be applied, using mathematical techniques, to determine the system response to any arbitrary command.

If the transient response of the servomechanism can be measured under actual operating conditions or by simulators, a rigorous analysis of the system behavior can be made.

In addition to analyzing the transient response to a prescribed input or to a random input corresponding to actual operating conditions, there is the possibility of using the frequency-response analyses to be evaluated subsequently. In regard to the relative merits of the two types of analyses, reference 3 presents the following views, ".... that dynamic stability specifications are more easily based on transients following a sudden disturbance than on the behavior following sinusoidal

disturbance of varying frequency. However, the design of conventional systems to fulfill the majority of performance specifications is more easily accomplished by studying the response to a sinusoidal disturbance of varying frequency."

A particular technique involving the transient response and yet not requiring the time history of the behavior of the mechanism to be ascertained is worthy of mention. Whiteley in reference 20 uses "standard forms" of the characteristic equations to specify the suitability of the system behavior. The standard forms are based on a given percentage of initial overshoot, a nonoscillatory response, and a satisfactory speed of response. Thus by comparing the numerical constants of the characteristic equation for any servomechanism with one of Whiteley's standard forms, some idea of changes in the constants, and thus in the system parameters required to match the performance of the servomechanism with that corresponding to the standard forms, can be obtained.

VI. Resonance Plots

The resonance plots are usually employed to show the closed-loop frequency-response characteristics of a system. Information about the parameters under consideration, however, can be obtained only indirectly from these plots. The speed of response (parameter 1), for instance, can be estimated from the location of the resonant peak through the relationship between resonant frequency and the natural frequency which has a correspondence to the speed of response. The existence of a steady-state error (parameter 2) is indicated in this type of plot. The time to damp (parameter 3) and the amount of initial overshoot (parameter 4) can be related to the magnitude of the peak response as described in the discussion of this technique of analysis.

Methods using open-loop resonance plots, as done in references 7 and 21, can be applied to determine gain or phase margins or related parameters such as the critical control gearing.

VII. Polar Plots

The Nyquist diagram (open-loop polar plot) is by far the most commonly employed type of polar plot. It is fairly convenient to construct and easily read by experienced analysts. Here again the information regarding the four behavior parameters is obtained indirectly through the correspondence of certain characteristics of the transfer locus with the transient behavior. The time to damp in terms of a value for a damping factor is not obtainable. However, quantitative information regarding the stability can be obtained in terms of gain or phase margins or critical control gearings.

Contour lines of constant magnitude can be superimposed on the Nyquist diagrams to determine the control gearing required for any desired peak response of the system. The peak response can be related

to the damping and initial overshoot as previously mentioned. If the frequency spectrum is indicated on the locus, the resonant peak location will give some indication of the resonant frequency which relates to the natural frequency and speed of response.

The type of steady-state error can be estimated from the position of the asymptote of the transfer locus (or the mathematical form of the transfer function) at low frequencies. (See reference 1.) The type of steady-state error is often used as a means of classifying the servomechanism as a zero-position error, zero-velocity error, or a zero-acceleration-error system. (See references 3 and 20.) If a steady-state error exists, its magnitude can be determined best from the differential equation for the system.

VIII. Logarithmic Plots

Essentially, everything that was said with regard to the information obtainable from the polar-plot technique applies to this technique as well. By enabling operations that required multiplication or division in the polar-plot technique to be performed by addition or subtraction and by breaking the transfer loci down into combinations of first- and second-order components that can be easily remembered and readily applied, the logarithmic-plot technique was developed as the most rapid procedure for analysis and synthesis. For synthesis there cannot be much argument about the improvement in facility gained by the use of logarithmic coordinates. From the analysis standpoint, the advantage of using logarithmic charts is questionable. The open-loop transfer loci on the log amplitude versus log frequency and phase angle versus log frequency charts give data which, unlike the polar plots, cannot be readily interpreted in terms of the closed-loop response for purposes of analysis. Therefore, another chart having an ordinate scale of the log modulus and an abcissa scale of the phase angle must be prepared. The transfer locus is then plotted and contours of constant amplitude and phase angle of the closed-loop response can be superimposed. From this type of log plot most of the stability and performance characteristics can be determined.

IX. Imlay's Method

This technique (reference 6) for analyzing two-control systems is a combination of the numerical root solving technique and the stability boundary chart technique previously discussed. The independent variables selected for the latter are usually the control gearings.

X. Greenberg's Method

This technique (reference 50) is an extension of the open-loop resonance plot technique to the two-control case. It is used mainly for determining critical control gearings and it is the only frequency-response technique reported that, at present, has been applied to an aircraft having two degrees of control.

CONCLUDING REMARKS

The commonly employed techniques of stability analysis for automatically controlled aircraft have been discussed and classified in this report. The survey was limited to continuous control and to linear closed-loop systems. A discussion of the components and concepts associated with controlled aircraft and similar servomechanisms was included in order that the descriptions of techniques could be made fairly concise. An attempt was made to evaluate the techniques on the basis of the kind and amount of information desirable. Furthermore, an illustrative example is included in an appendix that presents calculations for a typical case using all of the techniques discussed.

No attempt was made to establish satisfactory standards for the performance and stability of automatically controlled aircraft. Four performance and stability parameters were selected, however, to be used as a basis for comparison and evaluation of techniques. These parameters were: (1) speed of response, (2) steady-state error, (3) time to damp, and (4) amount of initial overshoot.

The evaluation of the techniques can be summarized briefly as follows: For a simple determination of system stability or instability, application of the Routh discriminants (or Hurwitz determinants) is a sufficient and relatively fast procedure. If knowledge of the rate of damping is desired in addition to the determination of stability, the roots of the characteristic equation can be calculated. When the design of the system is set except for the value of the control gearing to be used, application of the critical control-gearing method or the polar plot of the open-loop transfer locus is recommended. If the system is likely to require more adjustment than the setting of the control-gearing value, then the polar plot is the more suitable of the two methods. Use of the technique of plotting the transfer locus using logarithmic coordinates seems advisable only when a full-scale synthesis job is required. Analyses sufficiently complicated to warrant application of an elaborate technique, however, are more simply and intuitively handled by the polar plots. For the simultaneous investigation of two independent design variables with regard to system stability, the stability boundary charts are recommended. For the most elaborate and detailed analysis, that is, one that will provide information about each of the stability and performance parameters considered, a transient response analysis of some sort is the best. Transient-response techniques, however, are not as adaptable to synthesis as the frequency-response techniques.

Many of these techniques are only applicable to cases where one degree of control is employed. Extension of these techniques to cover the situation where two degrees of control must be considered, such as in the case of the lateral stability of an aircraft, has been done in

only two generally available references, 6 and 50. A discussion of these techniques is included in this report. The possibility of using simulators for solving the two-degrees-of-control case is mentioned also.

Ames Aeronautical Laboratory,
National Advisory Committee for Aeronautics,
Moffett Field, Calif., Oct. 5, 1950.

APPENDIX A

ILLUSTRATIVE EXAMPLE

For the purpose of demonstrating several of the techniques of stability and control analysis described in the body of this report, calculations have been made for the case of a typical high-speed fighter aircraft having an automatic pilot with proportional control based on the error in pitch angle E where $E = \theta_1 - \theta$. The following diagram defines the variables involved and their positive directions:

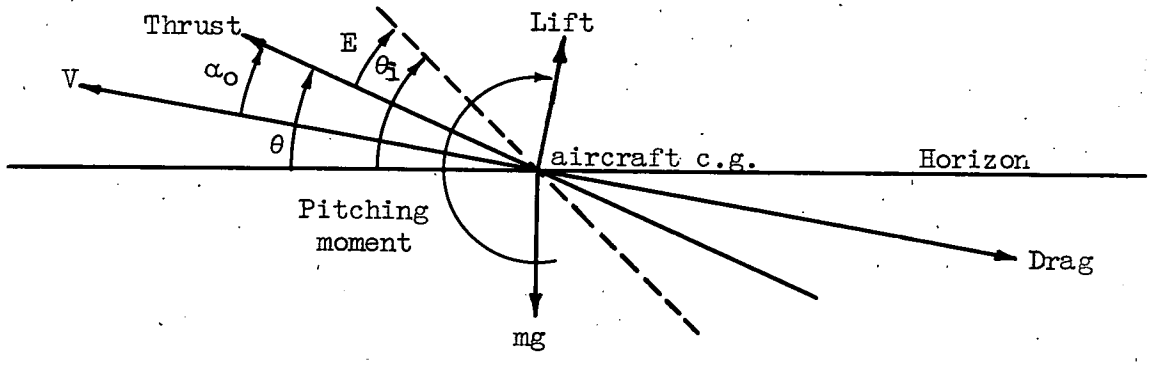

where

V aircraft velocity

u longitudinal perturbation velocity

α_o initial angle of attack

α perturbation angle of attack

θ angle of pitch

θ_1 input angle of pitch

m mass of the airplane

g acceleration due to gravity

For this arrangement the longitudinal equations of motion of the airplane in level flight with controls fixed can be written (for a derivation of a similar set of equations, see reference 39)

$$\left(-C_{T_o}\cos\alpha_o-\frac{\partial C_L}{\partial\alpha}\right)\alpha-2\tau D\alpha+2\tau D\theta+\left(-2C_{L_o}-2C_{T_o}\sin\alpha_o-\frac{\partial C_L}{\partial u'}\right)u'=0 \quad (A1)$$

$$\left(\frac{\partial C_D}{\partial\alpha}-C_{L_o}\right)\alpha+\left(C_{L_o}+C_{T_o}\sin\alpha_o\right)\theta+\left(2C_{D_o}-2C_{T_o}\cos\alpha_o+\frac{\partial C_D}{\partial u'}\right)u'+$$

$$\left(\frac{1}{\tau}\frac{\partial C_D}{\partial\dot{u}'}+2\right)\tau Du=0 \quad (A2)$$

$$\frac{\partial C_m}{\partial\alpha}\alpha+\frac{\partial C_m}{\partial\dot{\alpha}}D\alpha+\frac{\partial C_m}{\partial\dot{\theta}}D\theta+\left(\frac{1}{\tau^2}\frac{\partial C_m}{\partial\ddot{\theta}}-2K'\right)\tau^2D^2\theta+\frac{\partial C_m}{\partial u'}u'=0 \quad (A3)$$

where

C_T thrust coefficient

C_L lift coefficient

C_D drag coefficient

C_m pitching moment coefficient

K' nondimensional moment of inertia parameter $\left(\frac{K_y^2\rho S}{mc}\right)$

u' nondimensional longitudinal perturbation velocity $\left(\frac{u}{V_o}\right)$

τ aerodynamic time $\left(\frac{m}{\rho SV_o}\right)$, seconds

$\dot{\alpha}$, $\dot{\theta}$, etc. $\frac{d\alpha}{dt}$, $\frac{d\theta}{dt}$, etc.

$\ddot{\theta}$ $\frac{d^2\theta}{dt^2}$

and subscript o denotes initial condition.

For an altitude of 10,000 feet and a Mach number of 0.85 the numerical values of the mass and aerodynamic constants are assumed to be

$$\left(-C_{T_o}\cos\alpha_o-\frac{\partial C_L}{\partial\alpha}\right)=-5.325 \qquad \left(\frac{\partial C_m}{\partial\dot{\alpha}}\right)=-0.0165$$

$$\left(-2C_{L_o}-2C_{T_o}-\frac{\partial C_L}{\partial u'}\right)=5.39 \qquad \left(\frac{\partial C_m}{\partial\dot{\theta}}\right)=-0.034$$

$$\left(\frac{\partial C_D}{\partial \alpha} - C_{L_o}\right) = 0.1553$$

$$\left(C_{L_o} + C_{T_o} \sin \alpha_o\right) = 0.0687$$

$$\left(2C_{D_o} - 2C_{T_o} \cos \alpha_o + \frac{\partial C_D}{\partial u'}\right) = 0.553$$

$$\left(\frac{1}{\tau} \frac{\partial C_D}{\partial \dot{u}'} + 2\right) \approx 2$$

$$\frac{\partial C_m}{\partial \alpha} = -0.639$$

$$\left(\frac{1}{\tau^2} \frac{\partial C_m}{\partial \ddot{\theta}} - 2k'\right) = -0.0123$$

$$\frac{\partial C_m}{\partial u'} = 0.153$$

$$\tau = 0.967$$

$$\frac{\partial C_m}{\partial \delta} = -0.6299$$

Substituting these numerical values into equations (1A), (2A), and (3A) yields

$$(-5.325)\ \alpha - 2(0.967)\ D\alpha + 2(0.967)\ D\theta + (5.39)u' = 0 \qquad (A4)$$

$$(0.155)\ \alpha + (0.069)\theta + (0.553)\ u' + 2\ (0.967)\ D\ u' = 0 \qquad (A5)$$

$$(-0.639)\ \alpha + (-0.0165)D\alpha + (-0.034)\ D\theta + (-0.0123)(0.967)^2 D^2\theta + (0.1530)u' = 0 \qquad (A6)$$

where $D = \frac{d}{dt}$.

It is also necessary to choose some form for the autopilot equation. An electric motor having the usual inertia and viscous damping characteristics and an internal feedback was selected. The expression for this autopilot is

$$[\ J_m\ D^2 + (f_m + S_s)\ D + S_T\ ]\ \delta = S_T\ k\ E \qquad (A7)$$

where

J_m moment of inertia of motor

f_m damping coefficient of motor

S_s torque–speed sensitivity of motor

S_T torque–voltage sensitivity of motor

δ control deflection

k control gearing

With the numerical values assumed for these motor constants, the autopilot equation becomes

$$(0.058\ D^2 + D + 37.5)\ \delta = 37.5\ kE \qquad (A8)$$

For this problem k was chosen as one of the independent variables to be investigated. The other variable chosen for the calculation of a stability boundary chart was $\partial C_m/\partial\alpha$. This derivative, often referred to as the static stability factor, previously was set equal to -0.639. The loop diagram for the autopilot-aircraft combination is as follows:

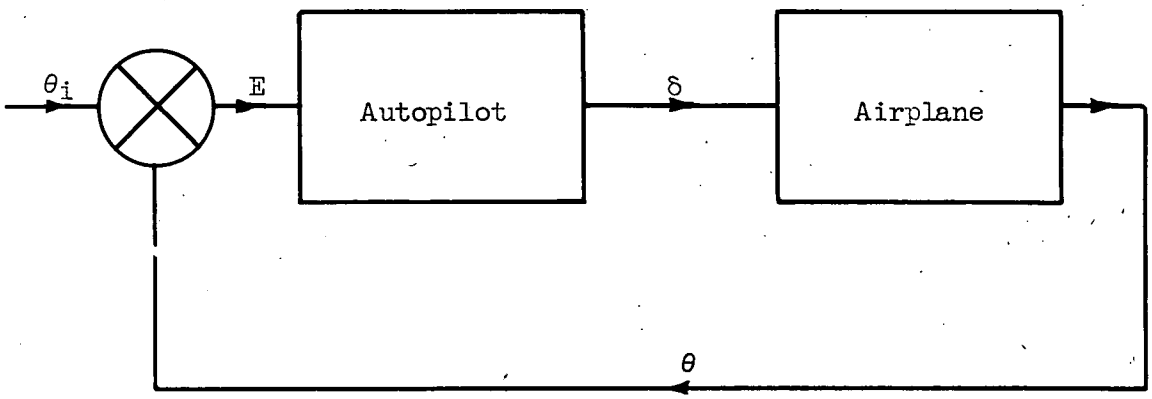

Having the equations representing the aircraft and autopilot behavior, it is now necessary to determine the algebraic signs that will tend to make the combined action of the two mechanisms stable. According to standard aircraft nomenclature, the displacements shown on the sketch are positive. Thus a positive control deflection δ gives a negative angle of pitch θ for the usual aerodynamic forces and moments involved. Since the elevator deflection for the conventional aircraft gives merely a pitching moment about the center of gravity, only the third equation of motion will be affected by the inclusion of the elevator action: With the elevator action $\delta \frac{\partial C_m}{\partial \delta}$ included as a forcing function, equation (A3) becomes

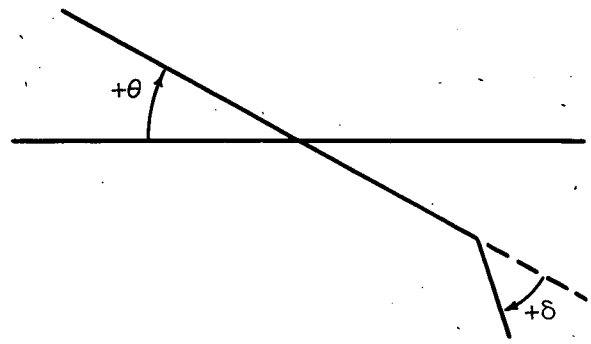

$$\frac{\partial C_m}{\partial \alpha}\alpha+\frac{\partial C_m}{\partial \dot{\alpha}}D\alpha+\frac{\partial C_m}{\partial \theta}D\theta+\left(\frac{1}{\tau^2}\frac{\partial C_m}{\partial \theta}-2K'\right)\tau^2 D^2\theta+\frac{\partial C_m}{\partial u'}u'=-\delta\frac{\partial C_m}{\partial \delta} \qquad (A9)$$

or numerically

$$(-0.639)\alpha+(-0.0165)D\alpha+(-0.034)D\theta+(-0.0123)(0.967)^2D^2\theta+(0.1530)u'=$$
$$-\delta\,(-0.6299) \qquad (A10)$$

As written, the autopilot equation (A8) gives a positive control deflection for a positive error since k is a positive quantity. In servomechanism nomenclature, the error is defined as

$$E = \theta_i - \theta \qquad (A11)$$

The following diagram represents the above relationship. Hence, to summarize, if a positive error gives a positive elevator deflection via the autopilot and a positive elevator deflection gives a negative increment to the pitch angle via the aerodynamics of the aircraft, the net result is an increase in the positive error and the system so defined is statically unstable. From the aeronautical engineer's point of view, the easiest way to repair the system is to make certain that the autopilot gives a negative deflection for a positive error, thus changing equation (A8) to read

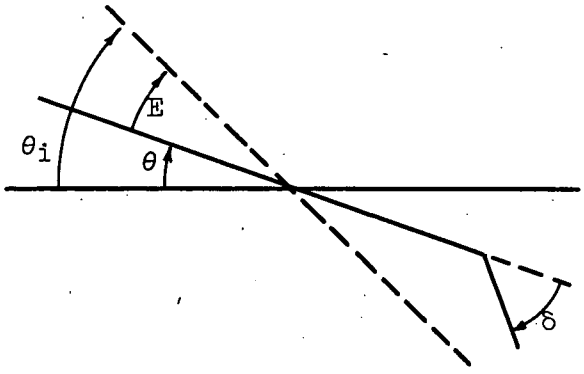

$$(0.058\,D^2 + D + 37.5)\,\delta = -37.5\,k\,E \qquad (A12)$$

Using equations (A1), (A2), (A9), and (A12), the system is stable and completely represented in mathematical form.

The results obtained by the applications of the various techniques demonstrated in the following sections of this appendix are summarized in table II.

The Routh or Hurwitz Criterion

By replacing δ in equation (A9) with the equivalent expression obtained from equation (A12), the equations of motion of the aircraft–autopilot become

$$\left(-C_{T_o}\cos\alpha_o - \frac{\partial C_L}{\partial \alpha}\right)\alpha - 2\tau D\alpha + 2\tau D\theta + \left(-2C_{L_o} - 2C_{T_o}\sin\alpha_o - \frac{\partial C_L}{\partial u'}\right)u' = 0 \quad (A1)$$

$$\left(\frac{\partial C_D}{\partial \alpha} - C_{L_o}\right)\alpha + (C_{L_o} + C_{T_o}\sin\alpha_o)\theta + \left(2C_{D_o} - 2C_{T_o}\cos\alpha_o + \frac{\partial C_D}{\partial u'}\right)u' +$$

$$\left(\frac{1}{\tau}\frac{\partial C_D}{\partial u'} + 2\right)\tau D u' = 0 \quad (A2)$$

$$\frac{\partial C_m}{\partial \alpha}\alpha + \frac{\partial C_m}{\partial \dot{\alpha}} D\alpha + \frac{\partial C_m}{\partial \dot{\theta}} D\theta + \left(\frac{1}{\tau^2}\frac{\partial C_m}{\partial \ddot{\theta}} - 2K'\right)\tau D^2\theta + \frac{\partial C_m}{\partial u'}u'$$

$$= 37.5\, k \frac{\partial C_m}{\partial \delta}\left(\frac{E}{0.058\, D^2 + D + 37.5}\right) \quad (A13)$$

Upon replacing the coefficients in the above equation by the numerical values, as was done previously, and setting k equal to unity, the equations become

$$-5.325\,\alpha - 1.934\, D\alpha + 1.934\, D\theta + 5.39\, u' = 0 \quad (A14)$$

$$0.1553\,\alpha + 0.0687\,\theta + 0.553\, u' + 1.934\, Du' = 0 \quad (A15)$$

$$-0.639\alpha - 0.0165D\alpha - 0.034\, D\theta - 0.01153D^2\theta + 0.153\, u' = \frac{(37.5)(-0.6299)\, E}{0.058\, D^2 + D + 37.5} \quad (A16)$$

As a further simplification, let $\theta_1 = 0$, so that $E = -\theta$. The characteristic equation of the above system is

$$\begin{vmatrix} (-5.325 - 1.934D) & 1.934D & 5.39 \\ 0.1553 & 0.0687 & (0.553 + 1.934D) \\ (-0.639 - 0.0165D) & \left(-0.034D - 0.01153D^2 - \frac{23.62}{0.058D^2 + D + 37.5}\right) & 0.153 \end{vmatrix} = 0 \quad (A17)$$

The expansion of this determinant results in the sixth-order polynomial:

$$0.00700D^6 + 0.164D^5 + 5.59D^4 + 39.8D^3 + 517D^2 + 801D + 219 = 0 \quad (A18)$$

It is seen that all of the coefficients of equation (A18) are positive.

The independent Hurwitz determinants for the sixth-order polynomial are

$$\begin{vmatrix} 0.164 & 39.800 \\ 0.007 & 5.590 \end{vmatrix} = 0.638 > 0 \qquad \text{(A19)}$$

$$\begin{vmatrix} 0.164 & 39.800 & 801.000 \\ 0.007 & 5.590 & 517.000 \\ 0 & 0.164 & 39.800 \end{vmatrix} = 12.41 > 0 \qquad \text{(A20)}$$

$$\begin{vmatrix} 0.164 & 39.800 & 801.000 & 0 & 0 \\ 0.007 & 5.590 & 517.000 & 219.000 & 0 \\ 0 & 0.164 & 39.800 & 801.000 & 0 \\ 0 & 0.007 & 5.590 & 517.000 & 219.000 \\ 0 & 0 & 0.164 & 39.800 & 801.000 \end{vmatrix} = 3,135,000 > 0 \qquad \text{(A21)}$$

Since the Hurwitz determinants are all greater than zero, the system is stable for the given values of the parameters.

Numerical Evaluation of Roots

The characteristic equation of the airplane-autopilot combination given by equation (A18) is a sixth-order polynomial. The roots can be obtained by the method described in reference 3 and outlined in the following paragraphs.

After division by the coefficient of D^6 the characteristic equation becomes

$$D^6 + 23.43\,D^5 + 798.6\,D^4 + 5686\,D^3 + 73860\,D^2 + 114400\,D + 31290 = 0 \qquad \text{(A22)}$$

The last three terms divided by the coefficient of D^2 yields

$$D^2 + 1.549\,D + 0.4236$$

as a first approximation to a quadratic factor. Division of the

polynomial by this factor results in a remainder of

$$3282\ D + 3227$$

and a second approximation of

$$D^2 + 1.699\ D + 0.4723$$

obtained from the next to the last remainder. Division by the second approximate factor results in a remainder of

$$105.0\ D + 93.00$$

Convergence is fairly rapid and only three more repetitions of the process are required to reduce the remainder to

$$-39.00\ D + 3.000$$

This is small enough to be accepted as negligible. The corresponding factor is

$$D^2 + 1.700\ D + 0.4737$$

and the roots obtained from it are $\lambda_1 = -0.351$ and $\lambda_2 = -1.35$. These real roots correspond to the damping constants of the two aperiodic modes shown in table I.

The remaining quartic is

$$D^4 + 21.73\ D^3 + 761.2\ D^2 + 4382\ D + 66050$$

which can be factored by the same process to yield

$$D^2 + 4.097\ D + 115.1$$

and

$$D^2 + 17.64\ D + 574.0$$

The roots obtained from these two quadratic factors are $-2.05 \pm i\ 10.5$ and $-8.82 \pm i\ 22.3$. Designating these as the roots for the long- and short-period oscillatory modes, the resulting damping constants and actual frequencies are

$$(\zeta\omega_n)_l = 2.05$$

$$\omega_l = \omega_{n_l}\sqrt{1-\zeta_l^2} = 10.5 \text{ radians/sec}$$

$$(\zeta \omega_n)_s = 8.82$$

$$\omega_s = \omega_{n_s}\sqrt{1-\zeta_s^2} = 22.3 \text{ radians/sec}$$

which yields

$$\zeta_l = 0.195$$

$$\omega_{n_l} = 10.8 \text{ radians/sec}$$

$$\zeta_s = 0.395$$

$$\omega_{n_s} = 24.3 \text{ radians/sec}$$

In this example the time to damp to half amplitude will be governed by the long-period root. Thus

$$t_{1/2} = \frac{0.693}{(\zeta\omega_n)_l} = \frac{0.693}{2.05} = 0.34 \text{ sec}$$

Cases for which the process is divergent can be handled by first transforming the equation by Graeffe's root squaring method or by Horner's root diminishing method. (See references 24 and 25.)

Stability Boundary Charts

A stability boundary chart will be constructed using the control gearing k and the so-called "static-stability" derivative $\frac{\partial C_m}{\partial \alpha}$ as the independent variables. In determinant form, corresponding to equation (A17), the characteristic equation for the aircraft-autopilot combination is (with θ_i arbitrarily set equal to zero)

$$\begin{vmatrix} (-5.325 - 1.934D) & 1.934\,D & 5.39 \\ 0.1553 & 0.0687 & (0.553 + 1.934D) \\ \left(\frac{\partial C_m}{\partial \alpha} - 0.0165D\right) & \left(-0.034D - 0.01153D^2 - \frac{23.62\,k}{0.058D^2 + D + 37.5}\right) & 0.153 \end{vmatrix} = 0 \quad \text{(A23)}$$

which reduces to the following polynomial form,

$$a_0D^6 + a_1D^5 + a_2D^4 + a_3D^3 + a_4D^2 + a_5D + a_6 = 0 \tag{A24}$$

For the case considered the coefficients of the polynomial become, in terms of k and C_{m_α} $\left(\text{a symbolic notation for } \partial C_m/\partial\alpha\right)$,

$$\left.\begin{aligned} a_0 &= 0.0000700 \\ a_1 &= 0.00164 \\ a_2 &= 0.05230 - 0.00576\, C_{m_\alpha} \\ a_3 &= 0.3340 - 0.1011\, C_{m_\alpha} \\ a_4 &= 2.343\, k + 0.4153 - 3.768\, C_{m_\alpha} \\ a_5 &= 7.154\, k + 0.1751 - 1.059\, C_{m_\alpha} \\ a_6 &= 2.379\, k + 0.05595 + 0.3703\, C_{m_\alpha} \end{aligned}\right\} \tag{A25}$$

The $n-1$ or 5th determinant for this sixth-order system is

$$\left[(a_1a_2-a_0a_3)(a_4a_3-a_2a_5 + a_1a_6) - (a_1a_4 - a_0a_5)^2\right] a_5 -$$

$$a_6(a_1a_2-a_0a_3)(a_3^2-a_1a_5) + a_1a_3a_6(a_1a_4-a_0a_5)-a_1^3a_6^2 \tag{A26}$$

The stability boundary can be determined by plotting this determinant equated to zero and the coefficient a_6 of constant or zero-order term equated to zero. For this particular example the detailed calculations cannot be conveniently presented because of their length but stability boundaries are presented in figure 1.

It is customary to restrict the range of values of the variables to a practical or sensible limit as has been done in figure 1. This often results in part of the bounded stability region being omitted from the chart. Such an omission is detrimental only from an academic point of view.

After plotting the loci, it is not always immediately evident which bounded region is the stable one. Perhaps the most direct way to resolve this problem is to select a point, substitute the values of the coordinates into the determinant and the expression for a_6 and check to see if they are positive. Since the point corresponding to the values $C_{m_\alpha} = -0.639$ and $k = 1$ is known to lie in the stable region

by virtue of the previous calculation, it is apparent that in this case the stable region lies between the locus of the upper branch of the 5th determinant and the locus of the coefficient a_6. The latter is the boundary of the stable aperiodic roots and the former is the boundary of the stable oscillatory roots. For the value of C_{m_α} of -0.639 used in the application of the Hurwitz determinants and the calculation of the roots, it is seen that stability exists for control gearings between the critical values of 0.07 to 2.3 approximately. These critical values of k shall be designated as $(k_{cr})_{low}$ and $(k_{cr})_{high}$, respectively.

The values of ω giving the frequency spectrum along the oscillatory boundary are not easily obtained if the technique just described is used for determining the boundaries. In fact, additional calculations of the roots must be made for points lying along the boundary in order that the frequencies may be determined from the imaginary parts of the roots. This is a tedious process for 4th or higher order systems.

The alternative method for calculating the oscillatory stability boundary, also described in the text of this report, provides the frequency spectrum as well as the boundary. In this application substitution of the pure imaginary root $i\omega$ into the characteristic equation yields the following real and imaginary parts which are equated to zero:

$$\left.\begin{aligned} -a_0\omega^6 + a_2\omega^4 - a_4\omega^2 + a_6 = 0 \\ a_1\omega^4 - a_3\omega^2 + a_5 = 0 \end{aligned}\right\} \qquad \text{(A27)}$$

Since $a_0, a_1 \ldots a_6$ are linear in C_{m_α} and k, equations (A27) are linear in C_{m_α} and k. Thus it is easy to solve these two equations simultaneously for values of C_{m_α} and k as the numerical value of the parameter ω is varied. In figure 1, it is seen that the range of values of ω lying on the part of the oscillatory boundary shown is from 0 to approximately 22.

It should be pointed out that the orientation of the static stability boundary shown in figure 1 indicates that for a given control gearing a decrease in the static stability of the aircraft–autopilot combination takes place as $-C_{m_\alpha}$, the static stability parameter of the aircraft itself, is increased. This undesirable effect plus the fact that the airplane by itself had a slightly divergent aperiodic mode (for $C_{m_\alpha} = -0.639$) indicates that the airplane, as represented by the aerodynamic data used, was flying in a critical Mach number range. Had the airplane been flying in a subcritical Mach number range, the static stability boundary for the aircraft–autopilot combination would have indicated increasing stability as $-C_{m_\alpha}$ was increased.

It is further noted that part of the stability boundary lies in the region where C_{m_α} is positive, that is, where the airplane itself is

statically unstable. This indicates that an automatic pilot can be used to extend the inherent stability limits of the aircraft.

This method of obtaining the oscillatory stability boundary is more expedient than the use of the Routh or Hurwitz criterion, at least for systems of fourth or higher order. It would seem, therefore, that the application of this method plus the use of the locus for the coefficient of the zero-order term is the most convenient way of obtaining this type of a stability boundary chart.

Transient-Response Analysis

Although it is possible to obtain an analytical solution for the transient response (time history) of the motion of this system following the application of a step input in θ by the operator methods used in references 47 and 48, this solution can be obtained more quickly and easily from an anologue computer. In figure 2, the time history as obtained from a Reeves Electronic Analogue Computer is presented for the case where $k=1$ and $C_{m_\alpha} = -0.639$.

From figure 2, it can be seen that although there is no initial overshoot there is an oscillation in the transient before the input signal is reached, a condition which commonly occurs in higher ordered systems. The steady-state error s_1 is approximately 0.06° or 6 percent of the step input magnitude. Approximate values for the long-period damping constant and frequency were measured and found to be

$$(\zeta\omega_n)_l = 2.00$$

$$\omega_l = \frac{2\pi}{0.60} = 10.5 \text{ radians/sec}$$

which yields

$$\omega_{n_l} = 10.7 \text{ radians/sec}$$

$$\zeta_l = 0.19$$

$$t_{1/2} = 0.35 \text{ sec}$$

Also by considering the time to reach the first peak in the response to be the response time, the speed of response is approximately 2.85° per second for a step input of 1°. In a linear system the speed of response is proportional to the magnitude of the disturbance. Thus the relative rates of response between systems should be measured on the basis of units per second per unit disturbance.

Resonance Plot

In order to plot the frequency-response characteristics of the closed-loop behavior of the aircraft-autopilot combination, it is convenient to put the transfer functions of the aircraft and autopilot into forms that can be readily combined to give the frequency-response function developed in the text, namely,

$$\frac{\theta}{\theta_i}(i\omega) = \frac{R_2}{R_1} e^{i\epsilon_c} \tag{A28}$$

Starting with equations (A4), (A5), and (A10) the operator form of the transfer function for the aircraft expressed in determinants becomes

$$\frac{\theta}{\delta} = \frac{\begin{vmatrix} (-5.325 - 1.934D) & 0 & (5.39) \\ (0.155) & 0 & (0.553 + 1.934\,D) \\ (-0.639 - 0.0165D) & (0.6299) & (0.153) \end{vmatrix}}{\begin{vmatrix} (-5.325 - 1.934D) & (1.934D) & (5.390) \\ (0.155) & (0.069) & (0.553 + 1.934\,D) \\ (-0.639 - 0.0165D) & (-0.034D - 0.0115D^2) & (0.153) \end{vmatrix}} \tag{A29}$$

which reduces to

$$\frac{\theta}{\delta} = A_\theta(D) = \frac{-(2.356D^2 + 7.162D + 2.383)}{0.043D^4 + 0.318D^3 + 2.839D^2 + 0.873D - 0.178} \tag{A30}$$

Substituting $i\omega$ for D to obtain the frequency response form of the transfer function yields

$$\left.\begin{aligned} \frac{\theta}{\delta} = A_\theta(i\omega) &= \frac{-[(-2.356\,\omega^2 + 2.383) + i\,(7.162\,\omega)]}{(0.043\,\omega^4 - 2.839\,\omega^2 - 0.181) + i(-0.318\omega^3 + 0.873\,\omega)} \\ &= \frac{b_1 + ib_2}{c_1 + ic_2} \end{aligned}\right\} \tag{A31}$$

This function can be written in exponential form as

$$\frac{\theta}{\delta} = A_\theta(i\omega) = R_\theta e^{i\epsilon_\theta} \tag{A32}$$

where

$$R_\theta = \sqrt{\frac{b_1^2 + b_2^2}{c_1^2 + c_2^2}} \tag{A33}$$

$$\epsilon_\theta = \tan^{-1} \frac{(b_2c_1 - b_1c_2)}{(b_1c_1 + b_2c_2)} \tag{A34}$$

A corresponding derivation for the autopilot transfer function begins with equation (A12) using $k = 1$.

$$(0.058\ D^2 + D + 37.5)\ \delta = -37.5\ E \tag{A35}$$

The operator form of the transfer function is

$$\frac{\delta}{E} = A_p(D) = \frac{-37.5}{(0.058\ D^2 + D + 37.5)} \tag{A36}$$

Substituting $i\omega$ for D gives

$$\frac{\delta}{E} = A_p(i\omega) = \frac{37.5}{(0.058\ \omega^2 - 37.5 - i\omega)} = \frac{d_3}{(d_1 + id_2)} \tag{A37}$$

and the exponential form can be written as

$$\frac{\delta}{E} = A_p(i\omega) = R_p e^{i\epsilon_p} \tag{A38}$$

where

$$R_p = \frac{d_3}{\sqrt{d_1^2 + d_2^2}} \tag{A39}$$

$$\epsilon_p = \tan^{-1} \frac{(-d_2)}{(d_1)} \tag{A40}$$

The open-loop transfer function of the combined airplane and autopilot can now be written as

$$\frac{\theta}{E} = \frac{\theta}{\delta}\frac{\delta}{E} = A_\theta(i\omega)\ A_p(i\omega) = R_\theta R_p e^{i(\epsilon_\theta + \epsilon_p)} \tag{A41}$$

By virtue of the relationship

$$\frac{\theta}{\theta_i} = \frac{\theta/E}{1+(\theta/E)} \tag{A42}$$

the frequency-response function of the closed loop becomes

$$\frac{\theta}{\theta_i} = A(i\omega) = \frac{A_\theta(i\omega)\ A_p(i\omega)}{1+A_\theta(i\omega)\ A_p(i\omega)} = \frac{R_\theta R_p e^{i(\epsilon_\theta+\epsilon_p)}}{1+R_\theta R_p e^{i(\epsilon_\theta+\epsilon_p)}} \tag{A43}$$

or, in the form (A28) desired at the beginning of the development

$$\frac{\theta}{\theta_i} = \frac{R_2}{R_1} e^{i\epsilon_c} \tag{A28}$$

where

$$\frac{R_2}{R_1} = \frac{R_\theta R_p}{\sqrt{1+R_\theta{}^2 R_p{}^2 + 2R_\theta R_p \cos\ (\epsilon_\theta+\epsilon_p)}} \tag{A44}$$

and

$$\epsilon_c = \epsilon_\theta+\epsilon_p - \tan^{-1}\ \frac{R_\theta R_p \sin\ (\epsilon_\theta+\epsilon_p)}{1+R_\theta R_p \cos\ (\epsilon_\theta+\epsilon_p)} \tag{A45}$$

Table III shows the calculations carried out in detail from $\omega = 0$ to $\omega = 20$. The plot of the frequency-response characteristics is shown in figure 3.

There is good correspondence between the resonant frequency, approximately 11 radians per second, and the long-period natural frequency, 10.64 radians per second, as calculated from the roots of the characteristic equation and measured from the transient-response data. The steady-state error is computed (table III) to be 8.2 percent compared to the less accurate value of 6.0 percent measured on the transient response. The relatively high peak amplitude of approximately 1.7 indicates that the damping of the dominant oscillatory mode is not very great. This is borne out by the damping ratio of approximately 0.2 for the long-period oscillation obtained from the roots and by the transient response. The assumed relationship between the peak amplitude and the peak overshoot was not borne out in view of the fact that no initial overshoot of the transient response occurred, although a relatively high peak amplitude is shown in figure 3. The oscillation of the transient

before reaching θ_i, which commonly occurs for systems of third or higher order having high peak amplitudes, did occur, however. The relatively high value of the resonant frequency indicates a high speed of response.

Greenberg's Method

This method will be applied to calculate the critical control gearings $(k_{cr})_{high}$ and $(k_{cr})_{low}$ for C_{m_α} fixed at -0.639. In Greenberg's notation the frequency-response form of the transfer function for the aircraft is

$$\frac{\theta}{\delta} = \frac{1}{K_r} e^{-i\epsilon_r} \tag{A46}$$

as contrasted with equation (A32) where

$$\frac{\theta}{\delta} = R_\theta e^{i\epsilon_\theta}$$

Also the autopilot response is designated as

$$\frac{\delta}{\theta} = K_p e^{i\epsilon_p} \tag{A47}$$

which corresponds to equation (A38) where

$$\frac{\delta}{E} = R_p e^{i\epsilon_p}$$

The two phase angles ϵ_p are not equal, however. In Greenberg's method the input θ_i is assumed to be zero and the error is assumed to be equal to the output, that is,

$$E = \theta \tag{A48}$$

rather than the usual assumption that

$$E = \theta_i - \theta \tag{A11}$$

or for $\theta_i = 0$

$$E = -\theta \tag{A49}$$

Diagrammatically this arrangement appears as follows:

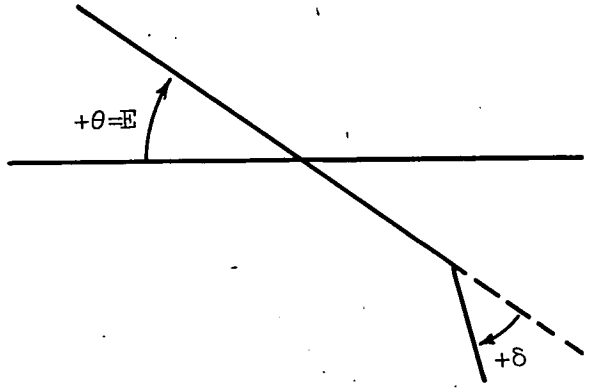

and in order for the aircraft–autopilot combination to be stable it is necessary to use the autopilot equation in the form of (A8)

$$(0.058D^2 + D + 37.5)\,\delta = 37.5\,k\,E$$

With the conventional notation and relationships the point $-1+0i$ is the critical stability point as established by Nyquist. In other words, when the phase angles add up to 180°, $\Phi_1 + \Phi_2 = \pi$ the product of the magnitudes R_θ, R_p, and k must be less than or equal to 1. Thus for comparison, and writing Greenberg's autopilot phase angle as ϵ_{p_1},

$$R_\theta = \frac{1}{K_r} \tag{A50}$$

$$\epsilon_\theta = -\epsilon_r \tag{A51}$$

and

$$R_p e^{i\epsilon_p} = -K_p e^{i\epsilon_{p_1}} \tag{A52}$$

or

$$R_p e^{i\epsilon_p} = K_p e^{-i\pi}\, e^{i\epsilon_{p_1}} \tag{A53}$$

so

$$R_p = K_p \tag{A54}$$

$$\epsilon_p = \epsilon_{p_1} - \pi \tag{A55}$$

In Greenberg's notation, at the point

$$\epsilon_\theta + \epsilon_p = -\epsilon_r + \epsilon_{p_1} - \pi = \pi \tag{A56}$$

or

$$\epsilon_{p_1} - \epsilon_r = 2\pi = 0 \tag{A57}$$

the magnitudes must satisfy

$$k\, R_\theta\, R_p = k\, \frac{K_p}{K_r} < 1 \tag{A58}$$

for stability.

To find the critical control gearings, therefore, the resonance plots of the autopilot and aircraft are compared and at the frequencies where the angles ϵ_{p_1} and ϵ_r are equal, the amplitudes K_p and K_r can be determined and substituted into the following expression:

$$k_{cr} = \left(\frac{K_r}{K_p} \right)_{\omega_{cr}} \tag{A59}$$

Thus if the control gearing is set equal to its critical value, equation (A58) is satisfied.

$$k_{cr} \frac{K_p}{K_r} = \frac{K_r}{K_p} \frac{K_p}{K_r} = 1$$

The values of the critical control gearings or gain margins based on the values of K_p and K_r at the critical frequencies shown in figure 4 are

$$(k_{cr})_{high} = \frac{2.80}{1.26} = 2.22 \quad \text{and} \quad (k_{cr})_{low} = \frac{0.075}{1.00} = 0.075$$

The phase margin, also available on this type of plot, is 50°. The computations are available in table III.

Open-Loop Transfer Locus Plot (Nyquist Diagram)

The transfer locus showing the open-loop response of the aircraft-autopilot combination for $C_{m_\alpha} = -0.639$ and $k=1$ was obtained by

plotting the individual transfer functions (A32) and (A38) and combining them vectorially. The results are shown in figures 5 and 6 at different scales and the computations are included in table III. Figure 5 shows a small-scale plot giving fairly good detail of the transfer locus in the region of high frequencies. The phase margin and the higher value of gain margin are evident as 48° and 2.22, respectively. From figure 6, which shows the transfer locus plotted for $\omega=0$ as well as the high frequencies, it can be seen that the lower value of critical control gearing is 0.076. It should be pointed out that although the airplane and autopilot are combined in the form of a single-loop system, the airplane by itself is unstable and should be considered as a multiple-loop system within the single loop. Thus the check of stability on the transfer locus plot should be made using the generalized Nyquist criterion relating the encirclements of the $-1+0i$ point to the number of zeros minus the number of poles as described in reference 11.

The effect of the simplifications in the equations of motion, used in the section of the report discussing damping, upon the frequency-response characteristics was of sufficient interest to warrant a comparison. The simplified transfer function of the aircraft in operator form is

$$A_{\theta_s}(D) = \frac{0.6299\ (5.325 + 1.933\ D)}{(0.967)(0.0231)\ D\ (D^2 + 7.12\ D + 63.4)} \tag{A60}$$

The frequency response form is

$$A_{\theta_s}(i\omega) = \frac{3.354 + 1.218\ i\omega}{-0.159\ \omega^2 + (-0.0223\ \omega^2 + 1.416)\ i\omega} \tag{A61}$$

$$= \frac{e_1 + ie_2}{f_1 + if_2} \tag{A62}$$

In polar form,

$$A_{\theta_s}(i\omega) = R_{\theta_s}\ e^{\epsilon\theta_s}$$

$$A_{\theta_s}(i\omega) = \sqrt{\frac{(e_1f_1+e_2f_2)^2+(e_2f_1-e_1f_2)^2}{f_1^2 + f_2^2}}\ \ e^{i\ \tan^{-1}\frac{(e_2f_1-e_1f_2)}{(e_1f_1+e_2f_2)}} \tag{A63}$$

The calculations are carried out in table IV. The simplified airplane transfer locus is plotted and combined with the autopilot transfer locus in figure 7. Comparison of these results with those shown in figure 5 indicates that the simplification was noticeable only at the low frequencies. No check on the lower critical control gearing was possible but the values of the phase margin and the higher critical control gearings are virtually the same.

Logarithmic Plots

The commonly used logarithmic form for plotting the transfer locus has the decibel as the unit of magnitude. To get the magnitude of the transfer function into this form the logarithm to the base 10 is taken

$$\mathrm{Log}_{10} \left| A(i\omega) \right|$$

and multiplied by 20. Thus the log modulus is defined, in decibels, as

$$\mathrm{Lm} \left| A(i\omega) \right| = 20 \log_{10} \left| A(i\omega) \right| \tag{A64}$$

The phase angles are not altered.

For the aircraft transfer function

$$\frac{\theta}{\delta} = A_\theta(i\omega) = \frac{b_1 + ib_2}{c_1 + ic_2} \tag{A31}$$

the log modulus is

$$\left.\begin{aligned} \mathrm{Lm} \left| A_\theta(i\omega) \right| &= 20 \log_{10} \sqrt{b_1^2+b_2^2} - 20 \log_{10} \sqrt{c_1^2 + c_2^2} \\ &= 10 \log_{10} (b_1^2+b_2^2) - 10 \log_{10} (c_1^2+ c_2^2) \end{aligned}\right\} \tag{A65}$$

Writing the phase angle in terms of the numerator and denominator components yields

$$\left.\begin{aligned} \mathrm{Ang}\ (b_1 + ib_2) &= \tan^{-1} \frac{b_2}{b_1} \\ \mathrm{Ang}\ (c_1 + ic_2)^{-1} &= \tan^{-1} \left(\frac{-c_2}{c_1} \right) \end{aligned}\right\} \tag{A66}$$

For the autopilot transfer function (A37)

$$\frac{\delta}{E} = A_p(i\omega) = \frac{d_3}{d_1 + id_2} \tag{A67}$$

the log modulus is

$$\left.\begin{aligned} Lm\ |A_p(i\omega)| &= 20 \log_{10} d_3 - 20 \log_{10} \sqrt{d_1^2 + d_2^2} \\ &= 10 \log_{10} \left(\frac{d_3^2}{d_1^2 + d_2^2} \right) \end{aligned}\right\} \tag{A67}$$

and the phase angle is

$$\text{Ang} \left(\frac{d_3}{d_1 + id_2} \right) = \tan^{-1} \left(\frac{-d_2}{d_1} \right) \tag{A68}$$

The over-all open-loop transfer function is

$$\frac{\theta}{E} = A_{\theta p}(i\omega) = A_\theta\ (i\omega)\ \ A_p(i\omega) \tag{A69}$$

The log modulus, therefore, is

$$\left.\begin{aligned} Lm\ |A_{\theta p}(i\omega)| &= Lm\ |A_\theta(i\omega)| + Lm\ |A_p(i\omega)| \\ &= 10 \log_{10} (b_1^2+b_2^2) + 10 \log_{10} (c_1^2+c_2^2) + \\ &\quad 10 \log_{10} \left(\frac{d_3^2}{d_1^2 + d_2^2} \right) \end{aligned}\right\} \tag{A70}$$

and the phase angle is

$$\text{Ang}\ A_{\theta p}(i\omega) = \tan^{-1} \frac{b_2}{b_1} + \tan^{-1} \left(\frac{-c_2}{c_1} \right) + \tan^{-1} \left(\frac{-d_2}{d_1} \right) \tag{A71}$$

The calculations are given in table V. The log modulus and phase-angle curves plotted against the log of the frequency are shown in figure 8. A graph showing the log modulus versus the phase angle is also presented as figure 9. From this curve the gain margins and phase margin are seen to be 6.9 decibels below the zero level, 22.4 decibels above the zero level, and 48°, respectively. The value of the gain margins, 6.9 and −22.4 decibels, correspond to the values of $G_{m_{high}} = 2.22$ and $G_{m_{low}} = 0.076$ which were found from the polar plots.

Approximate Factorization of Quartic

As mentioned in the body of this report, the log modulus analysis is particularly convenient if the system being analyzed is composed of only first- and second-order transfer elements. To take advantage of this situation in the case of longitudinal motion, the denominator of the aircraft transfer function often can be approximately factored into two quadratics by the method used in reference 39.

If the quartic is of the form

$$a_0 D^4 + a_1 D^3 + a_2 D^2 + a_3 D + a_4 = 0 \tag{A72}$$

it can be written as

$$(D^2 + z_1 D + z_2)\ (D^2 + z_3 D + z_4) = 0 \tag{A73}$$

where

$$\left.\begin{aligned} a_0 &= 1 \\ a_1 &= z_1 + z_3 \\ a_2 &= z_1 z_3 + z_2 + z_4 \\ a_3 &= z_1 z_4 + z_3 z_2 \\ a_4 &= z_3 z_4 \end{aligned}\right\} \tag{A74}$$

In reference 43, the following approximations are recommended for all practical cases of conventional aircraft:

$$\left.\begin{aligned} z_1 &= a_1 \\ z_2 &= a_2 \\ z_3 &= \frac{a_3}{a_2} - \frac{a_1 a_4}{a_2^2} \\ z_4 &= \frac{a_4}{a_2} \end{aligned}\right\} \qquad \text{(A75)}$$

From equation (A30) the denominator of the aircraft transfer function is

$$0.0431\ (D^4 + 7.424\ D^3 + 65.839\ D^2 + 20.235\ D - 4.190) \qquad \text{(A76)}$$

Substituting in the approximate relationships yields

$$0.0431\ (D^2 + 7.424\ D + 65.839)(D^2 + 0.314\ D - 0.064) \qquad \text{(A77)}$$

Thus in place of $c_1 + ic_2$ in equation (A31), the following quadratic factors can be used:

$$(g_1 + ig_2)\ (h_1 + ih_2) = (l_1 + il_2)$$

where with $i\omega$ substituted for D

$$\left.\begin{aligned} g_1 &= 2.838 - 0.0431\ \omega^2 \\ g_2 &= 0.3320\ \omega \\ h_1 &= -(0.064 + \omega^2) \\ h_2 &= 0.314\ \omega \end{aligned}\right\} \qquad \text{(A78)}$$

The calculations are given in table VI and the curves shown in figure 10. A comparison of the plots of the log modulus of $l_1 + il_2$ and $c_1 + ic_2$ can be made using figures 8 and 10. It is seen that in this particular case the approximation is very good.

APPENDIX B

SYMBOLS AND COEFFICIENTS

A, A_1, A_2, A_3	arbitrary transfer functions
A_c	closed-loop transfer function for aircraft and autopilot combined
A_p	autopilot transfer function
A_θ	aircraft transfer function for longitudinal motion
$A_{\theta p}$	open-loop transfer function, the product of A_θ and A_p
A_{θ_s}	simplified aircraft transfer function for longitudinal motion
AR	amplitude ratio (reference 9)
B	coefficient in arbitrary transfer function A
C	coefficient in arbitrary transfer function A
C_D	drag coefficient $\left(\frac{\text{drag}}{qS}\right)$
C_L	lift coefficient $\left(\frac{\text{lift}}{qS}\right)$
C_m	pitching-moment coefficient $\left(\frac{\text{moment}}{qSc}\right)$
C_T	thrust coefficient $\left(\frac{\text{thrust}}{qS}\right)$
C_{L_α}	rate of change of lift coefficient with angle of attack $\left(\frac{\partial C_L}{\partial \alpha}\right)$
C_{D_α}	rate of change of drag coefficient with angle of attack $\left(\frac{\partial C_D}{\partial \alpha}\right)$

C_{m_α} rate of change of pitching-moment coefficient with angle of attack $\left(\frac{\partial C_m}{\partial \alpha}\right)$

$C_{m_{\dot{\theta}}}$ rate of change of pitching-moment coefficient with pitching velocity $\left(\frac{\partial C_m}{\partial \dot{\theta}}\right)$

D differential operator $\left(\frac{d}{dt}\right)$

E error signal $(\theta_i - \theta)$

F arbitrary transfer function (reference 12)

G frequency dependent part of a transfer function (reference 3)

G_m gain margin

J moment of inertia

J_m moment of inertia of motor

K frequency invariant part of a transfer function (reference 3), also the loop sensitivity or gain

K' nondimensional moment of inertia parameter $\left(\frac{K_y^2 \rho S}{mc}\right)$

K_r aircraft amplitude ratio (reference 7)

K_p autopilot amplitude ratio (reference 7)

K_y radius of gyration of aircraft about axis of pitch

L [] Laplace transform of []

Lm log modulus

M constant magnitude parameter for closed-loop response

N constant phase angle parameter for closed-loop response

P period, seconds

PA	phase angle (reference 9)
$\phi P \phi$	performance operator (reference 9)
R, R_1, R_2, R_3, R_4	arbitrary magnitudes
R_p	amplitude of autopilot transfer function in polar form
R_θ	amplitude of aircraft transfer function in polar form
R_{θ_s}	amplitude of simplified aircraft transfer function in polar form
S	wing area
S_S	torque—speed sensitivity of motor
S_T	torque—voltage sensitivity of motor
T, T_1, T_2,	arbitrary time constants
V	velocity of aircraft
Y	arbitrary transfer function (reference 11)
a_o, a_1, a_2, a_3, a_4, a_5, a_6, a_n	coefficients of characteristic equation
b_1, b_2	coefficients in A_θ
c	mean aerodynamic chord
c_1, c_2	coefficients in A_θ
d	logarithmic decrement
d_1, d_2, d_3	coefficients in A_p
e	2.71828
e_1, e_2	coefficients in A_{θ_s}
f	damping coefficient (viscous)
f_{cr}	critical damping coefficient

f_m	damping coefficient of motor
f_1, f_2	coefficients in A_{θ_s}
g	acceleration due to gravity
g_1, g_2	coefficients in an approximate factorization of stability quartic for aircraft
h_1, h_2	coefficients in an approximate factorization of stability quartic for aircraft
i	$\sqrt{-1}$
j	proportional control constant
k	control gearing $\left(\left\|\frac{\delta(i\omega)}{E(i\omega)}\right\|_{\omega=0}\right)$
k_{cr}	critical control gearing
l	derivative control constant
l_1	$g_1h_1-g_2h_2$
l_2	$g_2h_1+g_1h_2$
m	mass of aircraft
n	arbitrary quantity
p	a variable introduced in the Laplace transformation
q	free-stream dynamic pressure $\left(\frac{1}{2}\rho V^2\right)$
r_1, r_2	roots of a second-order equation
s_1	steady-state error
s_2	amplitude of initial overshoot
t	time, seconds
$t_{1/2}$	time to damp to half amplitude

t_r	response time
u	longitudinal perturbation velocity
u'	nondimensional longitudinal perturbation velocity $\left(\frac{u}{V}\right)$
x	arbitrary dependent variable
z_1, z_2, z_3, z_4	coefficients in approximate factorization of aircraft stability quartic
α	angle of attack, radians
γ_m	phase margin, degrees
δ	arbitrary control deflection, radians
δ_a	aileron deflection, radians
δ_e	elevator deflection, radians
δ_r	rudder deflection, radians
ϵ	arbitrary phase angle, degrees
ϵ_c	phase angle for aircraft–autopilot closed–loop transfer function, degrees
ϵ_p	phase angle of autopilot response, degrees
ϵ_r	phase angle of aircraft response (reference 7), degrees
ϵ_θ	phase angle of aircraft response, degrees
ϵ_{θ_s}	phase angle of simplified aircraft response, degrees
ζ	damping ratio $\left(\frac{f}{f_{cr}}\right)$
θ	output angle of pitch, radians, unless otherwise noted
θ_i	input angle of pitch, radians, unless otherwise noted
	arbitrary exponential coefficient

$\lambda_1, \lambda_2, \lambda_3, \lambda_4, \lambda_5$	roots of a fifth-order characteristic equation
μ	spring constant
ρ	density of air
τ	aerodynamic time $\left(\frac{m}{\rho SV}\right)$, seconds
τ_d	time lag
Φ	angle of bank
$\varphi(t)$	arbitrary function of time
ψ	angle of yaw
ω	actual frequency $\left(\omega_n \sqrt{1-\zeta^2}\right)$, radians per second
ω_n	natural frequency, radians per second

Subscripts

l	long-period oscillatory mode
o	initial value
s	short-period oscillatory mode

REFERENCES

1. Craik, Kenneth J. W.: Theory of the Human Operator in Control Systems, II – Man as an Element in a Control System. British Journal of Psychology, vol. XXXVIII, part 3, March 1948, pp. 142–148.

2. Wiener, Norbert: Cybernetics. Technology Press, Cambridge, Mass., 1948.

3. Brown, Gordon S., and Campbell, Donald P.: Principles of Servomechanisms. John Wiley and Sons, Inc., N. Y., 1948.

4. Klemin, Alexander, Pepper, Perry A., and Wittner, Howard A.: Longitudinal Stability in Relation to the Use of an Autopilot. NACA TN 666, 1938.

5. Sternfield, Leonard: Effect of Automatic Stabilization of the Lateral Oscillatory Stability of a Hypothetical Airplane at Supersonic Speeds. NACA TN 1818, 1949.

6. Imlay, Fredrick H.: A Theoretical Study of Lateral Stability With an Automatic Pilot. NACA TR 693, 1940.

7. Greenberg, Harry: Frequency-Response Method for Determination of Dynamic Stability Characteristics of Airplanes with Automatic Control. NACA Rep. 882, 1947.

8. Moore, John R.: Application of Servo Systems to Aircraft. Aero. Eng. Rev., vol. 8, no. 1, Jan. 1949, pp. 32–43.

9. Seamans, Robert C., Jr., Bromberg, Benjamin G., and Payne, L. E.: Application of the Performance Operator to Aircraft Automatic Control. Jour. Aero. Sci., vol. 15, no. 9, Sept. 1948, pp. 535–555.

10. Flügge-Lotz, I., and Meissinger, H.: The Movements of an Oscillating Body – Under the Influence of a "Black-White" Type of Control. ZBW Report UM No. 1329, Berlin, 1944.

11. James, Hubert M., Nichols, Nathaniel B., and Phillips, Ralph S., ed.: Theory of Servomechanisms. McGraw-Hill Book Co., Inc., N. Y., 1947.

12. Oldenbourg, R. C., and Sartorius, H.: The Dynamics of Automatic Controls. American Soc. of Mech. Engineers, N. Y., 1948.

13. Lauer, Henri, Lesnick, Robert, and Matson, Leslie E.: Servomechanism Fundamentals. McGraw-Hill Book Co., Inc., N. Y., 1947.

14. MacColl, LeRoy A.: Fundamental Theory of Servomechanisms. D. Van Nostrand Co., N. Y., 1945.

15. Graham, R. E.: Linear Servo Theory. Bell System Tech. Jour., vol. 25, Oct. 1946, pp. 616–651.

16. Haus, Fr.: Automatic Stability of Airplanes. NACA TM 695, 1932.

17. Haus, Fr.: Automatic Stabilization. NACA TM 815, 1936.

18. Haus, Fr.: Automatic Stabilization. NACA TM 802, 1936.

19. Meredith, F. W., and Cooke, P. A.: Aeroplane Stability and the Automatic Pilot. Jour. of the Royal Aero. Soc., vol. 41, no. 318, June 1937.

20. Whitely, A. L.: Theory of Servo Systems With Particular Reference to Stabilization. Inst. of Elec. Engineers Jour., vol. 93, 1946, pp. 353–372.

21. Jones, Robert T., and Sternfield, Leonard: A Method for Predicting the Stability in Roll of Automatically Controlled Aircraft Based on the Experimental Determination of the Characteristics of an Automatic Pilot. NACA TN 1901, 1949.

22. Harris, Herbert, Jr.: The Frequency Response of Automatic Control Systems. Trans. AIEE., vol. 65, Aug. – Sept. 1946, pp. 539–546.

23. Sternfield, Leonard, and Gates, Ordway B., Jr.: A Theoretical Analysis of the Effect of Time Lag in an Automatic Stabilization System on the Lateral Stability of an Airplane. NACA TN 2005, 1950.

24. Whittaker, E. T., and Robinson, G.: The Calculus of Observations. Blackie and Sons, Ltd., Glasgow, 3rd ed., 1940.

25. Uspensky, J. V.: Theory of Equations. McGraw-Hill Book Co., Inc., N. Y., 1948.

26. Vazsonyi, Andrew: Transient Analysis of a Speed Regulator Servomechanism. NAVORD Rep. 1147, Apr. 1949.

27. Ansoff, H. I.: Stability of Linear Oscillating Systems With Constant Time Lag. Jour. of Applied Math., vol. 16, no. 2, June 1949, pp. 158–164.

28. Callender, A., Hartree, D. R., and Porter, A.: Time Lag in Control Systems. Philosophical Transactions of the Royal Society of London, series a, vol. 235, 1936, pp. 415–444.

29. Vazsonyi, Andrew: Transient Analysis of an Angular-Position Servomechanism. NAVORD Rep. 1149, May 1949.

30. Beckhardt, Arnold R.: A Theoretical Investigation of the Effect on the Lateral Oscillations of an Airplane of an Automatic Control Sensitive to Yawing Accelerations. NACA TN 2006, 1950.

31. Gardner, Robert A., Zarovsky, Jacob, and Ankenbruck, H. O.: An Investigation of the Stability of a System Composed of a Subsonic Canard Airframe and a Canted-Axis Gyroscope Automatic Pilot. NACA TN 2004, 1950.

32. Marcy, H. Tyler: Parallel Circuits in Servomechanisms. Transactions of the American Institute of Electrical Engineers, vol. 65, 1946, pp. 521-529.

33. Andronow, A. A., Chaikin, C. E.: Theory of Oscillations. Princeton University Press, Princeton, N. J., 1949.

34. Brown, G. S., and Hall, A. C.: Dynamic Behavior and Design of Servomechanisms. Transactions of the A.S.M.E., vol. 68, 1946, pp. 503-524.

35. Jones, B. Melvill: Dynamics of the Airplane. Vol. V, div. N, Aerodynamic Theory, W. F. Durand, ed., J. Springer (Berlin), 1934.

36. Vazsonyi, Andrew: Longitudinal Stability of Autopilot-Controlled Aircraft. NAVORD Rep. 1150, June 1949.

37. Routh, E. J.: Advanced Rigid Dynamics. Vol. II, 5th ed., MacMillan Co., N. Y., 1905.

38. Brown, W. S.: A Simple Method of Constructing Stability Diagrams. R.& M. No. 1905, British A.R.C., 1942.

39. Zimmerman, Charles H.: An Analysis of Longitudinal Stability in Power-Off Flight With Charts for Use in Design. NACA TR 521, 1935.

40. Zimmerman, Charles H.: An Analysis of Lateral Stability in Power-Off Flight With Charts for Use in Design. NACA TR 589, 1937.

41. Weiss, Herbert K.: Constant Speed Control Theory. Jour. Aero. Sci., vol. 6, no. 4, Feb. 1939, pp. 147-152.

42. Oppelt, W.: Comparison of Automatic Control Systems. NACA TM 966, 1941.

43. Gates, S.B.: A Survey of Longitudinal Stability Below the Stall, With an Abstract for Designers Use. R.& M. No. 1118, British A.R.C., 1927.

44. Sternfield, Leonard, and Gates, Ordway B., Jr.: A Method of Calculating a Stability Boundary That Defines a Region of Satisfactory Period-Damping Relationship of the Oscillatory Mode of Motion. NACA TN 1859, 1949.

45. Lyon, H. M., Truscott, P. M., Auterson, E. I., and Whatham, J.: A Theoretical Analysis of Longitudinal Dynamic Stability in Gliding Flight. R.& M. No. 2075, British A.R.C., 1942.

46. Whatham, J., and Lyon, H. M.: A Theoretical Investigation of Dynamic Stability With Free Elevators. R.& M. No. 1980, British A.R.C., 1943.

47. Jones, Robert T.: A Simplified Application of the Method of Operators to the Calculation of Disturbed Motions of an Airplane. NACA TR 560, 1936.

48. Harper, Charles W., and Jones, Arthur L.: A Comparison of the Lateral Motion Calculated for Tailless and Conventional Airplanes. NACA TN 1154, 1947.

49. Vazsonyi, Andrew: A Generalization of Nyquist's Stability Criterion. NAVORD Rep. 1148, Apr. 1949.

50. Greenberg, Harry: Application of the Frequency Response Method to the Calculation of the Dynamic Stability Limits of Airplanes With Two Independent Autopilots. Aero. Eng. Lab. Rep. No. 119, Princeton University, Princeton, N. J., 1947.

B I B L I O G R A P H Y

Routh-Hurwitz Determinants:

Frazer, R. A., Duncan, W. J., and Collar, A. R.: Elementary Matrices and Some Application to Dynamics and Differential Equations. Cambridge University Press, England, 1938, pp. 154-155.

Cascade Networks:

Prinz, D. G.: Contributions to the Theory of Automatic Controllers and Followers. Journal of Scientific Instruments, vol. 21, no. 4, 1944, pp. 53-64.

Transient and Frequency-Response Correlation:

Mack, C.: The Calculation of the Optimum Parameters for a Following System. Philosophical Magazine, 7th series, vol. 40, Sept. 1949, pp. 922-928.

TABLE I

DAMPING CONSTANTS $\zeta \omega_n$

[for k=1]

Form of equations	Aircraft alone θ/δ	Aircraft–autopilot combination	
		θ/E (open loop)	θ/θ_i (closed loop)
Rigorous aircraft equations	3.54 Oscillatory mode	8.625, 3.54 Oscillatory modes	8.82, 2.05 Oscillatory modes
	0.467, −0.141 Aperiodic modes	0.467, −0.141 Aperiodic modes	1.35, 0.351 Aperiodic modes
Approximate factorization of aircraft stability quartic	3.71 Oscillatory mode	8.625, 3.71 Oscillatory modes	9.041, 1.97 Oscillatory modes
	0.455, −0.141 Aperiodic modes	0.455, −0.141 Aperiodic modes	1.28, 0.40 Aperiodic modes
Approximate aircraft stability equation based on two degrees of freedom	3.56 Oscillatory mode	8.625, 3.56 Oscillatory modes	9.52, 1.97 Oscillatory modes
	0 Aperiodic mode	0 Aperiodic mode	1.39 Aperiodic mode

TABLE II

SUMMARY OF THE RESULTS OF THE CALCULATIONS
FOR THE ILLUSTRATIVE EXAMPLE

Technique (See p.49)	Roots		Stability margins		Performance parameters		Stability parameters	
	Damping factors	Actual frequencies	Gain margins or critical control gearings	Phase margin	Speed of response	Steady-state error	$t_{1/2}$	Initial overshoot
I	---[1]	---	---	---	---	---	---[1]	---
II	$(\zeta\omega_n)_1 = 0.35$ $(\zeta\omega_n)_2 = 1.35$ $(\zeta\omega_n)_l = 2.05$ $(\zeta\omega_n)_s = 8.82$	$\omega_l = 10.5$ rad./sec $\omega_s = 22.3$ rad./sec	---	---	high	---	0.34 sec	---
III	---[2]	---[2]	2.3; 0.07	---	---[2]	---	---[2]	---
IV & V	$(\zeta\omega_n)_l = 2.00$	$\omega_l = 10.5$ rad./sec	---	---	2.85 $\frac{\text{unit}}{\text{sec}}$ (for a unit input)	6%	0.35 sec	None
VI	---	---	2.22;0.076[3]	49°[3]	high	8%	high	---[4]
VII	---	---	2.22;0.076	48°	---[5]	---	---	---[5]
VIII	---	---	2.22;0.076	48°	---[5]	---	---	---[5]

[1]Positive damping indicated.

[2]Could have been indicated by lines of constant damping and period.

[3]By Greenberg's method (reference 6).

[4]Indicated occurrence of oscillation before θ_1 is reached.

[5]Could have been indicated qualitatively by use of M and N contour lines.

TABLE III

RESONANCE PLOT CALCULATIONS
[See equations (A28) through (A45) and fig. 3.]

(1)	(2)	(3)	(4)	(5)	(6)	(7)	(8)
ω	b_1	b_2	c_1	c_2	d_1	(2)^2	(3)^2
0	−2.38215	0	−0.18064	0	−37.5	5.67464	0
.1	−2.35859	−.71607	−.20902	.08691	−37.49942	5.56294	.51275
.5	−1.79314	−3.58036	−.88753	.39616	−37.48550	3.21535	12.81905
1	−.02611	−7.16073	−2.97588	.55226	−37.44200	.00068	51.27605
1.5	2.91894	−10.74109	−6.34868	.22821	−37.36950	8.52021	115.37123
2	7.04201	−14.32146	−10.84428	−.81582	−37.26800	49.58990	205.10422
3	18.82221	−21.48219	−22.23388	−6.02538	−36.97800	354.27559	461.48449
4	35.31449	−28.64292	−34.55808	−16.99636	−36.57200	1,247.113	820.41687
5	56.51885	−35.80365	−44.19564	−35.64950	−36.05000	3,194.380	1,281.901
6	82.43529	−42.96438	−46.49268	−63.90533	−35.41200	6,795.577	1,845.938
7	113.06381	−50.12511	−35.75268	−103.68442	−34.65800	12,783	2,512.527
8	148.40441	−57.28584	−5.25648	−156.90728	−33.78800	22,024	3,281.667
9	188.45709	−64.44657	52.75772	−225.49446	−32.80200	35,516	4,153.360
10	233.22185	−71.60730	147.08436	−311.36550	−31.70000	54,392	5,127.605
15	527.72685	−107.41095	1,551.179	−1,067.218	−24.45000	278,495	11,537.
20	940.03385	−143.21460	5,762.079	−2,543.273	−14.30000	883,664	20,510.

TABLE III – CONTINUED

1	(9)	(10)	(11)	(12)	(13)	(14)	(15)
ω	$(4)^2$	$(5)^2$	(9) + (10)	$\frac{(7)+(8)}{(11)}$	$R_\theta=\sqrt{(12)}$	(2)(4) + (3)(5)	$\frac{(3)(4)-(2)(5)}{(14)}$
0	0.03263	0	0.03263	173.90800	13.1874	0.43031	0
.1	.04368	.00755	.05124	118.57300	10.8889	.43075	.82333
.5	.78770	.15695	.94465	16.97390	4.1243	.17307	22.46512
1	8.85586	.30499	9.16085	5.59737	2.3666	-3.87688	-5.50027
1.5	40.30574	.05209	40.35783	3.06982	1.7541	-20.98264	-3.21816
2	117.59841	.66589	118.26430	2.15360	1.4694	-64.68179	-2.48989
3	494.34541	36.30520	530.65061	1.53728	1.2409	-289.05240	-2.04467
4	1,194.226	288.87600	1,483.102	1.39405	1.1807	-733.57524	-2.16755
5	1,953.254	1,270.887	3,224.131	1.38836	1.1798	-1,221.505	-2.94491
6	2,161.569	4,083.892	6,248.461	1.38298	1.1760	-1,086.984	-6.68416
7	1,278.254	10,750	12,028	1.27166	1.1277	1,154.859	11.70272
8	27.63058	24,619	24,647	1.02672	1.0133	8,208	2.87493
9	2,783.377	50,848	53.631	.73967	.8600	24,474	1.59740
10	21,633.	96,949	118,582	.50193	.7085	56,599	1.09690
15	2,406,156.	1,138,955	3,545,111	.08181	.2860	933,229	.42500
20	33,201,554.	6,468,235	39,669,789	.02279	.1509	5,760,783	.27081

NACA

TABLE III – CONTINUED

(1)	(16)	(17)	(18)	(19)	(20)	(21)	(22)
ω	$\epsilon_\theta = \tan^{-1}$ (15)	$\frac{(1)}{(6)}$	$\epsilon_p = \tan^{-1}$ (17)	$(6)^2 + \omega^2$	$\sqrt{(19)}$	$R_p = \frac{37.5}{(20)}$	(13) (21)
0	0°	0	−180°	1406.250	37.5000	1	13.1874
.1	−320.51°	−.00266	−180.15°	1406.216	37.5000	1	10.8889
.5	−272.54°	−.01333	−180.76°	1405.413	37.4887	1.0003	4.1252
1	−259.69°	−.02670	−181.54°	1402.903	37.4455	1.0015	2.3701
1.5	−252.74°	−.04013	−182.30°	1398.729	37.3996	1.0027	1.7588
2	−248.11°	−.05366	−183.06°	1392.904	37.3216	1.0048	1.4765
3	−243.93°	−.08112	−184.64°	1376.374	37.0995	1.0108	1.2543
4	−245.24°	−.10937	−186.24°	1353.511	36.7901	1.0193	1.2035
5	−251.25°	−.13869	−187.89°	1324.603	36.3950	1.0304	1.2157
6	−261.50°	−.16943	−189.62°	1290.009	35.9166	1.0441	1.2279
7	−274.89°	−.20197	−191.42°	1250.177	35.3579	1.0606	1.1960
8	−289.18°	−.23677	−193.32°	1205.629	34.7222	1.0800	1.0944
9	−302.05°	−.27437	−195.35°	1156.971	34.0143	1.1025	.9482
10	−312.36°	−.31545	−197.51°	1104.890	33.1400	1.1315	.7993
15	−336.90°	−.61349	−211.54°	822.803	28.6845	1.3073	.3739
20	−344.15°	−1.39860	−234.44°	604.490	24.5864	1.5252	.2301

TABLE III – CONTINUED

(1)	(23)	(24)	(25)	(26)	(27)	(28)	(29)
ω	$(22)^2$	(16) + (18)	sin (24)	cos (24)	$1 + \frac{1}{2}\frac{(23)}{(22)} + (26)$	$\sqrt{(27)}$	$R_2/R_1 = \frac{(22)}{(28)}$
0	173.9075	−180°	0	−1	148.5327	12.1872	1.0820
.1	118.5681	−140.66°	−.6378	−.7701	105.6766	10.2798	1.0592
.5	17.0173	−93.23°	−.9983	−.0575	17.5429	4.1892	.9847
1	7.4534	−81.23°	−.9883	.1524	9.1758	3.0291	.7824
1.5	3.0934	−75.04°	−.9661	.2579	5.0006	2.2364	.7864
2	2.1801	−71.17°	−.9465	.3228	4.1333	2.0033	.7370
3	1.5733	−68.61°	−.9312	.3646	3.3370	1.8267	.6866
4	1.4527	−71.48°	−.9483	.3173	3.2164	1.7933	.6711
5	1.4779	−79.14°	−.9821	.1882	2.9355	1.7132	.7096
6	1.5077	−91.12°	−.9998	−.0195	2.4598	1.5682	.7829
7	1.4304	−106.31°	−.9598	−.2809	1.7585	1.3026	.9181
8	1.1977	−122.50°	−.8434	−.5373	1.0216	1.0008	1.0935
9	.8991	−139.56°	−.6486	−.7612	.4556	.6749	1.4049
10	.6389	−149.87°	−.5020	−.8649	.2463	.4963	1.6105
15	.1398	−188.44°	.1467	−.9892	.4001	.6325	.5910
20	.0529	−219.59°	.6238	−.7815	.6932	.8325	.2763

TABLE III – CONCLUDED

(1)	(30)	(31)	(32)	(33)
ω	$1 + (22)(26)$	$\frac{(22)(25)}{(30)}$	$\tan^{-1}(31)$	$\epsilon_c = (24) - (32)$
0	−12.1871	0	−180°	0°
.1	−7.3859	.9403	−136.76°	−3.90°
.5	.7628	−5.3986	−79.50°	−13.80°
1	1.3612	−1.7207	−59.50°	−21.73°
1.5	1.4536	−1.1688	−49.45°	−25.59°
2	1.4766	−.9464	−43.42°	−27.75°
3	1.4573	−.8014	−38.71°	−29.90°
4	1.3819	−.8258	−39.55°	−31.93°
5	1.2288	−.9715	−44.17°	−34.97°
6	.9761	−1.2576	−51.50°	−39.62°
7	.6640	−1.7287	−59.95°	−46.36°
8	.4119	−2.2408	−65.95°	−56.55°
9	.2782	−2.2106	−65.66°	−73.90°
10	.3087	−1.2996	−52.41°	−97.46°
15	.6301	.0869	−355.04°	−193.40°
20	.8201	.1749	−350.08°	−228.51°

TABLE IV

CALCULATIONS FOR THE SIMPLIFIED TRANSFER LOCUS OF THE AIRCRAFT

[See equation (A63) and fig. 7.]

(1)	(2)	(3)	(4)	(5)	(6)	(7)	(8)
ω	e_2	f_1	f_2	$f_1^2 + f_2^2$	$e_1f_1 + e_2f_2$	$e_2f_1 - e_1f_2$	$\frac{e_2f_1 - e_1f_2}{e_1f_1 + e_2f_2}$
0	0	0	0	0	0	0	≈
.5	.609	−.039	.705	.499	.297	−2.389	−8.044
1	1.218	−.159	1.394	1.969	1.166	−4.869	−4.176
1.5	1.827	−.357	2.049	4.326	2.546	−7.525	−2.955
2	2.436	−.636	2.654	7.448	4.332	−10.451	−2.413
3	3.654	−1.431	3.645	15.333	8.552	−17.484	−2.044
4	4.872	−2.544	4.236	24.416	12.105	−26.602	−2.198
5	6.090	−3.975	4.295	34.248	12.824	−38.613	−3.011
6	7.308	−5.724	3.678	46,292	7.681	−54.167	−7.052
7	8.526	−7.791	2.261	65.810	−6.854	−73.994	10.796
8	9.744	−10.176	−.096	103.560	−35.066	−98.745	2.816
9	10.962	−12.879	−3.510	178.189	−81.672	−129.407	1.584
10	12.180	−15.900	−8.140	319.069	−152.474	−166.360	1.091
15	18.270	−35.700	−54.030	4,193.730	−1106.865	−471.022	.426
20	24.360	−63.600	−150.080	26,568	−3869.263	−1045.927	.270

TABLE IV – CONCLUDED

(1)	(9)′	(10)	(11)	(12)	(13)	(14)
ω	$(6)^2 + (7)^2$	$\sqrt{(9)}$	$R_{\theta_s} = (10)/(5)$	$\tan^{-1}(8)$	$R_p R_{\theta_s}$	$\epsilon_{\theta_s} + \epsilon_p$
0	0	0	~	~	~	~
.5	5.796	2.405	5.36	−262.90°	5.36	−83.66°
1	25.067	5.010	2.54	−256.54°	2.54	−78.08°
1.5	63.107	7.95	1.84	−251.31°	1.84	−73.61°
2	127.989	13.40	1.80	−247.50°	1.80	−70.59°
3	378.827	19.43	1.27	−243.94°	1.28	−68.58°
4	854.197	29.21	1.195	−245.54°	1.22	−71.79°
5	1,655.42	40.70	1.187	−251.64°	1.222	−79.55°
6	2,993.06	54.70	1.181	−261.94°	1.231	−91.57°
7	5,522.09	74.40	1.130	−275.30°	1.200	−106.73°
8	10,980	104.6	1.011	−289.55°	1.092	−122.89°
9	23,416	152.7	.856	−302.26°	.949	−137.61°
10	50,923	225.5	.707	−312.50°	.800	−150.02°
15	1,440,370	1,200	.287	−336.96°	.375	−188.47°
20	16,065,000	4,000	.151	−344.89°	.230	−219.18°

TABLE V

CALCULATIONS FOR THE LOGARITHMIC PLOTS
[See equations (A64) through (A71) and fig. 8.]

(1)	(2)	(3)	(4)	(5)	(6)
ω	$b_1^2+b_2^2$	$c_1^2+c_2^2$	$d_1^2+d_2^2$	$\frac{d_3^2}{d_1^2+d_2^2}$	$10 \log_{10}$ (5)
0	5.67464	0.03263	1,406.250	1	0
.5	16.03440	.94465	1,405.413	1.00059	.0026
1	51.27673	9.16085	1,402.903	1.00238	.0103
1.5	123.89144	40.35783	1,398.730	1.00538	.0233
2	254.69419	118.26430	1,392.904	1.00958	.0415
3	815.76008	530.65061	1,376.372	1.02170	.0932
4	2,067.52987	1,483.1020	1,353.511	1.03896	.1660
5	4,476.28100	3,224.141	1,324.602	1.06163	.2596
6	8,641.515	6,245.461	1,290.010	1.09010	.3747
7	15,295.527	12,028	1,250.177	1.12484	.5108
8	25,305.667	24,647	1,205.629	1.16640	.6685
9	39,669.360	53,031	1,156.971	1.21545	.8472
10	59,519.605	118,582	1,104.890	1.27275	1.0473
15	290,032	3,545,111	822.802	1.70909	2.3277
20	904,174	39,669,789	604.490	2.32634	3.6667

NACA

TABLE V.- CONTINUED

(1)	(7)	(8)	(9)	(10)	(11)
ω	$10 \log_{10}$ (2)	$-10 \log_{10}$ (3)	b_2/b_1	$\tan^{-1}$ (9)	$-c_2/c_1$
0	7.443	14.864	0	-180°	0
.5	12.049	0.248	1.99669	-116.60°	.44636
1	17.098	-9.619	275.29600	-90.21°	.18557
1.5	20.968	-16.058	-3.67979	-74.79°	.03594
2	24.062	-20.726	-2.03371	-63.81°	-.07523
3	29.155	-27.248	-1.14132	-48.10°	-.27099
4	33.155	-31.711	-.81108	-39.05°	-.49182
5	36.508	-35.084	-.63348	-32.35°	-.80662
6	39.365	-37.948	-.52118	-27.53°	-1.37452
7	41.873	-40.803	-.44333	-23.91°	-2.90004
8	44.032	-43.918	-.38601	-21.11°	29.85025
9	45.984	-47.294	-.34196	-18.88°	4.27415
10	47.746	-50.741	-.30703	-17.06°	2.11691
15	54.623	-65.496	-.20353	-11.44°	.68800
20	59.731	-75.984	-.15235	-8.66°	.44138

TABLE V.– CONCLUDED

1	(12)	(13)	(14)	(15)	(16)
ω	$\tan^{-1}$ (11)	$-d_2/d_1$	$\tan^{-1}$ (13)	(6) + (7) + (8)	(10) + (12) + (14)
0	–180°	0	–180°	22.307	–180°
.5	–155.95°	–.01333	–180.76°	12.299	–93.31°
1	–169.49°	–.02670	–181.54°	7.489	–81.24°
1.5	–177.93°	–.04013	–182.30°	4.933	–75.02°
2	–184.30°	–.05366	–183.09°	3.378	–71.20°
3	–195.15°	–.08112	–184.64°	2.000	–67.89°
4	–206.20°	–.10937	–186.25°	1.610	–71.50°
5	–218.88°	–.13869	–187.91°	1.684	–79.14°
6	–233.96°	–.16943	–189.63°	1.792	–91.12°
7	–250.96°	–.20197	–191.43°	1.581	–106.30°
8	–268.90°	–.23677	–193.34°	.783	–123.35°
9	–283.16°	–.27437	–195.35°	–.463	–137.39°
10	–295.29°	–.31545	–197.52°	–1.948	–149.87°
15	–325.47°	–.61349	–211.51°	–8.545	–188.42°
20	–336.19°	–1.39860	–234.29°	–12.586	–219.14°

TABLE VI

CALCULATIONS FOR THE APPROXIMATE FACTORIZATION OF THE AIRCRAFT STABILITY QUARTIC

[See equations (A72) through (A78) and fig. 10.]

(1)	(2)	(3)	(4)	(5)	(6)	(7)	(8)	(9)
ω	g_1	g_2	h_1	h_2	g_2/g_1	h_2/h_1	$\tan^{-1}\frac{-g_2}{g_1}$	$\tan^{-1}\frac{-h_2}{h_1}$
0	2.838	0	-0.064	0	0	0	0	-180°
.5	2.827	.166	-.314	.157	.059	-.500	-3.37°	-153.45°
1	2.795	.332	-1.064	.314	.119	-.295	-6.79°	-163.56°
1.5	2.741	.498	-2.314	.471	.182	-.204	-10.32°	-168.47°
2	2.666	.664	-4.064	.628	.249	-.154	-13.79°	-171.26°
3	2.450	.996	-9.064	.942	.407	-.104	-22.15°	-174.06°
4	2.148	1.328	-16.064	1.256	.618	-.078	-31.72°	-175.54°
5	1.761	1.660	-25.064	1.570	.943	-.063	-43.34°	-176.38°
6	1.286	1.992	-36.064	1.884	1.549	-.052	-57.14°	-177.03°
7	.726	2.324	-49.064	2.198	3.049	-.045	-71.85°	-177.42°
8	.079	2.656	-64.064	2.512	33.620	-.039	-88.30°	-177.76°
9	-.653	2.988	-81.064	2.826	-4.576	-.035	-102.33°	-178.00°
10	-1.472	3.320	-100.064	3.140	-2.255	-.031	-113.20°	-178.21°
15	-6.859	4.980	-225.064	4.710	-.726	-.021	-144.03°	-178.80°
20	-14.402	6.640	-400.064	6.280	-.461	-.016	-155.25°	-179.09°

TABLE VI – CONCLUDED

(1)	(10)	(11)	(12)	(13)	(14)	(15)
ω	$g_1^2 + g_2^2$	$h_1^2 + h_2^2$	$-(10)\log_{10}(10)$	$-(10)\log_{10}(11)$	(8)+(9)	(12) + (13)
0	8.054	0.004	−9.060	23.980	−180°	14.920
.5	8.019	.123	−9.041	9.101	−156.86°	.060
1	7.922	1.136	−8.988	−.554	−170.35°	−9.542
1.5	7.761	5.576	−8.899	−7.463	−178.79°	−16.362
2	7.548	16.910	−8.778	−12.281	−185.05°	−21.059
3	6.995	83.043	−8.448	−19.193	−196.21°	−27.641
4	6.377	259.629	−8.046	−24.143	−207.26°	−32.189
5	5.857	630.669	−7.676	−27.998	−219.72°	−35.674
6	5.622	1,304.16	−7.530	−31.153	−234.17°	−38.683
7	5.928	2,412.11	−7.729	−33.824	−249.27°	−41.553
8	7.061	4,110.51	−8.488	−36.138	−266.06°	−44.626
9	9.355	6,579.36	−9.710	−38.182	−280.33°	−47.892
10	13.189	10,022	−11.202	−40.009	−291.41°	−51.211
15	72.341	50,675	−18.594	−47.047	−322.83°	−65.641
20	251.507	160,090	−24.005	−52.044	−334.34°	−76.049

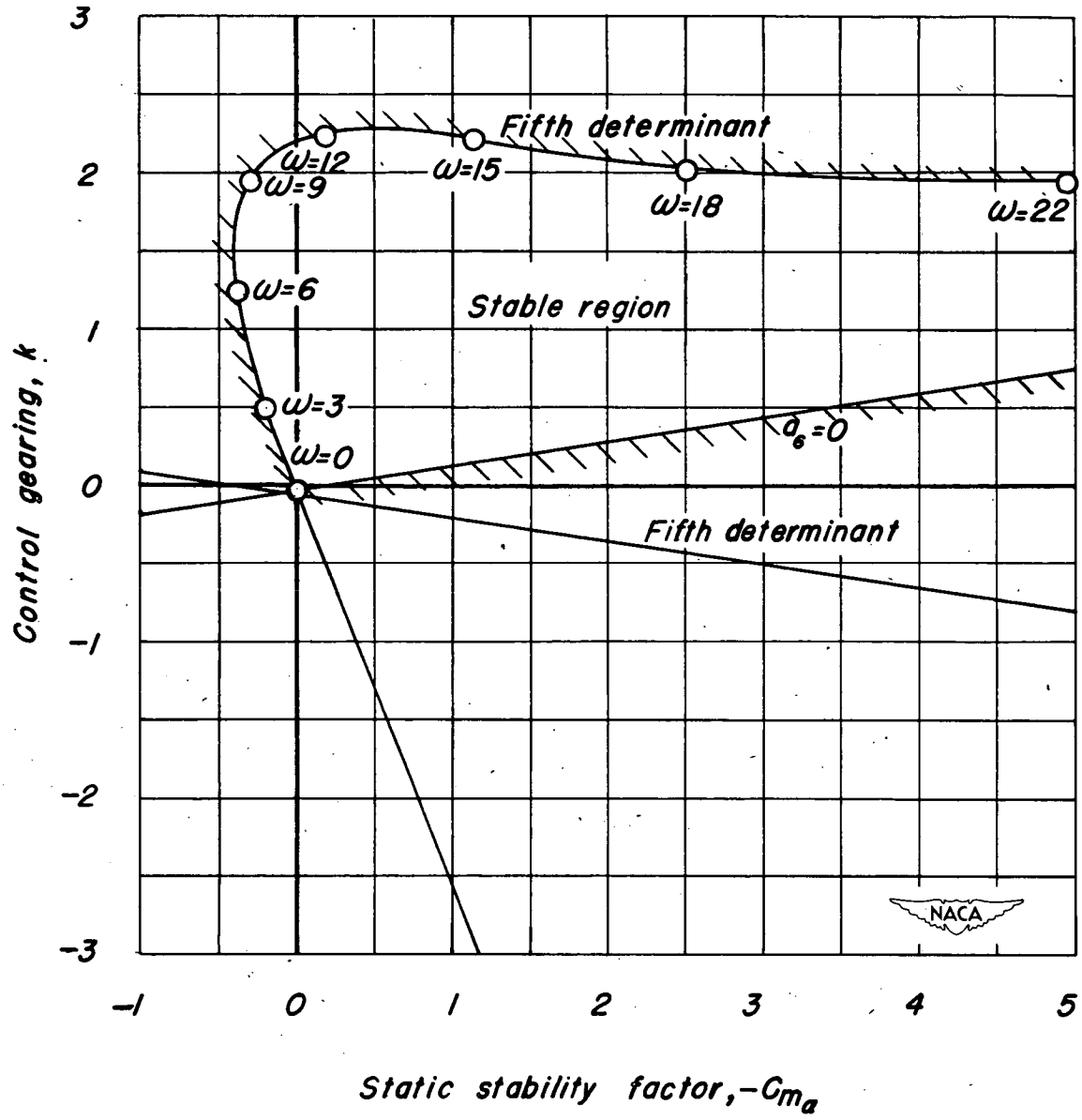

Figure 1.— Stability boundary chart for the aircraft–autopilot combination.

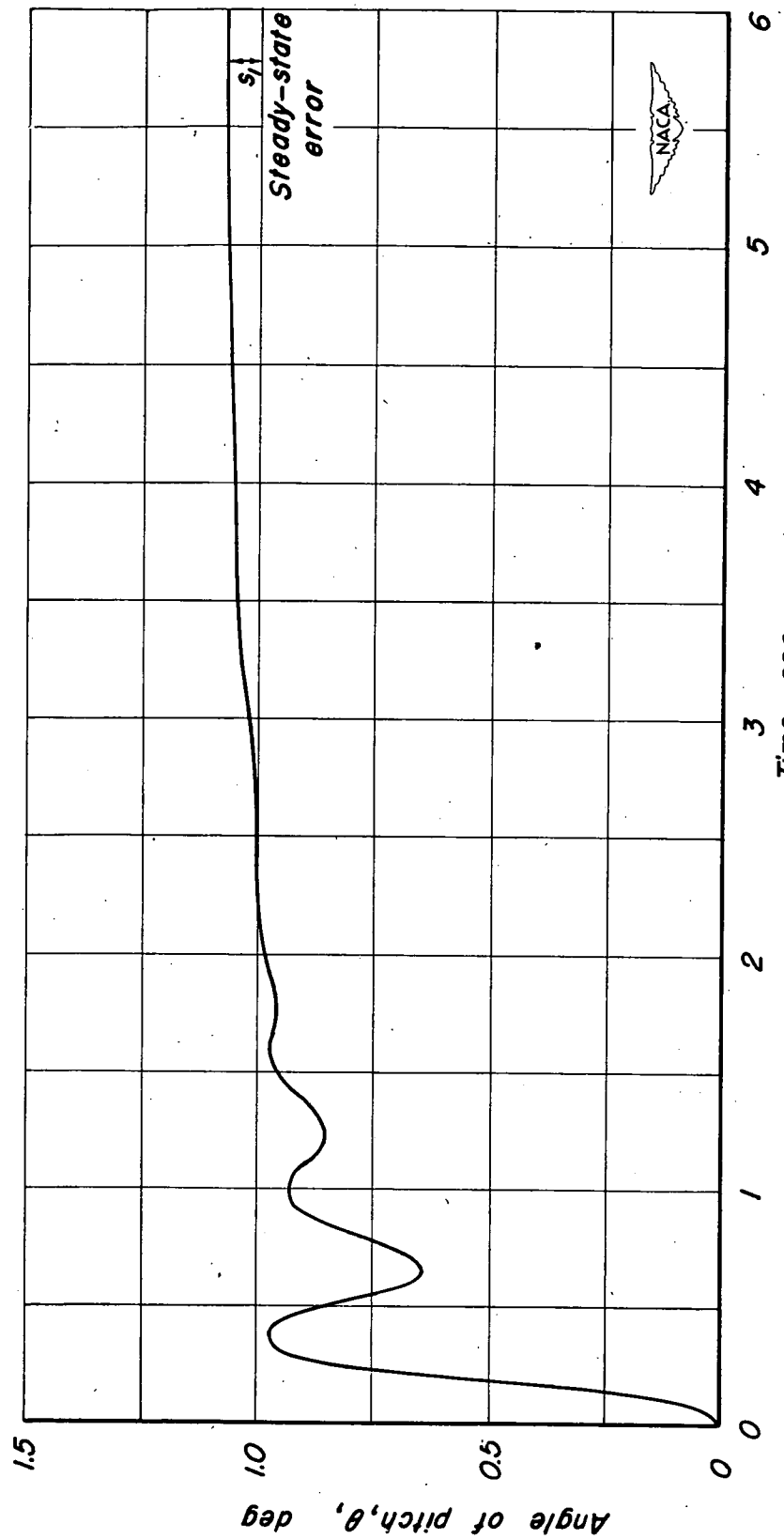

Figure 2.—The transient response of the airplane–autopilot combination following a step input in θ. $k = 1$, $C_{m_\alpha} = -0.639$.

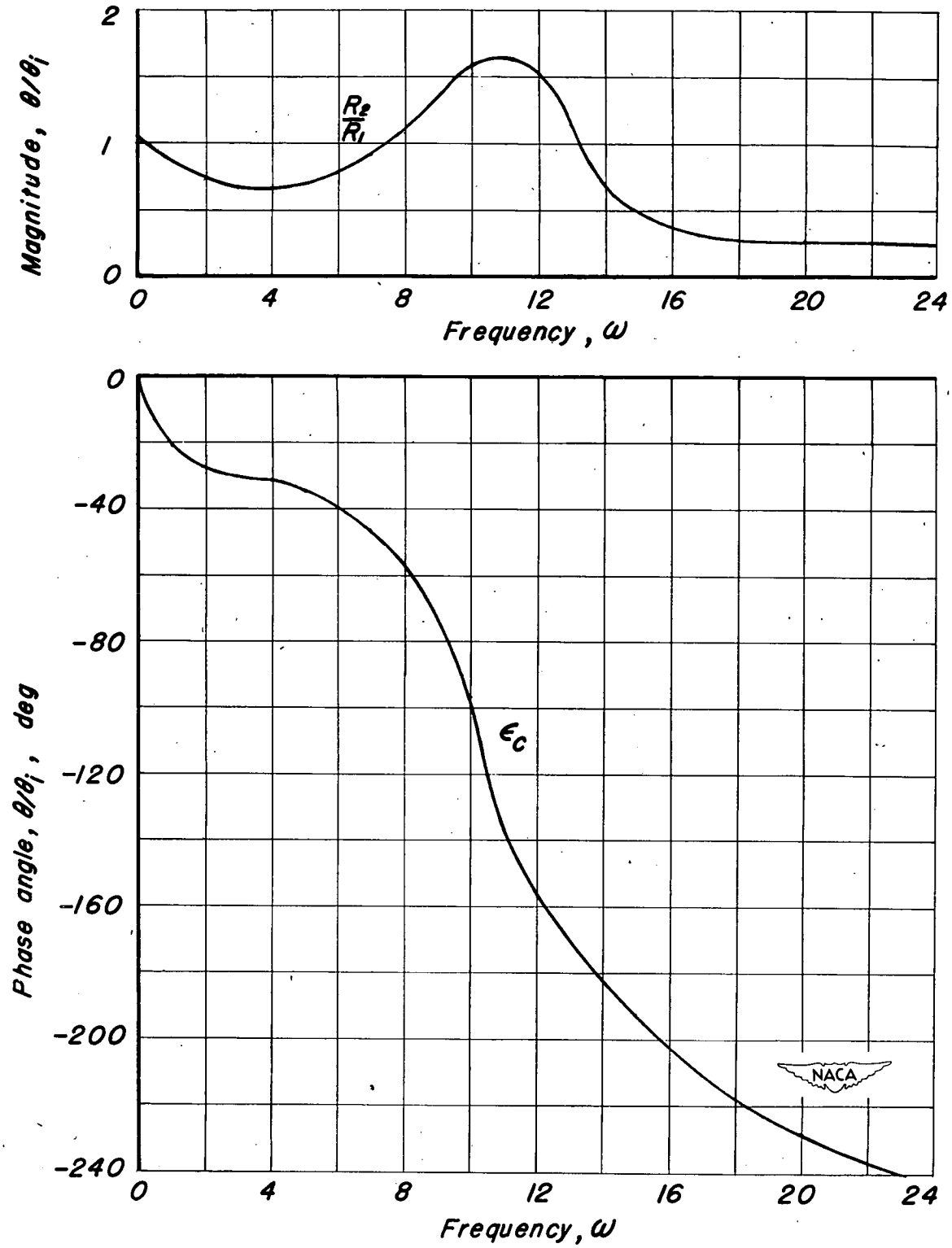

Figure 3.- Closed-loop frequency-response characteristics of the aircraft-autopilot combination. $k=1$, $C_{m_\alpha}=-0.639$.

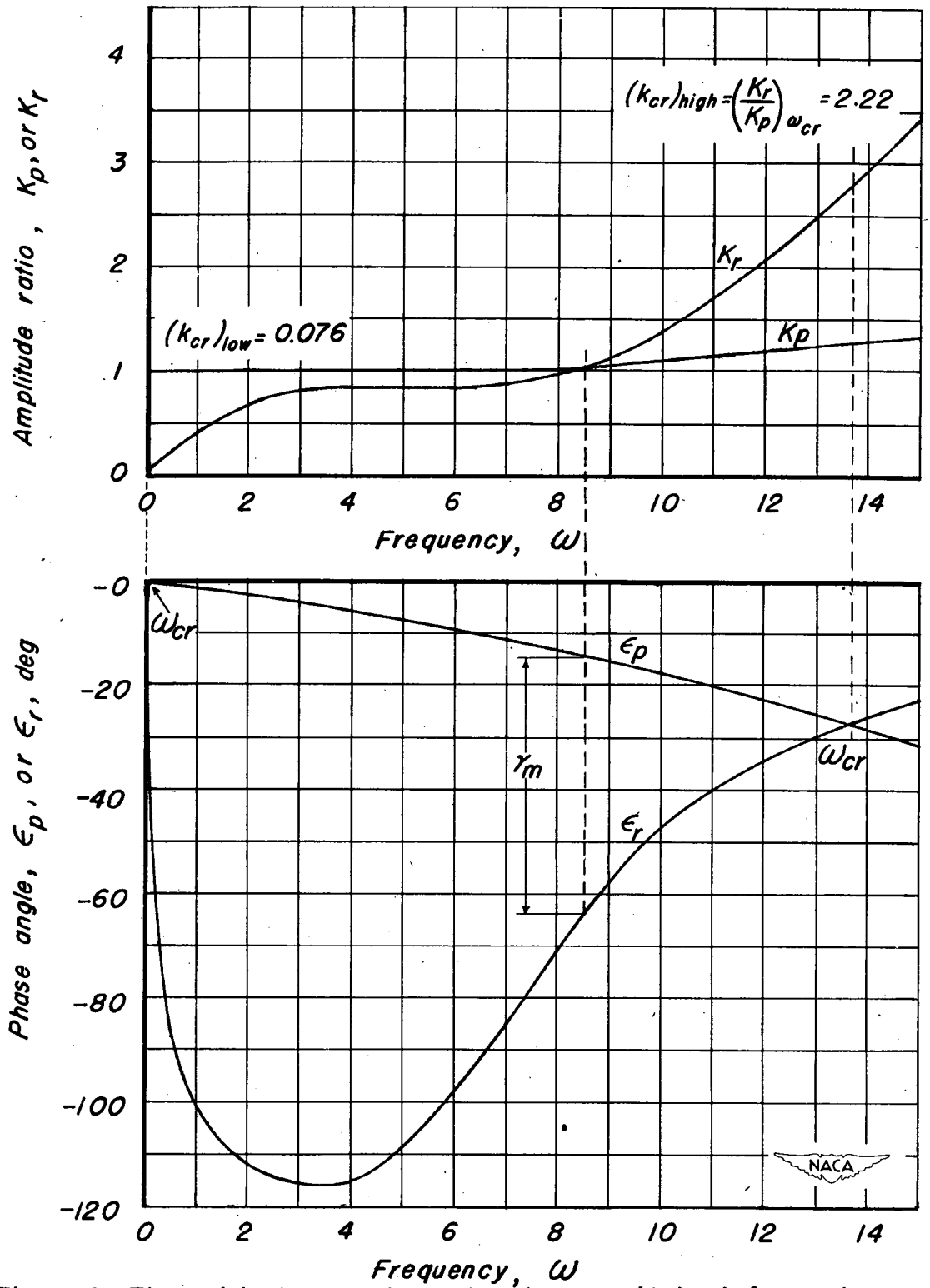

Figure 4.– The critical control gearing, k_{cr}, as obtained from the frequency–response characteristics of the aircraft and autopilot.

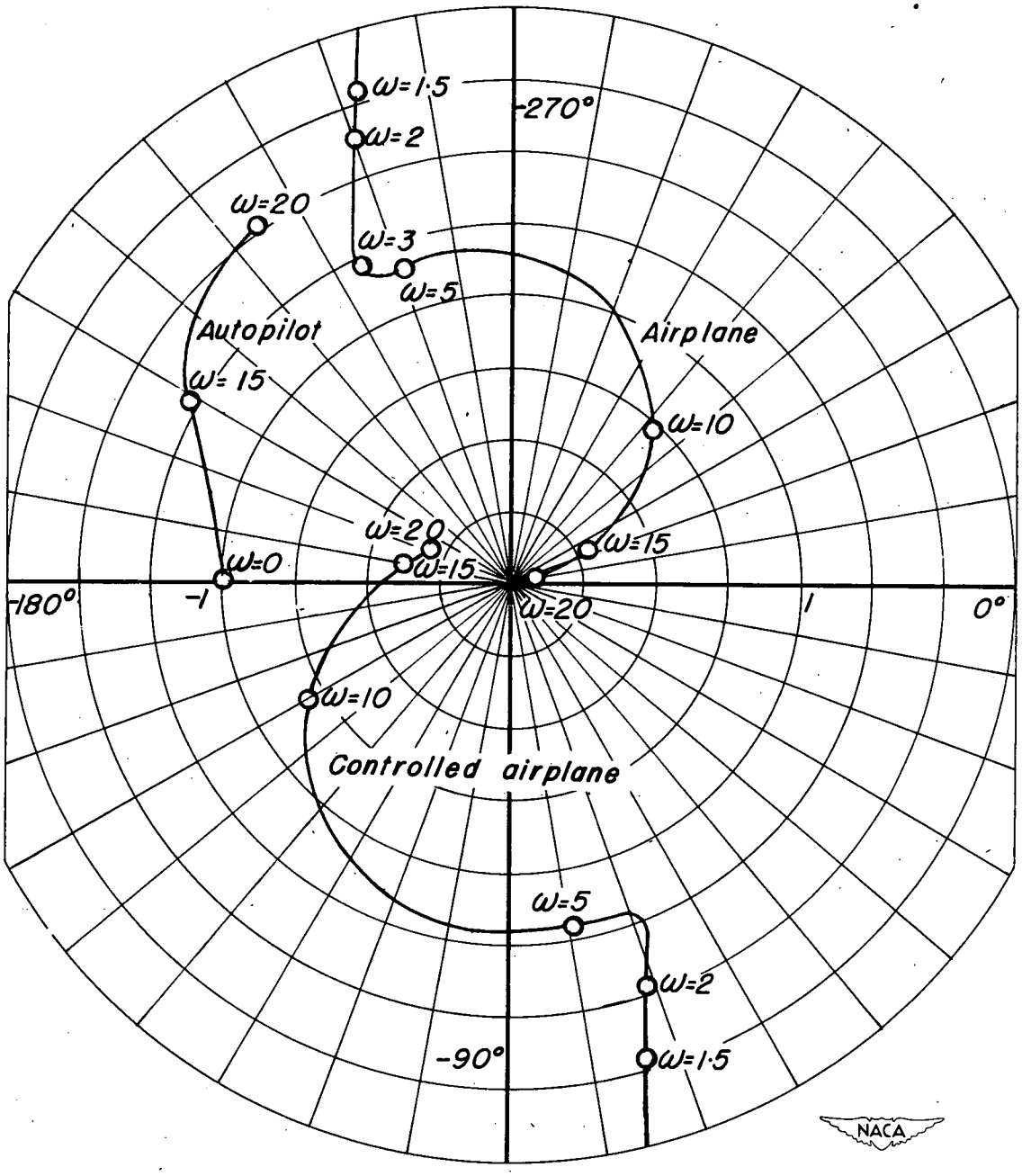

Figure 5.—The open-loop transfer loci of the aircraft, the autopilot, and the aircraft-autopilot combination.

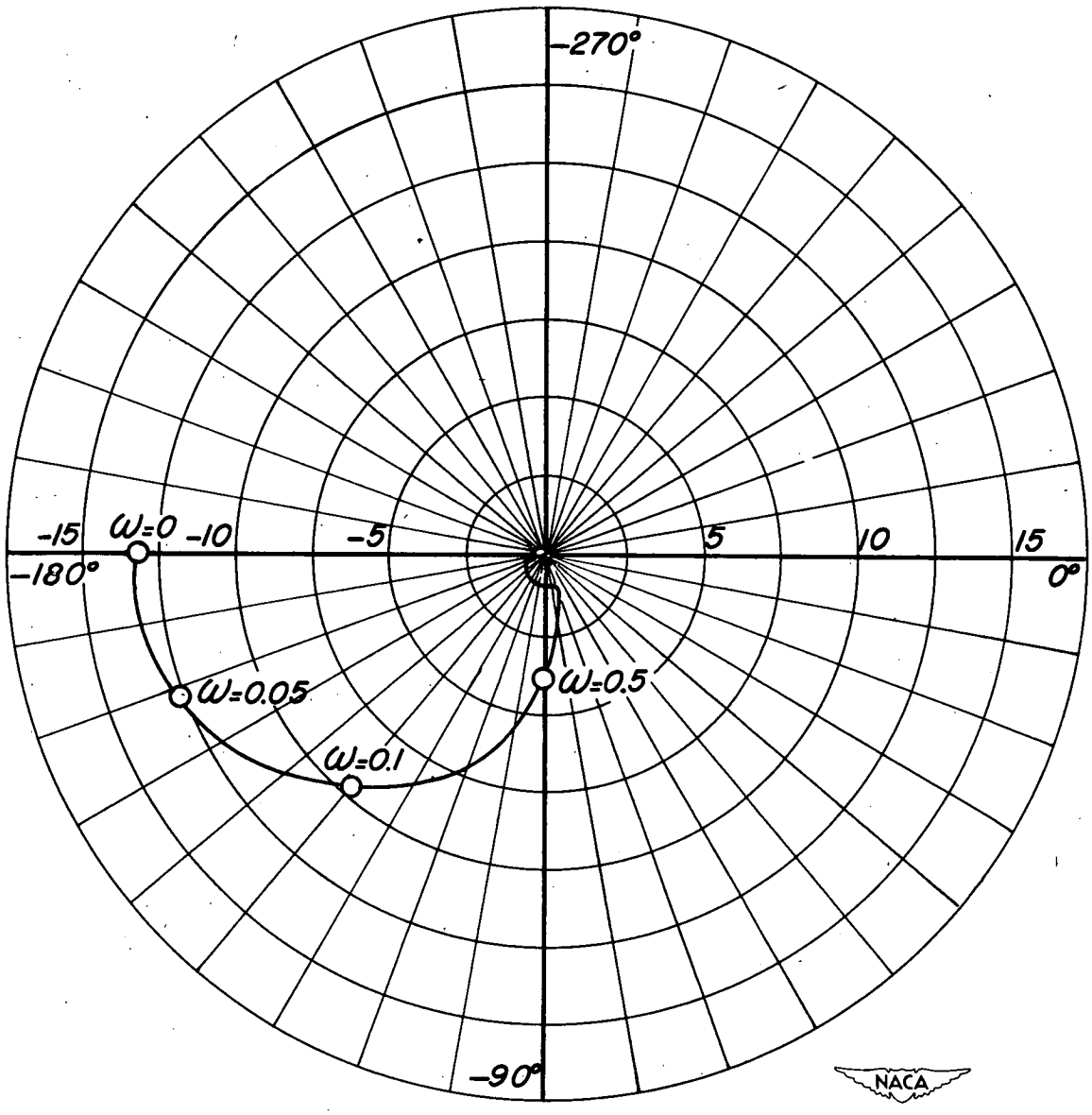

Figure 6.– The open-loop transfer locus of the aircraft-autopilot combination showing the low frequency region.

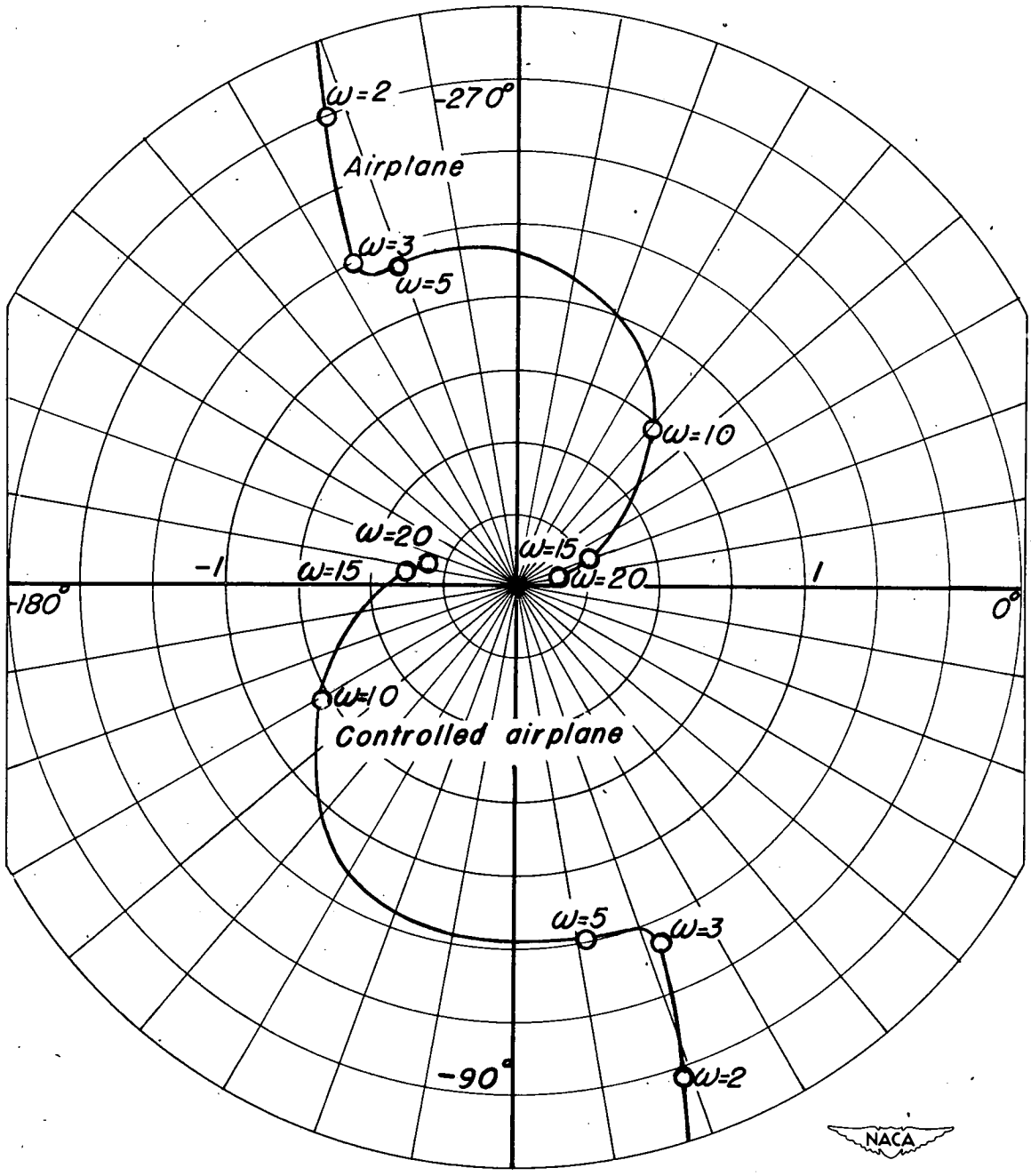

Figure 7.- The open-loop transfer locus of the aircraft using simplified response equations, and the locus of the corresponding aircraft-autopilot combination.

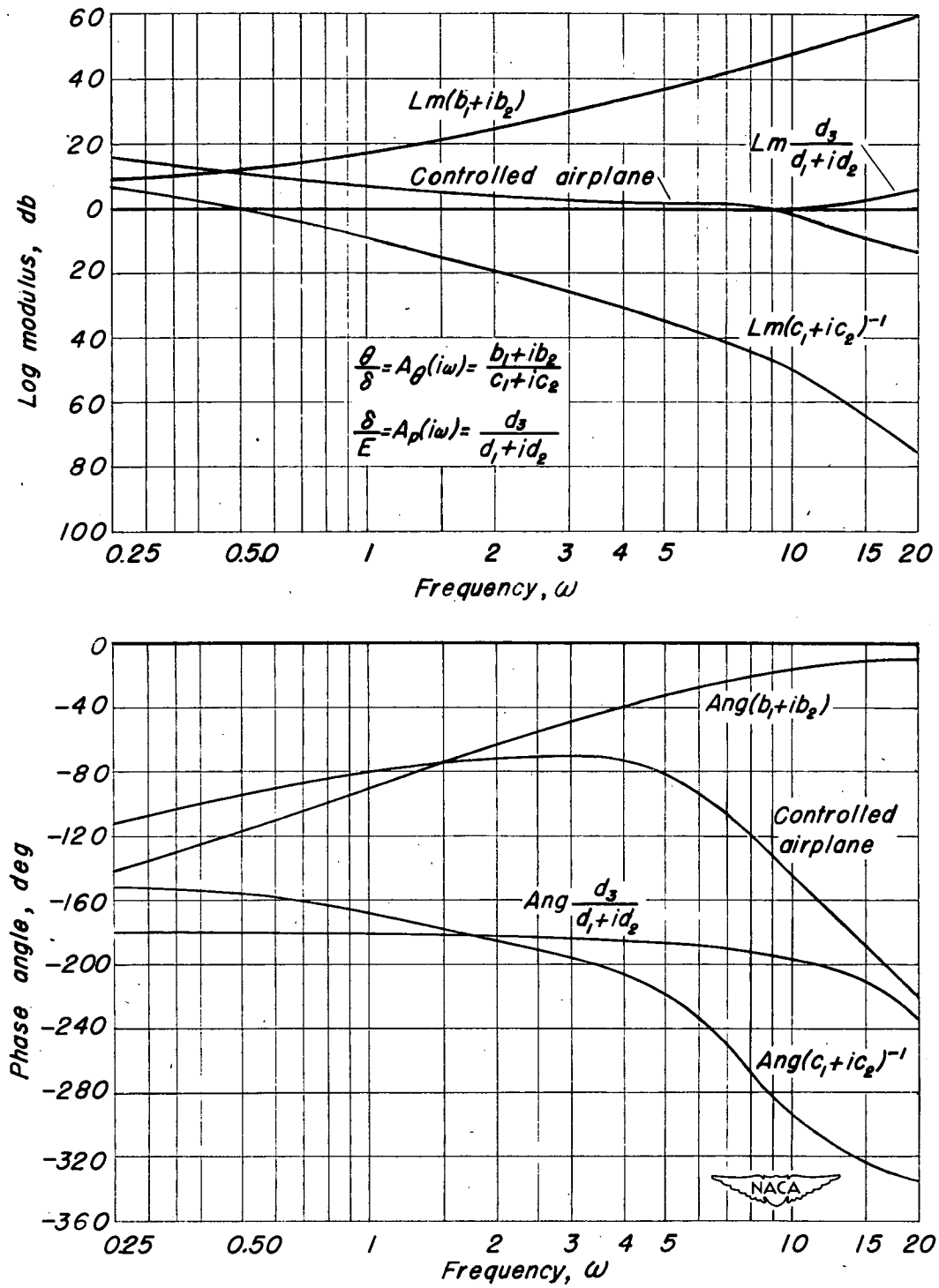

Figure 8.- Logarithmic plots of the transfer loci of the autopilot $d_3/(d_1+id_2)$, the aircraft $(b_1+ib_2)/(c_1+ic_2)$, and the combination representing the controlled airplane.

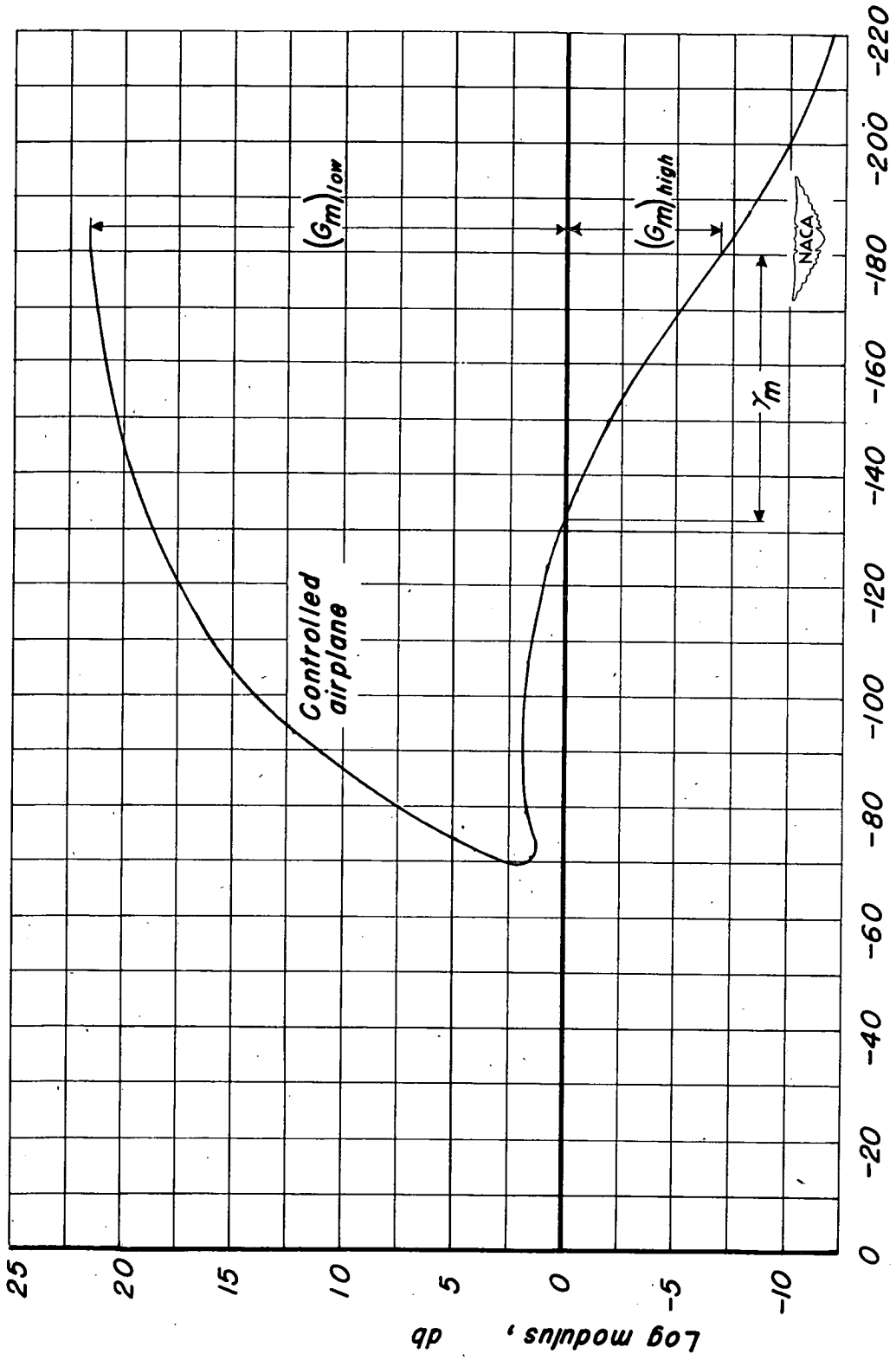

Figure 9.— Open-loop transfer locus of the aircraft-autopilot combination on the Lm-Ang chart showing the gain and phase margins.

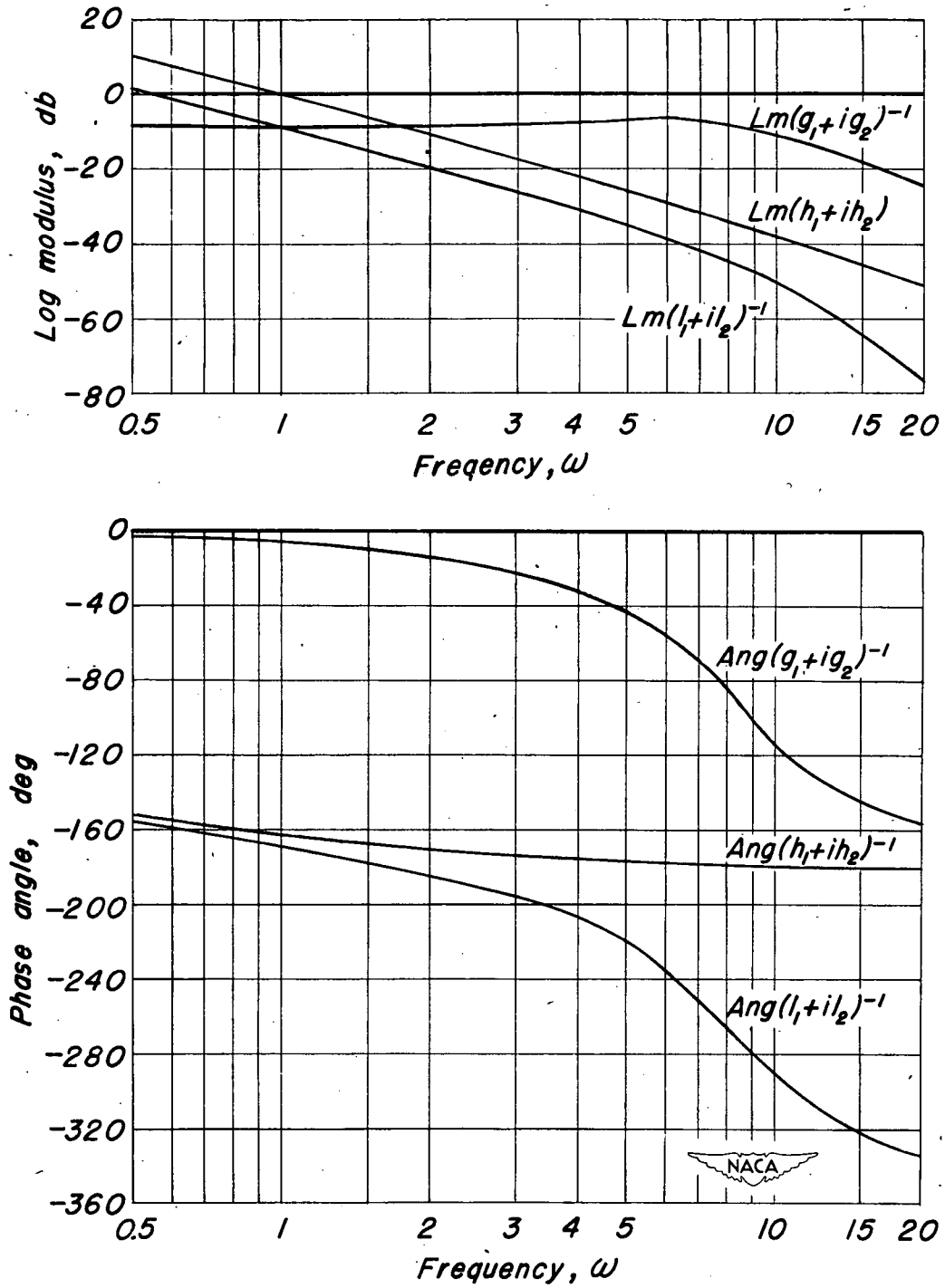

Figure 10.- Logarithmic plots of the transfer loci representing the approximate factorization of the aircraft stability quartic c_1+ic_2 into the quadratic factors $(g_1+ig_2)(h_1+ih_2)=l_1+il_2$.